EVALUATION OF ALTERNATIVE RETRIEVAL METHODS FOR TIROS-N AND NOAA-6 SOUNDINGS

Department of Meteorology
University of Wisconsin—Madison
1225 W. Dayton Street
Madison, Wisconsin 53706

Contributions by

L. H. Horn

T. L. Koehler

J. P. Nelson III

C. J. Seman

Lyle H. Horn, Principal Investigator
Thomas L. Koehler, Co-Principal Investigator

FINAL REPORT

The research in this report has been supported by the Department of Commerce, National Oceanic and Atmospheric Administration under Grant NA81AA-D-00087

July 1986

EVALUATION OF ALTERNATIVE RETRIEVAL METHODS FOR TIROS-N AND NOAA-6 SOUNDINGS

Department of Meteorology
University of Wisconsin—Madison
1225 W. Dayton Street
Madison, Wisconsin 53706

Contributions by

L. H. Horn

T. L. Koehler

J. P. Nelson III

C. J. Seman

Lyle H. Horn, Principal Investigator
Thomas L. Koehler, Co-Principal Investigator

FINAL REPORT

The research in this report has been supported by the Department of Commerce, National Oceanic and Atmospheric Administration under Grant NA81AA-D-00087

July 1986

TABLE OF CONTENTS

PREFACE

The following series of articles summarizes research completed on NOAA Grant NA81AA-D-00087, administered first by the U. S. FGGE Project Office with Dr. Wayne McGovern as grant monitor, and more recently by the Climate and Atmospheric Research Program with Dr. Joseph Huang as grant monitor. Work on this project began in late August, 1981. Before summarizing the research, it is beneficial to review the previous experience of our research group and the overall goals of the project.

1. Background

Our University of Wisconsin-Madison research group has been involved since the mid 1960's in various aspects of the physical problem of deriving vertical profiles of temperature and moisture from satellite-based radiance measurements, and the application of these satellite profiles to weather analysis and forecasting problems. Much of the work in the early and mid 1970's assessed the ability of satellite soundings derived from Nimbus-5 measurements to define the hyperbaroclinic zones found beneath upper tropospheric wind maxima. This work included the simulation study of Togstad and Horn (1974), and the observational studies of Kapela and Horn (1975) and Horn et al. (1976), where some relatively positive results were achieved in locating the thermal wind jet core and defining its intensity. Since the scan mechanism on Nimbus-5 failed, the observational studies were confined mainly to comparisons of satellite and radiosonde cross sections oriented normal to the direction of the upper tropospheric flow.

The launch of the Nimbus-6 satellite in 1975 permitted the first opportunity to examine the horizontal structure of satellite-derived thermal fields. Some of the studies from our group using the standard NESS operational retrievals included Petersen and Horn (1977) and Koehler (1981). The study by Petersen and Horn from an August 1975 case showed that the Nimbus-6 fields agreed remarkably well with bracketing (in time) radiosonde fields. Koehler's results from a February 1976 period indicated that while the satellite data correctly positioned tropospheric troughs and ridges, they underestimated the thermal gradients. Other research with Nimbus-6 soundings investigated the effect of making retrievals at higher horizontal resolution than offered by NESS operations. The studies involved include Koehler (1981), Blechman and Horn (1981) and Paulson and Horn (1981). Of these, the results from Paulson and Horn provided the most promising results with very fine resolution retrievals derived using only a few infrared fields-of-view as input to the software developed on the University of Wisconsin-Madison Man-computer Interactive Data Acquisition System (McIDAS). The Paulson and Horn study determined that the combination of satellite radiance information over large regions in the operational procedures could, at least in part, be responsible for some of the loss of thermal gradient information evident in the Koehler study.

Finally, our most recent work with operational soundings performed in the early 1980's examined the accuracy of operational TIROS-N and NOAA-6 retrievals. Streit and Horn (1981) demonstrated that the jet streak associated with

the April 10, 1979 Wichita Falls tornado outbreak could be successively tracked in its eastward propagation across the Eastern Pacific and across the Rockies for a period of several days using TIROS-N satellite soundings. In more detailed work summarized in Koehler et al. (1983), the accuracy of TIROS-N and NOAA-6 soundings from a January, 1980 period was investigated. This work involved not only a comparison of satellite versus radiosonde fields, but also examined the effect of retrieval accuracy on subsequent numerical model predictions. The results from Koehler et al. for TIROS-N and NOAA-6 retrievals were very similar to the Koehler (1981) results from Nimbus-6, indicating that the satellite retrievals tend to underestimate thermal gradients, being too warm in troughs and slightly too cold in ridges. Furthermore, these weaker gradients were retained in numerical forecasts initialized with the satellite retrievals. Our findings of weaker thermal gradients in the satellite soundings compared to conventional observations are quite consistent with other reported satellite sounding assessments fron TIROS-N and NOAA-6 such as Phillips et al. (1979), Schlatter (1981), and Gruber and Watkins (1982).

In summary, our research group has had considerable experience in the evaluation of retrieval accuracy, with an interest not only in statistical representations of retrieval errors, but also in their spatial distributions both in the horizontal and vertical. Our evaluations involve direct comparisons of satellite and conventional data, without mixing data from different observing systems together, with the careful editing of data from both sources receiving considerable attention. This research philosophy has been continued in the studies reported in this project report.

2. Purpose of the Project

The primary purpose of this project was to evaluate alternatives to the operational retrieval method employed by the National Environmental Satellite Service (NESS) in producing satellite soundings from TIROS-N and NOAA series satellites. By evaluating alternative methods, we hoped to identify sources of error in the operational NESS retrievals and to suggest possible avenues for improving their accuracy. Of primary importance is the fact that the operational soundings from TIROS-N and NOAA-6 were included in the Level IIa data sets archived during the First GARP Global Experiment (FGGE) from December 1978 through November 1979. These data sets are certainly the most complete ever gathered on a global basis, and have been the focus of a considerable research effort. Although the FGGE data produced some forecasting improvement, the addition of satellite data had a less positive impact than expected. Reducing errors in the satellite temperature retrievals included in this data set could have a significant impact on much of the FGGE research.

3. The NESS Operational Retrieval Technique

A description of the NESS operational retrieval technique is necessary before we can present the results from alternative methods. Only a brief description will be presented here. For more details see for example Smith et al. (1979).

Three instruments were carried aboard the TIROS-N and NOAA series polar orbiting satellites for the determination of satellite soundings: the 20 channel second generation High Resolution Infrared Sounder (HIRS/2), the 4 channel Microwave Sounding Unit (MSU), and the 3 channel Stratospheric Sounding Unit (SSU). Of primary importance in the troposphere are the HIRS/2 and MSU measurements, which have nominal horizontal fields-of-view (FOV) of 17.4 km and 109.3 km respectively (at nadir). The operational NESS retrieval method is based on the HIRS/2 scan geometry, combining the information from several HIRS/2 FOV to produce a single temperature retrieval. A step-by-step description of the NESS retrieval algorithm is provided below.

1. Translate the digital instrument counts by the HIRS/2, MSU and SSU instruments to radiance or brightness temperature values using calibration information included with the raw data.

2. Apply a statistical limb correction to the HIRS/2 and MSU data. This technique attempts to remove the effect of scan angle from the measurements, making all the data appear to have been measured at nadir. The MSU limb correction also attempts to remove the effects of relatively low emissivity found over bodies of water in the lowest sounding channels and the effects of heavy precipitation which also degrades the microwave data.

3. Interpolate the MSU data to the HIRS/2 observation locations.

4. Organize the HIRS/2 resolution radiances into 63 FOV arrays, oriented with 9 FOV across the path of the satellite orbit, and 7 FOV along the path.

5. Determine the extent of cloud cover in each 9x7 array, through various checks of the HIRS/2 channels peaking in the lower troposphere with both HIRS/2 window channels and the MSU channel peaking near 700 mb. The radiances for a given array are then classified in one of three categories: clear, partly cloudy or cloudy. If the partly cloudy path is chosen, the infrared radiances are corrected to remove the effect of clouds using an N* technique similar to that presented in Smith (1968).

6. Derive temperature and moisture profiles using a statistical eigenvector approach from the composite radiances (Smith and Woolf, 1976). The statistical coefficients are based on the previous week's satellite-vs-raob matches. The coefficients are also categorized in 5 latitudinal zones: 2 polar zones (one in each hemisphere), 2 midlatitude zones, and a tropical zone. Coefficients used in a particular retrieval are selected on the basis of the latitude of the observation and an interpolation of coefficients between the two closest latitudinal zones based on MSU Ch. 4. This latter interpol-

ation attempts to identify different air masses in regions of strong air mass contrast. The resulting temperature retrievals at 40 selected pressure levels from 1000 to 0.1 mb, and water vapor mixing ratio from 1000 to about 100 mb are converted to thicknesses between mandatory pressure levels and precipitable water in selected atmospheric layers, which are then entered onto the NESS archive tapes along with the composite brightness temperatures for the 9x7 array in question.

The TIROS-N and NOAA-6 soundings included in the FGGE Level IIa data sets were derived in this manner. The research described in this project report involves alternatives to several steps in the operational approach.

4. Research Design

Our basic plan was to first evaluate the final step of the retrieval procedure, the determination of temperatures from radiances using a statistical technique, and then evaluate alternatives to some of the earlier steps, such as those involving cloud cover determination and radiance compositing in 9x7 regions. The principal alternative retrieval method considered was a physically-based iterative retrieval technique available from the NESDIS Development Laboratory at Madison, WI in November, 1981, called the TOVS Export Package. This software was designed for use on McIDAS computer systems and combined radiance data over 3x3 HIRS/2 FOV. It was modified for transfer to the University of Wisconsin's Univac 1100 system, and to meet our specifications for data input. These modifications are outlined in one of the later papers in this report.

A related area of investigation did not involve an alternative approach but did evaluate the accuracy of the microwave limb correction procedure applied early in the operational method. The microwave information is quite important to several steps in the retrieval procedure, particularly the cloud cover determination steps. Thus, inadequacies in the limb correction procedure could have a significant effect on the final satellite sounding accuracy.

5. Summary of the Papers Presented

The following summary provides a description of the overall scope of our research and briefly outlines the major results from several of our different topics of study. For more detail, refer to the papers themselves. The first two papers describe the modifications to the iterative retrieval package and the determination of the verification data from radiosonde observations, respectively, while the following three papers present the main body of alternative method evaluations. Each of the papers are briefly described below.

A. "A Modified Version of the NESDIS TOVS Export Package for Use in Alternative Retrieval Method Studies" by Thomas L. Koehler and Charles J. Seman.

This first paper outlines the modifications made to the NESDIS software so that true alternatives to the operational NESS retrievals could be examined. Some of the major changes include the option of producing cloudy path retrievals, incorporating additional first guess alternatives to the zonal climatology originally provided, and adding a statistically-derived guess profile in the cloud cover determination algorithm. The original NESDIS software consisted of over 60 subprograms, which made the modification of the programs for our purposes a time consuming effort.

B. "High Quality Radiosonde-Derived Temperature and Thickness Data for Alternative Satellite Retrieval Evaluation Experiments" by Thomas L. Koehler.

A method for deriving vertical temperature profiles from radiosonde measurements that can be transferred in time and space to specific satellite soundings is described. These verification data are derived for the specific needs of this project and can be applied to data from different conventional sources. Particular care is given to checking the data for both vertical and horizontal consistency and supplementing the data archive whenever possible. Colocations to satellite soundings are made from temperature analyses instead of individual radiosonde observations.

C. "An Evaluation of a Physical Retrieval Method as an Alternative to the Statistical Method Used in the NESS Operational Sounding Processing during FGGE", by Thomas L. Koehler, James P. Nelson III and Lyle H. Horn.

This study investigates the effect of replacing the last step in the operational retrieval technique with a physical retrieval method outlined in Smith (1970). This iterative technique has demonstrated a first guess dependence, therefore three different guesses were evaluated: two guesses based on climatologies of varying spatial and temporal resolution, and the NESS operational statistical retrieval. The same 9x7 FOV resolution radiances used in deriving the operational sounding were used in the retrieval. Results from two periods, one in January, 1980, just after completion of the FGGE data collection, and the other in mid April, 1979, indicate that the operational retrieval provides the more accurate initial guess. However, only small improvements over the operational retrieval are realized in applying the iterative technique.

D. "An Evaluation of Different Horizontal Resolution in Radiance Compositing for TIROS-N Retrievals" by Charles J. Seman, Lyle H. Horn and Thomas L. Koehler.

This study examined the effect of using a 3x3 set of HIRS/2 FOV in the cloud cover determination and radiance compositing steps, yielding higher

horizontal resolution in the resulting soundings. A subset of the January, 1980 case from the previous paper was evaluated, and a statistical retrieval was used as the first guess in the iterative retrieval method. Several subsets of the high resolution sounding sets were examined, including the complete set of soundings, and a set that was colocated to the operational NESS retrieval locations.

The findings from the edited high resolution subsets indicate only minor changes in atmospheric thermal representations from each subset. Some modest improvements were made over corresponding 9x7 retrievals, with more improvement being realized for the clear path retrievals and little improvement for the cloudy path retrievals which make up almost half of the sample. The soundings still exhibited a loss of thermal gradient information similar to that found in the operational soundings. This result was somewhat disappointing considering the success found by Paulson and Horn (1981) in using higher resolution retrievals with Nimbus-6 data.

E. "An Examination of Scan Angle Dependence in Limb-Corrected MSU Brightness Temperatures from TIROS-N" by Thomas L. Koehler.

Unlike the previous two papers, this study does not involve evaluations of alternative temperature retrievals. Instead, simulated brightness temperatures derived from radiosonde temperature measurements are compared to observed microwave brightness temperatures both before and after the limb correction method is applied. The results indicate a definite left-to-right bias in MSU Ch. 2 peaking near 700 mb in the early January, 1980 period. Some of this bias could be removed by using the original angle-dependent brightness temperatures and modeling the microwave FOV using known asymmetries in the antenna pattern. Some of these limb correction problems could in part be responsible for some of the loss of thermal gradient information evident at the end of the retrieval process.

6. Conclusions

A vital component of the FGGE observing system was the retrieval of vertical temperature profiles from radiances measured by the TIROS-N and NOAA-6 polar orbiting satellites. Although these soundings provided nearly global coverage, their impact on improving global numerical model forecasts was less than expected. Consequently, a significant post-FGGE effort has involved attempts to improve the satellite soundings. The research in this report has investigated the use of a physical iterative retrieval method as an alternative to the statistical method used during FGGE. However, the physical method did not significantly improve the accuracy of the retrievals when the same array of fields-of-view (9x7) were employed as in the operational retrieval. In an attempt to provide increased horizontal resolution, 3x3 field-of-view arrays were also employed. Although the higher resolution soundings provided some slight improvements in the lower and mid-troposphere, the overall improvement was negligible. Both the FGGE statistical operational retrievals and the physical iterative retrievals show a definite tendency for synoptically correlated errors, with temperatures too warm in troughs and too cold in ridges,

thus reducing thermal gradients. This tendency suggests that the problem in the satellite soundings may arise from the radiance information provided to the retrieval technique. In response to this possibility, a study of the limb correction procedures was undertaken. The results from that study indicate that limb correction of the microwave data may indeed have a negative impact on retrieval accuracy in several ways. For example, the limb-corrected brightness temperatures from TIROS-N exhibit a left-to-right asymmetry, and differences between observed and simulated brightness temperatures exhibit some of the same synoptically correlated error evident in the retrievals.

7. Acknowledgements

We wish to gratefully acknowledge the valuable assistance provided by the following persons. First, sincere thanks go to Dr. Christopher Hayden and Mr. Hal Woolf of the NESDIS Development laboratory in Madison, Wisconsin, who provided the TOVS Export Package and frequent and sometimes lengthy descriptions of how the software works. Dr. John Derber proved a tremendous help in the transfer and modification of the NESDIS routines to the Univac 1100 computer. The extraction of the radiance data from the NESS sounding archive tapes was performed by Mr. Anthony Schreiner, along with the production of the MSU brightness temperature data sets with and without limb correction. Hal Woolf also provided important documentation of the NESS limb correction procedure. We wish to thank Dr. Norman Grody of NESDIS in Suitland, MD for providing the TIROS-N antenna patterns used in the MSU limb correction study. Finally, we acknowledge assistance of Linda Whittaker and Brad Bramer in preparing the final report.

Lyle H. Horn
Principal Investigator

Thomas L. Koehler
Co-Principal Investigator

8. References

Blechman, A.G. and L.H. Horn, 1981: The influence of higher resolution Nimbus-6 soundings in locating jet maxima. Case Studies Employing Satellite Indirect Soundings, Final Report, NOAA Grant 04-4-158-2, Dept. of Meteorology, University of Wisconsin, Madison, 1-30.

Gruber, A. and C. D. Watkins, 1982: Statistical assessment of the quality of TIROS-N and NOAA-6 satellite soundings. Mon. Wea. Rev., 110, 867-876.

Horn, L.H., R.A. Petersen and T.M. Whittaker, 1976: Intercomparisons of data derived from Nimbus-5 temperature profiles, rawinsonde observations and initialized LFM model fields. Mon. Wea. Rev., 104, 1362-1371.

Kapela, A. and L.H. Horn, 1975: Nimbus-5 satellite soundings in a strongly baroclinic region. Meteorological Applications of Satellite Indirect Soundings, Project Report, NOAA Grant 04-4-158-2, Dept. of Meteorology, University of Wisconsin-Madison.

Koehler, T.L., 1981: A case study of height and temperature analyses derived from Nimbus-6 satellite soundings. Evaluation of Satellite Soundings Using Anlyses and Model Forecasts, Final Report, NASA Grant NSG5252, Dept. of Meteorology, University of Wisconsin-Madison, 1-50.

Koehler, T.L., J.C. Derber, B.D. Schmidt and L.H. Horn, 1983: An evaluation of soundings, analyses and model forecasts derived from TIROS-N and NOAA-6 satellite data. Mon. Wea. Rev., 111, 562-571.

Paulson, B.A. and L.H. Horn, 1981: Nimbus-6 temperature soundings obtained using interactive video-graphics computer techniques. Bull. Amer. Meteor. Soc., 62, 1308-1318.

Petersen, R.A. and L.H. Horn, 1977: A evaluation of 500 mb height and geostrophic wind fields derived from Nimbus-6 soundings. Bull. Amer. Meteor. Soc., 58, 1195-1201.

Phillips, N., L. McMillin, A. Gruber and D. Wark, 1979: An evaluation of early operational temperature soundings from TIROS-N. Bull. Amer. Meteor. Soc., 60, 1188-1197.

Schlatter, T.W., 1981: An assessment of operational TIROS-N temperature retrievals over the United States. Mon. Wea. Rev., 109, 110-119.

Smith, W.L., 1968: An improved method for calculating tropospheric temperature and moisture from satellite radiometer measurements. Mon. Wea. Rev., 96, 387-396.

Smith, W.L., 1970: Iterative solution of the radiative transfer equation for the temperature and absorbing gas profile of an atmosphere. Applied Optics, 9, 1993-1999.

Smith, W.L. and H.M. Woolf, 1976: The use of eigenvectors of statistical covariance matrices for interpreting satellite sounding radiometer measurements. J. Atmos. Sci., 33, 1127-1140.

Smith, W.L., H.M. Woolf, C.M. Hayden, D.Q. Wark and L.M. McMillin, 1979: The TIROS-N operational vertical sounder, Bull. Amer. Meteor. Soc., 60, 1177-1187.

Streit, D.F. and L.H. Horn, 1981: Intercomparisons of TIROS-N satellite soundings, radiosonde data and NMC analyses in tracking jet streaks. Synoptic-Dynamic Applications of Meteorlogical Satellite Data, Final Report, NOAA Grant NA79AA-H-00011, Dept. of Meteorology, University of Wisconsin-Madison, 1-27.

Togstad, W.E. and L.H. Horn, 1974: An application of the satellite indirect sounding technique in describing the hyperbaroclinic zone of a jet streak. J. Appl. Meteor., 13, 264-276.

A MODIFIED VERSION OF THE NESDIS TOVS EXPORT PACKAGE FOR USE IN ALTERNATIVE RETRIEVAL METHOD STUDIES

by

Thomas L. Koehler and Charles J. Seman

Abstract

The computer software used to generate the alternate retrievals evaluated in our research was developed from a version of the TOVS Export Package produced by the NESDIS Development Laboratory at Madison, WI in November, 1981. A fairly detailed description of the Export Package is presented, followed by a description of the modified version used in the research studies presented in this project report.

1. Introduction

A major step in our research project was the modification of the NESDIS iterative retrieval software to meet the special needs of our project. For example, the final software had to be flexible enough to accept radiances from composites over either 9x7 or 3x3 fields-of-view, apply one of three first guess fields, and produce temperatures for sets of soundings classified as clear, partly cloudy or cloudy. Consistent changes also had to be made in the cloud cover determination and compositing software so that 3x3 FOV resolution radiances could be entered into the same temperature retrieval programs as the operational resolution 9x7 radiances included in the original NESS archive tapes.

The paper is organized in the following manner. First, a reasonably detailed description of the original TOVS Export Package software will be provided. Then, the modified versions of the temperature retrieval and 3x3 radiance compositing software will be presented.

2. A Description of the NESDIS TOVS Export Package

The NESDIS Development Laboratory at Madison, WI has developed several versions of the TOVS Export Package for use at several other research and operational institutions. The version of the software used in our studies was obtained from NESDIS in November, 1981. Smith et al. (1983) documents a later version of the Export Package. It is important to document the version we used so that it can be clearly differentiated from subsequent versions.

The software is designed to make temperature retrievals from radiances measured by any of the satellites carrying the TIROS-N Operational Vertical Sounder (TOVS) instruments, including not only TIROS-N but also the NOAA series satellites starting with NOAA-6. The TOVS instruments include the 20 channel HIRS/2 the 4 channel MSU and the 3 channel SSU. A brief description of the channels, and a depiction of their atmospheric weighting functions are presented in Table 1 and Fig. 1, respectively, from Smith et al. (1979). Refer to that article for further details on these instruments. Limb-corrected HIRS/2 and MSU brightness temperature data at the HIRS/2 observation locations serve as input to the routines, and temperature and moisture values determined from 3x3 composites of this data are the output. The entire procedure was broken into 62 subprograms. The major steps included entering the required data sets, determining a climatological first guess for each attempted retrieval, determining the extent of cloud cover over a 3x3 region, producing a temperature and moisture retrieval for those soundings designated either clear or partly cloudy, and producing the final output in the form of heights at mandatory pressure levels up to 100 mb.

After initializing several arrays needed in the atmospheric transmittance calculations, the routine proceeds to step through the brightness temperature data in a organized fashion, attempting a retrieval at input-specified increments of scan line and scan position within an individual line. Default values are 3 for both the line and element steps. The basic sounding information is then entered for each stepped position, which will form the center point for a 3x3 FOV retrieval. A surface elevation is determined from the location's latitude and longitude using a surface topography file with a 1^0 latitude and longitude resolution. Regression coefficients needed in the cloud determination routines are then extracted from a retrieval coefficient file that is updated weekly, as described in Smith et al. (1979). These coefficients are kept in five latitudinal zones, one tropical zone from 30^oS to 30^oN, two midlatitude zones from 30^o to 60^o in each hemisphere, and two regions poleward of 60^o in each hemisphere. Coefficients for the particular sounding being attempted are determined from the sounding's latitude and MSU channel 2 (Ch. 2) value. The next step in the procedure is to determine a climatological "first guess" estimate for the retrieval.

A. The climatological first guess.

The first guess for the retrieval is determined from a climatology available at the 40 pressure levels from 1000 to 0.1 mb used in the retrieval algorithm. Values are defined at 5 latitudes from 15^oN to 75^oN in 15^o increments, for January and July. Points in the Northern Hemisphere south of 15^oN are assigned the values for 15^oN, and those poleward of 75^oN are assigned the value at 75^oN. A linear interpolation in latitude is employed between 15^o and 75^o. An additional linear interpolation by month is done for soundings not occurring in either January or July. Soundings in the Southern Hemisphere use the climatology at the same latitude in the Northern Hemisphere, except the values for January and July are interchanged.

After the climatological temperature and relative humidity values for a sounding location have been determined, the surface temperature and pressure

TABLE 1. Characteristics of TOV sounding channels.

HIRS Channel number	Channel central wavenumber	Central wavelength (μm)	Principal absorbing constituents	Level of peak energy contribution	Purpose of the radiance observation
1	668	15.00	CO_2	30 mb	*Temperature sounding.* The 15-μm band channels provide better sensitivity to the temperature of relatively cold regions of the atmosphere than can be achieved with the 4.3-μm band channels. Radiances in Channels 5, 6, and 7 are also used to calculate the heights and amounts of cloud within the HIRS field of view.
2	679	14.70	CO_2	60 mb	
3	691	14.50	CO_2	100 mb	
4	704	14.20	CO_2	400 mb	
5	716	14.00	CO_2	600 mb	
6	732	13.70	CO_2/H_2O	800 mb	
7	748	13.40	CO_2/H_2O	900 mb	
8	898	11.10	Window	Surface	*Surface temperature* and cloud detection.
9	1 028	9.70	O_3	25 mb	*Total ozone* concentration.
10	1 217	8.30	H_2O	900 mb	*Water vapor sounding.* Provides water vapor corrections for CO_2 and window channels. The 6.7-μm channel is also used to detect thin cirrus cloud.
11	1 364	7.30	H_2O	700 mb	
12	1 484	6.70	H_2O	500 mb	
13	2 190	4.57	N_2O	1 000 mb	*Temperature sounding.* The 4.3-μm band channels provide better sensitivity to the temperature of relatively warm regions of the atmosphere than can be achieved with the 15-μm band channels. Also, the short-wavelength radiances are less sensitive to clouds than those for the 15-μm region.
14	2 213	4.52	N_2O	950 mb	
15	2 240	4.46	CO_2/N_2O	700 mb	
16	2 276	4.40	CO_2/N_2O	400 mb	
17	2 361	4.24	CO_2	5 mb	
18	2 512	4.00	Window	Surface	*Surface temperature.* Much less sensitive to clouds and H_2O than the 11-μm window. Used with 11-μm channel to detect cloud contamination and derive surface temperature under partly cloudy sky conditions. Simultaneous 3.7- and 4.0-μm data enable reflected solar contribution to be eliminated from observations.
19	2 671	3.70	Window	Surface	
20	14 367	0.70	Window	Cloud	*Cloud detection.* Used during the day with 4.0- and 11-μm window channels to define clear fields of view.

MSU	Frequency (GHz)	Principal absorbing constituents	Level of peak energy contribution	Purpose of the radiance observation
1	50.31	Window	Surface	*Surface emissivity* and *cloud attenuation* determination.
2	53.73	O_2	700 mb	*Temperature sounding.* The microwave channels probe through clouds and can be used to alleviate the influence of clouds on the 4.3- and 15-μm sounding channels.
3	54.96	O_2	300 mb	
4	57.95	O_2	90 mb	

SSU	Wavelength (μm)	Principal absorbing constituents	Level of peak energy contribution	Purpose of the radiance observation
1	15.0	CO_2	15.0 mb	*Temperature sounding.* Using CO_2 gas cells and pressure modulation, the SSU observes thermal emissions from the stratosphere.
2	15.0	CO_2	4.0 mb	
3	15.0	CO_2	1.5 mb	

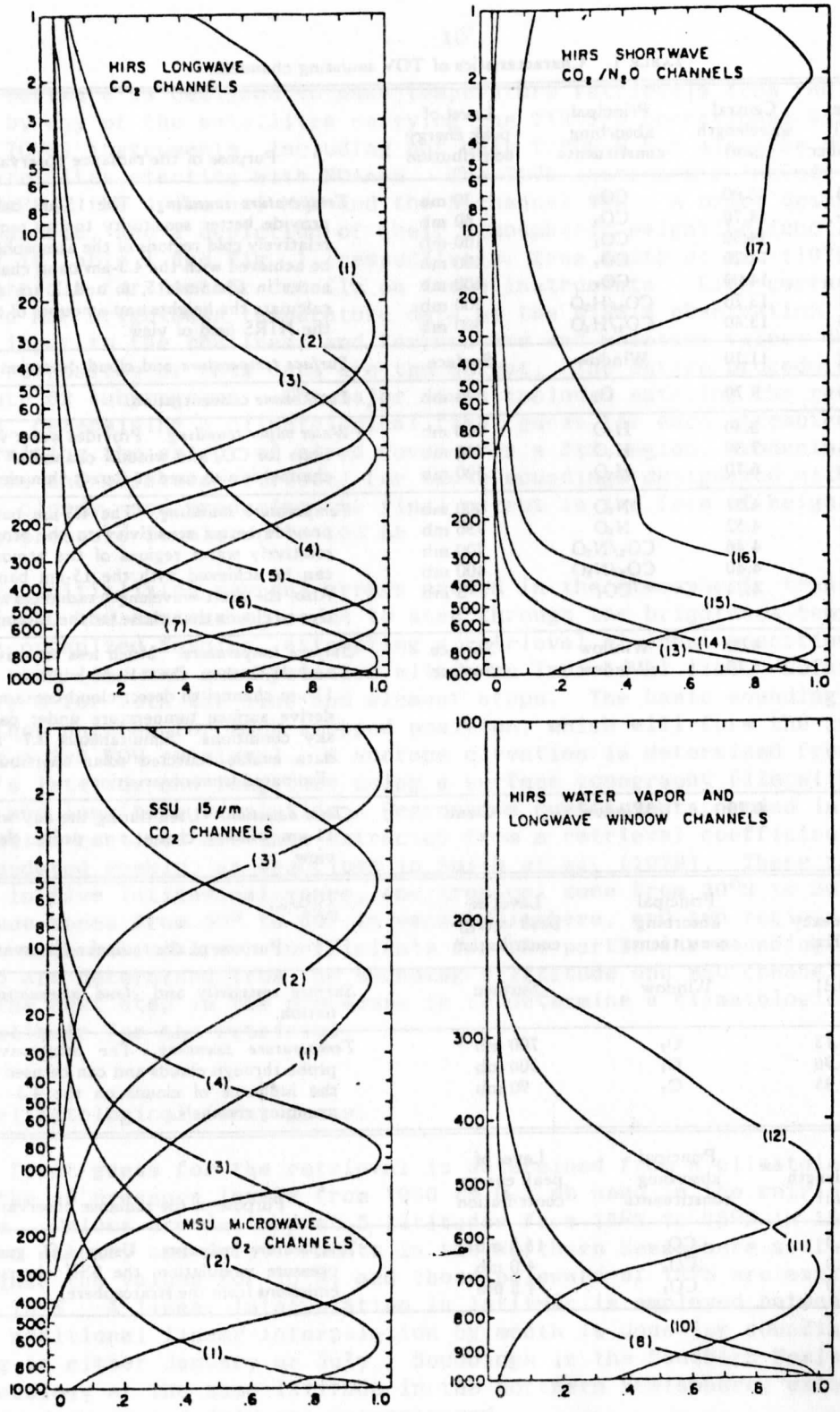

Figure 1. Normalized TOVS weighting functions for the standard atmosphere.

for the retrieval is estimated using the 1000 mb temperature and assuming a standard atmospheric lapse rate of 0.0065°C/m. If the estimated surface pressure is less than 700 mb, no retrieval will be attempted. Finally, mixing ratio values are computed for the levels at or below 100 mb using the temperature and relative humidity information.

The routine then moves on to read the complete HIRS/2 and MSU brightness temperature data sets for the entire 3x3 array, averaging the values for the HIRS/2 Ch. 1, 2, 3 and 17, which peak near the top of the atmosphere. If no data is found for either the HIRS/2 or MSU at the center location, no retrieval is attempted. Some window channel checks are then made before the routine attempts a temperature retrieval using only MSU Ch. 2, 3 and 4.

As indicated in Table 1, there are three HIRS/2 window channels: a longwave IR channel (8) and two shortwave IR channels (18 and 19). A series of three checks are now made to ascertain the effect of cloud contamination at this point in the retrieval. First, Ch. 18 is corrected for possible reflection of solar radiation from the surface. This corrected Ch. 18 value is then compared to the Ch. 8 window, and if they differ by more than 2°C, the sounding is assumed to be affected by clouds. A regression estimate of MSU Ch. 2 is then derived from the regression coefficients discussed earlier and the longwave IR channels (1-12). If the regression estimate is colder than the measured MSU Ch. 2 brightness temperature by some specified limit (also from the coefficient file, but around 2.5°C), clouds are again assumed. A final check is then made to see whether the difference between the corrected Ch. 18 value and the guess surface temperature is greater than 30°C. If not, the sounding is assumed clear and the surface temperature is replaced with the Ch. 18 value. Note that no conventional surface air temperatures are used in this version. Transmittance profiles for the MSU channels are then computed from the climatological temperature and moisture profiles.

B. The microwave-only retrieval.

Before proceeding directly to a more detailed determination of cloud cover, the Export Package routine makes some adjustments to the climatological guess temperature profile by performing one set of iterations using only the three atmospheric microwave channels (2, 3 and 4). This procedure removes much of the overall bias in the guess profile, such as the entire lower troposphere being too warm or too cold. Thus a more accurate temperature estimate can be provided to the cloudiness determination programs. An iterative physical retrieval method is applied in these temperature adjustments.

The iterative retrieval method applied in several steps of the TOVS Export Package is quite similar to the method described in Smith and Woolf (1981). The physical basis for the method comes from the radiative transfer equation (Eq. 1) given below.

$$R(\lambda) = B(\lambda,T_S)\tau_S - \int_o^{p_s} B(\lambda,T) \frac{\partial \tau}{\partial \ln p} \, d \ln p \qquad (1)$$

In this form the radiance at some wavelength λ [$R(\lambda)$] can be subdivided into a contribution radiated by the earth's surface [$B(\lambda,T_s)\tau_s$] and an integral of the Planck radiance emitted by the atmosphere [$B(\lambda,T)$] at some pressure (p) and a weighting function ($\partial\tau/\partial \ln p$) from the top of the atmosphere to the earth's surface. The variable τ is the atmospheric transmittance which defines the fraction of emitted radiation at a given level that arrives at the top of the atmosphere after absorption by the intervening atmosphere. The transmittance profile for a given wavelength varies as a function of temperature and moisture, and the weighting functions at different wavelengths exhibit varying structures for a given atmospheric profile (see for example Fig. 1). After linearization of Eq. 1 about a first guess profile, it can be shown that

$$T_B(\lambda) = \tilde{T}_B(\lambda) + \int_o^{p_s} [T(p) - \tilde{T}(p)]\, \tilde{W}(\lambda,p)\, d \ln p \tag{2}$$

where

$$\tilde{W}(\lambda,p) = \left[\frac{\partial B(\lambda,T)}{\partial T} \Big/ \frac{\partial B(\lambda,\tilde{T}_B)}{\partial T}\right] \frac{\partial \tilde{\tau}(\lambda,p)}{\partial \ln p} \tag{3}$$

and the variables designated with a ~ represent first guess quantities. The inverse problem of finding adjustments to the vertical temperature profile based on observed minus calculated brightness temperatures is solved in the following empirical manner.

$$T_i = \tilde{T}_i + \sum_{n=1}^{N} \tilde{W}^*_{n,i}\, (T_{B_n} - \tilde{T}_{B_n}); \; i = 1, 40 \tag{4}$$

where

$$\tilde{W}^*_{n,i} = \left[\tilde{W}_{n,i} \Big/ \varepsilon_n\right] \Big/ \sum_{n=1}^{N} \left[\tilde{W}_{n,i} \Big/ \varepsilon_n\right] \tag{5}$$

ε is an RMS noise level for a given channel and the subscripts i and n refer to an atmosphere level and a particular wavelength, respectively. A finite difference form of Eq. 1 is then used to compute new values of the brightness temperatures to be used in the next iteration.

For the microwave-only retrieval, up to 10 iterations are allowed, with convergence occuring if the differences between the observed and computed brightness temperatures is less than the specified error level for each of the three channels. Transmittance profiles are only redetermined if the change in computed brightness temperatures changes by more than 3°C from one iteration to the next. No changes are made to the mixing ratio profile. Brightness temperatures for HIRS/2 Ch. 5, 6, 7 13, 14 and 15, and MSU Ch. 2 at the central spot in the 3x3 array are then computed for use in the cloud detection routines that follow.

C. Cloud cover determination and brightness temperature compositing

This is the most involved part of the routine where each location in the 3x3 array is examined for the presence of cloud contamination in the IR channels, an attempt is made to correct for partial cloud cover between pairs of observations, and the observations passing all the requirements are averaged together to produce a single set of brightness temperatures to be used in the final retrieval. As noted earlier, the central point in the array has already been checked for possible cloud contamination at this stage in the routine. If it was determined that the spot was clear, no further cloud determination is performed, and the central location's brightness temperatures are passed to the retrieval step. However, if the location did not pass the preliminary clear checking, the examination of the entire 3x3 array proceeds.

The process begins by rechecking the central location for clouds using an altered set of criteria. As was done earlier, a regression estimate of MSU Ch. 2 is produced from the longwave IR channels, and if the observed MSU Ch. 2 value exceeds it by more than some error limit, the presence of clouds is assumed. Note that if this check caused a clear failure in the previous checks with the central location, it will fail again here, because exactly the same error limits are applied. If it is night, a similar regression check against MSU Ch. 2 is also made using the shortwave IR channels. Finally, a series of three checks between different window channels and the surface temperature estimate are made. First, if the Ch. 19 window is more than 4°C colder than the Ch. 8 window, heavy cloud cover is assumed. If the brightness temperatures for these two channels differs by more than 2°C at night or 10°C during the day, cloud contamination is assumed. Lastly, if the estimated surface temperature exceeds the longwave IR window channel (Ch. 8) by 6°C or less during the day (or 10°C at night), the location is assumed clear.

One last test is then done to the brightness temperatures before the scan spot is declared clear. Differences between the observed brightness temperatures and the brightness temperatures calculated from the updated guess profile are computed for the six selected HIRS/2 channels and MSU Ch. 2. The microwave channel difference is subtracted from the 6 IR differences, and the RMS of the resulting differences computed. If the RMS exceeds 5°C the location is deemed too "noisy" for use in the retrieval. If this final test is passed, the central location is then designated as clear.

Next, the cloudiness in the surrounding 8 HIRS/2 locations is scrutinized in a slightly different manner. Each of the eight points is matched with the

central location in what is called the N^* determination, originally described in Smith (1968) and again in Smith and Woolf (1976). This method uses the differences between the measured MSU Ch. 2 brightness temperature and a regression estimate of that temperature from the HIRS/2 channels as a measure of relative cloud cover between the two locations. A regression estimate in a mostly cloudy region will generally be much colder than the observed MSU value than one in a less cloudy region. A comparison between the differences for the two locations is then used to classify the particular location as clear, partly cloudy, or cloudy. If the point is classified as partly cloudy, the radiances are adjusted to estimate equivalent clear column values using the N^* approach, and these adjusted radiances must pass the same window channel and noise checks described for the central location, with relaxed limits in the comparisons.

Any of the nine locations found to be clear are averaged together, and the retrieval is labeled as clear. If no clear locations are found, successful pairs from the N^* correction are then averaged, and the subsequent retrieval would be termed partly cloudy. If no clear spots or N^* pairs are available, the region is assumed to be cloudy, and no retrieval is attempted.

D. The retrieval of temperature and moisture profiles

The starting point of the retrieval process is the temperature profile derived from the microwave-only retrieval performed earlier. A set of temperature iterations is performed first using HIRS/2 Ch. 2-5 and 13-16, and MSU channels 2-4. The low level longwave channels (6 and 7) are not yet used because they are quite sensitive to the vertical moisture distribution, and no update to the climatological moisture profile has yet been made. Additional channels may also be removed based upon yet another window channel check. If the Ch. 18 value after correction for reflected solar radiation and Ch. 8, the longwave IR window, differ by more than 3°C, a problem with solar reflection in the lowest shortwave sounding channels (13 and 14) is assumed, and these channels are removed from the iteration. The basic procedure is identical to that used in the microwave-only update, with the temperature profile from the latest iteration serving as the guess profile for the next iteration. A maximum of ten iterations is allowed, and transmittances are calculated only at the beginning of the iterations, unless one of the calculated brightness temperatures changes by more than 3°C from one iteration to the next.

A set of four moisture iterations then follows using HIRS/2 Ch. 10, 11 and 12. A finite difference form of Eq. 1 is still used to calculate brightness temperatures, but the form of the updates for specific humidity (q) is slightly different than that presented in Eq. 4 and 5 for the temperature iteration.

$$(q/\tilde{q})_i = \sum_{n=1}^{N} \tilde{M}^*_{n,i}\, \tilde{r}_n;\ i = 1,\ 20 \qquad (6)$$

where

$$\tilde{r}_n = \exp\left[(T_{B_n} - \tilde{T}_{B_n}) \Big/ \sum_{n=1}^{20} \tilde{M}_{n,i} \right] \tag{7}$$

$$\tilde{M}_{n,i} = \tilde{\tau}_{n,i} \ln \tilde{\tau}_{n,i} \left[\frac{\partial B(\lambda,\tilde{T}_i)}{\partial T} \Big/ \frac{\partial B(\lambda,\tilde{T}_{B_n})}{\partial T} \right] \frac{(T_{i+1} - T_{i-1})}{2\varepsilon_n} \tag{8}$$

In this case, transmittance profiles are computed for each channel at every iteration because this is the only way to change the calculated brightness temperatures.

Another set of up to 10 temperature iterations follows, with HIRS/2 Ch. 6 and 7 added to the retrieval, and MSU Ch. 2 removed, followed by a maximum of 8 moisture iterations. If any of the mandatory levels in the final retrieval differs from the climatological first guess by more than 10°C, the retrieval is processed no further. The temperature profile is then checked for superadiabatic layers, and mandatory level heights and layer precipitable water values are computed for output.

In summary, the version of the TOVS Export Package provided by the NESDIS Development Laboratory in November, 1981 uses limb-corrected HIRS/2 and MSU brightness temperatures at the HIRS/2 scan locations as input. Each 3x3 array in the data set is carefully tested for the presence of cloud contamination in the IR channels, and an effort is made to correct the HIRS/2 channels in regions of partial cloud cover. These clear or partly cloudy brightness temperatures are then used to update a climatological first guess using the iterative physical method introduced in Smith (1970). No retrieval is attempted in regions of total cloud cover, and no surface temperature data from conventional measurements is included in the retrieval process.

3. The Modified Versions of the Retrieval Software

As noted briefly in the introduction, our research studies required a much more flexible software package. For example, brightness temperatures from the operational resolution 9x7 arrays were available on the NESS archive tapes, along with the operational statistical retrievals, and we wanted to apply the iterative retrieval technique to these brightness temperatures using not only the climatological first guess available in the Export Package, but also using the statistical retrieval as a first guess. In other studies, the 3x3 compositing of the HIRS/2 resolution radiances was needed, but again using a statistical guess in place of the climatological guess provided in the original software. Since the retrieval and compositing features of the TOVS Export Package were intertwined, these steps were separated in the modified version, to accomodate brightness temperature input from alternative sources. Since the original subroutines also included several options that would never be invoked

in our studies, considerable streamlining of all the subroutines was performed to reduce the expense of operating the software. The integrity of the original method was, however, preserved in the modifications. Thus, much of the detailed discussion of the Export Package's features will also apply to the modified versions, and the streamlining has little effect on the final product. Therefore, the descriptions of the modified software that follow will concentrate on the substantial changes made to the routines. The modified retrieval package will be presented first, since it was applied in both of the primary studies presented in this report (Koehler et al., 1986, and Seman et al. 1986). The modified cloud detection and data compositing used in Seman et al. (1986) will then follow.

A. The modified temperature and moisture retrieval technique

The major additions made to this routine are the ability to make cloudy path retrievals and some new choices for a first guess profile. Input variables for each vertical profile to be processed include the location's latitude and longitude, the HIRS/2 and MSU brightness temperatures, the type of sounding to produce (clear, partly cloudy or cloudy), and a statistically derived temperature profile at the 40 pressure levels from 1000 to 0.1 mb at which the retrieval is made.

Three first guess options are now available. The first is the zonal climatology provided in the original Export Package. The second is a more detailed climatology available at 5° latitude-longitude intersections for each month of the year taken from Crutcher and Meserve (1970) and is called the regional climatology. The third option is the statistical retrieval provided in the input data.

The regional climatology includes 1000 mb heights, temperatures from 1000 to 0.1 mb at the 40 satellite sounding levels, and relative humidities at the 20 tropospheric levels below 100 mb. The original data from Crutcher and Meserve was available only at mandatory levels in the troposphere. Data at higher levels came either from the monthly zonally averaged statistics of Oort and Rasmusson (1971), or at very high levels, from the zonal climatology of the Export Package. Appropriate interpolations were made to the satellite sounding levels in developing the guess files accessed by the software. Guess values for a particular sounding location are interpolated bilinearly from the four surrounding 5° latitude-longitude intersections.

The statistical guess option is provided external to the retrieval program from one of two sources. For most of the operational resolution (9x7) soundings, the values were interpolated from the layer mean temperatures reported in the NESS retrieval archive tapes. For the 3x3 resolution soundings, the temperatures were derived from brightness temperatures via linear regression. In both cases, the temperature data was supplemented with 1000 mb height and tropospheric moisture information from the regional climatology.

The surface pressure and temperature estimates for the retrieval were determined in a slightly different manner than in the export package. Instead of extrapolating either upward or downward from 1000 mb based on a comparison

of the surface elevation and the 1000 mb height as done in the Export Package, heights for the sounding levels were computed hypsometrically from the 1000 mb height and the guess temperature profile, and the surface pressure interpolated between the two height levels surrounding the surface elevation. If the surface elevation was less than the 1000 mb height, an extrapolation downward was made using the lapse rate in the layer above 1000 mb.

The retrieval process itself has been consolidated into one routine involving three passes. The first pass replaces the microwave only pass in the Export Package and differs only by using HIRS/2 Ch. 1, 2 and 3 from the stratosphere in addition to the MSU channels. These are the same channels used in the cloudy path statistical retrievals. If the sounding type is cloudy, the retrieval stops here. If not, the mixing ratios are recomputed using the guess relative humidities and the updated temperature profile, to provide a slightly better estimate of the moisture distribution, something not done in the Export Package. The remaining two passes involve first a set of temperature iterations, followed by a set of moisture iterations in exactly the same arrangement as in the Export Package. Some details have been changed. A window check is done again to detect possible problems in the solar reflection correction, but some of the criteria are changed. In the temperature iterations, HIRS/2 Ch. 1 is now included, but Ch. 16 removed. Also, the surface air temperature is changed in the iterative process.

Other more substantial changes have been made in the moisture iterations. First, the exponent in the r factor in Eq. 7 is only allowed to vary between plus or minus one, keeping the moisture retrieval more stable. Also, the moisture channel transmittances and brightness temperatures are computed at the end of an iteration before the check for convergence, instead of at the beginning of the next iteration as done in the Export Package.

B. The modified cloud detection and data compositing procedure

The techniques for detecting the presence of cloud in a 3x3 region and combining the brightness temperature data over that region underwent considerable change, although the basic principles of identifying cloudy FOV in the Export Package were not affected. The statistical retrieval method was incorporated into this procedure to provide a reasonably accurate guess for the cloud cover determination and to determine a statistical guess profile that could be used in the modified retrieval software.

The guess profile for the cloud detection profile is determined from a cloudy path statistical retrieval using HIRS/2 channels 1, 2 and 3, and the MSU channels which have been averaged over all available spots in the 3x3 area. The guess moisture profile comes from the regional climatology presented earlier, as is an estimate of the surface pressure. Guess brightness temperatures for these temperature and moisture profiles are then computed for use in the cloud contamination checking procedures.

The next major change in the procedure is that the method for determining whether the central location was clear is now used at all available points in the 3x3 array. This method included regression estimates of the MSU Ch. 2 from

the IR observations, various checks of the window channel information, and the extent of noise in the low level IR channels. Some changes were made, such as including a measure of cold bias in the IR noise check, and removing the window check against the estimated surface temperature. If no clear locations are found, N^* processing then proceeds in exactly the same manner as before. If no successful clear-column corrections for partly cloudy solutions can be derived, the area is designated cloudy. For clear and partly cloudy solutions, brightness temperatures, latitudes, and longitudes for the fields-of-view passing the appropriate tests are averaged together to provide the resultant information for that array. A statistical retrieval using the complete set of brightness temperatures is then computed to provide input into the retrieval routines. For a cloudy solution, only the previously averaged HIRS/2 channels 1, 2 and 3 and the MSU channels are reported, along with the cloudy path statistical retrieval produced earlier in the routine.

In summary, two modules were developed for our alternative retrieval method studies, both of which originated from the TOVS Export Package. One module performs cloud detection and satellite data compositing over 3x3 arrays of HIRS/2 locations, producing both the average brightness temperatures for the different sounding channels, and a statistical first guess profile for use in the retrieval module. The second module takes the brightness temperature information from either the first module for 3x3 resolution data or from the NESS retrieval archive tapes for 9x7 resolution, and produces iterative, physical retrievals using a first guess based on a zonal climatology, a regional climatology, or a statistically derived sounding.

4. Acknowledgements

We would like to sincerely thank those who assisted in many ways to the development of the modifications to this retrieval software. Dr. John Derber helped considerably in the initial installation of the McIDAS version of the TOVS Export Package on the Univac 1100 computer, and in the documentation of that software, a crucial step in understanding how the routines worked before modifications could be made. Mr. Hal Woolf and Dr. Christopher Hayden of the NESDIS Development Laboratory were quite helpful in answering our many questions regarding their software during its modification. Also, Dr. Robert Gallimore and Dr. Bette Otto-Bliesner were quite helpful in providing the data for the regional climatology.

5. References

Crutcher, H.R. and J.M. Meserve, 1970: Selected heights, temperatures, and dew points for the Northern Hemisphere. NAVAIR 50-1C-52, revised Chief Nav. Op., Washington, D.C.

Koehler, T.L., J.P. Nelson and L.H. Horn, 1986: An evaluation of a physical retrieval method as an alternative to the statistical method used in the NESS operational sounding processing during FGGE. Evaluation of Alternative Retrieval Methods for TIROS-N and NOAA-6 Soundings. Final Report, NOAA Grant NA81AA-D-00087, Dept. of Meteorology, University of Wisconsin-Madison, 26-46.

Oort, A.H. and E.M. Rasmusson, 1971: Atmospheric circulation statistics. NOAA Professional Paper 5, NOAA, Rockville, MD.

Seman, C.J., L.H. Horn and T.L. Koehler, 1986: An evaluation of different horizontal resolution in radiance compositing for TIROS-N retrievals. Evaluation of Alternative Retrieval Methods for TIROS-N and NOAA-6 Soundings. Final Report, NOAA Grant NA81AA-D-00087, Dept. of Meteorology, University of Wisconsin-Madison, 47-64.

Smith, W.L., 1968: An improved method for calculating tropospheric temperature and moisture from satellite radiometer measurements. Mon. Wea. Rev., 96, 387-396.

Smith, W.L., 1970: Iterative solution of the radiative transfer equation for the temperature and absorbing gas profile of an atmosphere. Applied Optics, 9, 1993-1999.

Smith, W.L. and H.M. Woolf, 1976: The use of eigenvectors of statistical covariance matrices for interpreting satellite sounding radiometer observations. J. Atmos. Sci., 33, 1127-1140.

Smith, W.L. and H.M. Woolf, 1981: Algorithms used to retrieve surface skin temperature and vertical temperature and moisture profiles from VISSR Atmospheric Sounder (VAS) radiance observations. Fourth Conference on Atmospheric Radiation, June 15-18, 1981, Toronto, Ont., Canada. Published by the AMS, Boston, MA.

Smith, W.L., H.M. Woolf, C.M. Hayden, A.J. Schreiner and J.M. LeMarshall, 1983: The physical retrieval TOVS Export Package. Presented at the First International TOVS Study Conference, Igls, Austria, August 29 - September 2, 1983.

Smith, W.L., H.M. Woolf, C.M. Hayden, D.Q. Wark and L.M. McMillin, 1979: The TIROS-N operational vertical sounder. Bull. Amer. Meteor. Soc., 60, 1177-1187.

HIGH QUALITY RADIOSONDE-DERIVED TEMPERATURE AND THICKNESS DATA FOR ALTERNATIVE SATELLITE RETRIEVAL STUDIES

by

Thomas L. Koehler

Abstract

Methods employed to determine the conventional radiosonde values colocated to the satellite soundings used in the papers in this project report are described. The original radiosonde profiles are carefully checked, and a special effort is made to produce the raob verification data at the levels used in the satellite retrieval methods.

1. Introduction

An important component in the verification of satellite-derived data sets is a high quality conventional data set that provides a standard of comparison. One of the more common comparisons made is a direct comparison between a satellite temperature profile and a radiosonde profile taken near the satellite sounding within a specified time interval. In the research presented in this project report, a more sophisticated colocation technique is used. First, a series of objective analyses at the synoptic times from radiosonde observations is performed, followed by both spatial and temporal interpolations to the locations and times of the satellite sounding observations. Careful attention is paid to editing the radiosonde data and to supplementing missing data when possible. Both level temperatures and layer mean temperatures for a standard set of NESS sounding retrieval layers are produced for a particular satellite sounding location.

This paper describes the procedures used to determine the radiosonde-based data sets used in several of the other studies presented in this report. The editing and preparation of the basic radiosonde data is described first, followed by an overview of the objective analysis routine. Finally, a description of the spatial and temporal interpolations is provided.

2. Basic Radiosonde Data Handling

The studies presented in this report were performed during only two periods, one in early January, 1980, and the other in mid April, 1979. The raob data for both periods included both mandatory and significant pressure level temperature and dewpoint information. The January soundings were extrac-

ted from the NMC PE model archive tapes, while the April data were taken from the data archive kept at University of Wisconsin-Madison for the McIDAS system. Normal checking procedures, which include checks for superadiabatic lapse rates and anomalous vertical moisture gradients, were applied to both data sets. Efforts were made to supplement this data with the original upper air teletype messages, including late reports, whenever possible.

The next step in the procedure was to interpolate the temperature values to the 21 pressure levels between 1000 and 100 mb inclusive used in the satellite retrieval algorithms (1000, 950, 920, 850, 780, 700, 670, 620, 570, 500, 470, 435, 400, 350, 300, 250, 200, 150, 135, 115 and 100 mb), followed by an integration to determine the layer mean virtual temperature in the corresponding 20 satellite layers. Soundings with surface pressures less than 1000 mb are extrapolated downward to 1000 mb using the approach applied in Koehler (1979), and 1000 mb heights are computed using the observed surface temperature, instead of an average over the last 24 hours. Heights of the 300 mb isobaric surface were then computed from the 1000 mb height and layer mean temperature information, and hand analyses of these 300 mb heights were constructed to identify poor soundings.

3. The Objective Analysis

Grid point analyses of the level temperature, layer mean temperature and 1000 mb height fields are constructed using an optimum interpolation method described in Koehler (1979). The eight closest observations to a particular grid point are used in the univariate analysis, with the same set of weights being applied at every level for each parameter. First guess fields for the analyses are derived from one of two sources: NMC's LFM analyses for the January period, and NMC's Final Cycle (OI) analyses for the April period. In both cases, the first guess is derived using data valid at the same time as the verification analyses being produced, and the original LFM or OI data sets must be modified to produce the appropriate first guess fields.

Fewer operations are needed to produce the first guess fields from the LFM analyses compared to that from the OI. Since the final verification analyses are performed on the LFM grid, no grid-to-grid interpolation in the horizontal is necessary. Also, both height and temperature data at mandatory levels are available. Thus, vertical interpolations to the satellite sounding levels must be made. The vertical interpolations for temperatures are made linearly in ln p, while height interpolations are made using overlapping quadratic polynomials. The first guess virtual temperatures are then computed from the isobaric height values using the hypsometric equation.

The determination of the OI first guess fields is more complicated because less information is available from the archive tapes. First, values are available from a subset of the coarse resolution PE grid, making a grid-to-grid interpolation to the LFM grid necessary. Also, only mandatory level height data are available, which are interpolated vertically to intermediate satellite sounding levels in the same manner as the LFM guess. However, the guess for the level temperatures must be estimated from a linear ln p interpolation of the layer mean temperature values. While the vertical interpolations used in

both the LFM and OI processing are known to produce errors, these fields only serve as first guess values which will be updated using the raob data.

For the analysis at a specified time, those radiosonde observations designated as poor in the editing procedure are not included in the determination of the analysis weights. Incomplete raob reports were included in the weight determination, but a zero deviations from the first guess were entered at upper levels not included in the incomplete reports. In any event, a radiosonde ascent had to reach at least 700 mb to be included in the analysis.

As in most objective analysis schemes, the first guess value at a grid point is modified using the weighted deviations of the raob data from the guess values. The analysis is then filtered using a smoother-desmoother, that removes some of the small scale noise generated in the interpolation.

4. Spatial and Temporal Interpolations to the Satellite Observation Locations

One of the last steps in producing a raob value at a particular satellite sounding location and time is the interpolation of the synoptic raob analyses in space and time. Both operations involve overlapping quadratic polynomial interpolations.

First, the spatial interpolation in the horizontal is performed at the four synoptic time periods centered on the satellite observation, using overlapping quadratics as first decribed by Bleck and Haagenson (1968), and more recently by Koehler (1977). These four values are then interpolated to the time of the satellite sounding observation, producing the final colocated value.

5. Grid Point Interpolations of Satellite-minus-Raob Differences

One other type of interpolation is made in the research studies presented in this project that does not involve only raob verification data: the interpolation of the satellite-minus-raob colocation differences to a uniform grid for contour analysis purposes. In this case, a form of optimum interpolation with normalized weights is performed, as described in Koehler (1981). The advantage of using this type of optimum interpolation is that no first guess is required for the analysis.

6. Summary

The procedures used to colocate the conventional raob observations to the locations and times of satellite soundings has been described. The specifications of the types of data transferred is unique to the particular needs of our research studies. For example, all of the variables were determined at the pressure levels used in the satellite retrieval methods. Thus, full use was made of the typically fine vertical resolution in the radiosonde reports. The layer mean temperature values are used as the basic verification values in Koehler et al. (1986) and Seman et al. (1986), while the level temperatures

were applied in the MSU brightness temperature simulations in Koehler (1986).

7. Acknowledgements

I want to thank two persons who aided considerably in the original data processing for the LFM tapes from the January, 1980 period. First, Dr. Christopher Hayden made a special effort to save the LFM and PE archive tapes from NMC. Without his help, these data tapes would have been recycled 30 days after they were generated. Also, thanks are due Dr. John Derber for the original transfer of the LFM analysis data from the LFM archive tapes.

8. References

Bleck, R. and P.L. Haagenson, 1968: Objective analysis on isentropic surfaces. NCAR Technical Notes, NCAR-TN-39, Boulder, CO, 27 pp.

Koehler, T.L., 1977: A test of seven methods which perform grid to observation interpolations. Meteorological Applications of Satellite Indirect Soundings II, Project Report, NOAA Grant 04-4-158-2, Dept. of Meteorology, University of Wisconsin-Madison, 55-65.

Koehler, T.L., 1979: A case study of height and temperature analyses derived from Nimbus-6 satellite soundings on a fine mesh model grid. Ph.D. Thesis, University of Wisconsin-Madison, 186 pp.

Koehler, T.L., 1981: Satellite sounding to grid interpolation tests. Case Studies Employing Satellite Indirect Soundings, Final Report, NOAA Grant 04-4-158-2, Dept. of Meteorology, University of Wisconsin-Madison, 57-81.

Koehler, T.L., 1986: An examination of scan angle dependence in limb-corrected MSU brightness temperatures from TIROS-N. Evaluation of Alternative Retrieval Methods for TIROS-N and NOAA-6 Soundings. Final Report, NOAA Grant NA81AA-D-00087, Dept. of Meteorology, University of Wisconsin-Madison, 65-93.

Koehler, T.L., J.P. Nelson and L.H. Horn, 1986: An evaluation of a physical retrieval method as an alternative to the statistical method used in the NESS operational sounding processing during FGGE. Evaluation of Alternative Retrieval Methods for TIROS-N and NOAA-6 Soundings. Final Report, NOAA Grant NA81AA-D-00087, Dept. of Meteorology, University of Wisconsin-Madison, 26-46.

Seman, C.J., L.H. Horn and T.L. Koehler, 1986: An evaluation of different horizontal resolution in radiance compositing for TIROS-N retrievals. Evaluation of Alternative Retrieval Methods for TIROS-N and NOAA-6 Soundings. Final Report, NOAA Grant NA81AA-D-00087, Dept. of Meteorology, University of Wisconsin-Madison, 47-64.

AN EVALUATION OF A PHYSICAL RETRIEVAL METHOD AS AN ALTERNATIVE TO THE STATISTICAL METHOD USED IN THE NESS OPERATIONAL SOUNDING PROCESSING DURING FGGE

by

Thomas L. Koehler, James P. Nelson III and Lyle H. Horn

Abstract

A physical iterative retrieval method is used in an attempt to improve the FGGE year operational soundings. The method is tested using periods from January 1980 and April 1979. Three retrieval first guesses are employed: two are climatological while the third is derived directly from the NESS operational FGGE soundings.

The physical method is evaluated using colocation statistics and 700-300 mb thickness temperature difference maps. The colocation statistics indicate that the substantial corrections are made to the climatological first guesses during the retrieval procedure, but only minor corrections are evident for the operational sounding guess. The 700-300 mb thickness difference charts reveal that troughs are too warm and ridges too cold, thus reducing the thickness gradients and indicating that the satellite sounding errors are correlated to the synoptic pattern. In general, the physical iterative retrieval method tested here does not provide any significant improvement over the FGGE operational soundings.

1. Introduction

A major problem facing the meteorological community has been the lack of upper air data over remote land and oceanic regions of the earth. With the advent of the meteorological satellite came the ability to sense the atmosphere in these data-poor regions. During the First GARP Global Experiment (FGGE), conducted from 1 December 1978 to 30 November 1979, satellite soundings made by TIROS-N and NOAA-6 were a vital component of the observing system.

The FGGE soundings were derived in an operational manner by NESS using an algorithm described in Smith et al. (1979), which was outlined in the preface to this report. The final temperature soundings are estimated from the radiance information in a statistical manner. These soundings have been evaluated in several studies, such as Phillips et al. (1979), Schlatter (1981) and Gruber and Watkins (1982). In a recent study, Koehler et al. (1983) examined the performances of both TIROS-N and NOAA-6 soundings over the United States for a

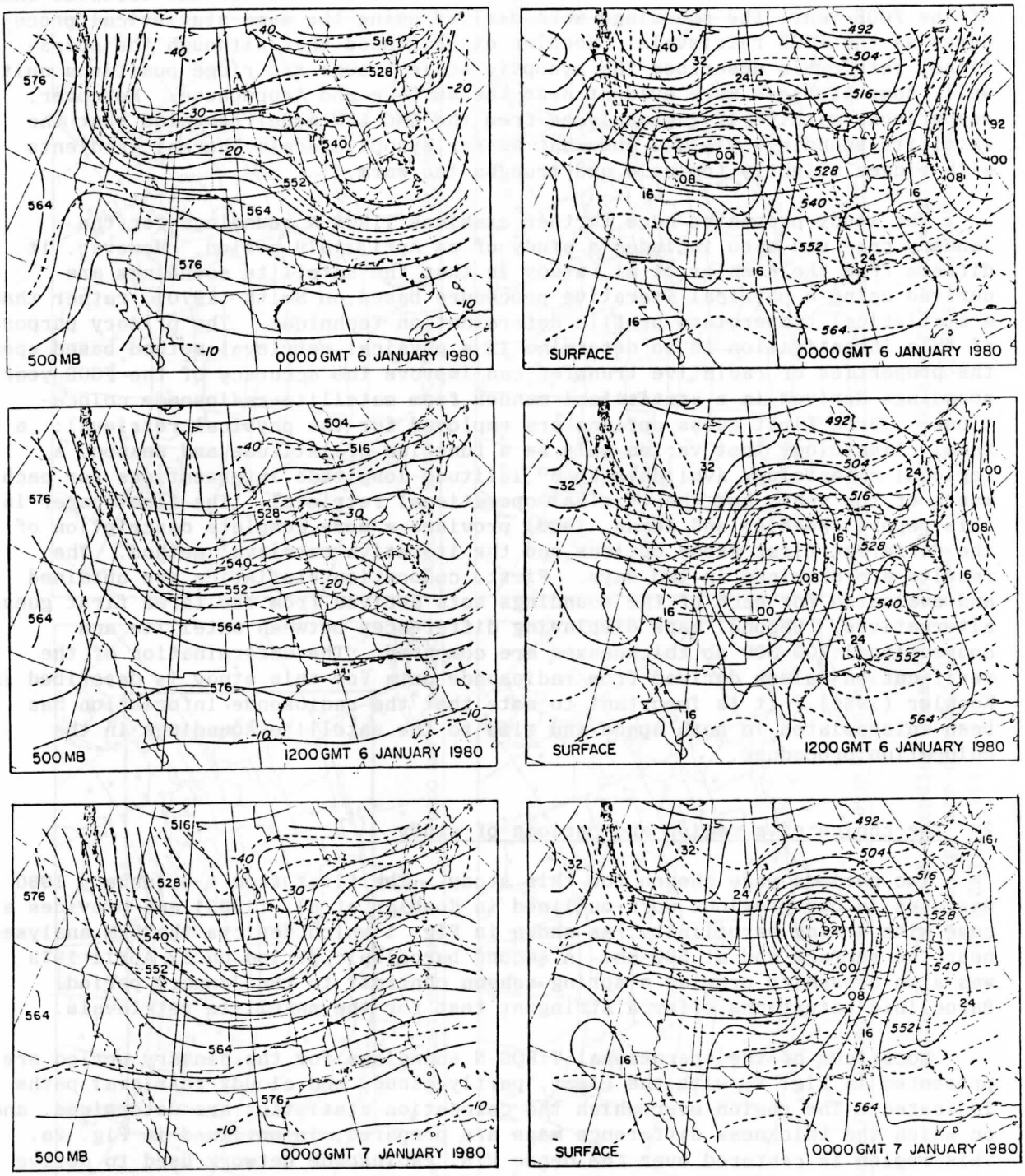

Figure 1. LFM 500 mb height (solid) and isotherm (dashed) analyses (left), and sea level pressure (solid) and 1000-500 mb thickness (dashed) analyses (right) for 0000 GMT 6 January through 0000 GMT 7 January 1980.

period in early January 1980. Although this period was after the official end of the FGGE year, the soundings were derived using the same statistical procedures as the FGGE retrievals. Koehler et al. found that although the operational retrievals described the synoptic scale trough and ridge positions quite well, some problems were evident near the surface and tropopause. Moreover, comparisons with verifying analyses from the NMC LFM model revealed that the satellite soundings yielded somewhat weaker synoptic scale thermal gradients with ridges slightly too cold and troughs too warm.

The study presented here further examines TIROS-N soundings for the January case and also includes a study of an April 1979 period. However, it differs from the Koehler et al. study in that the satellite soundings are derived using a physical iterative procedure based on Smith (1970), rather than a statistical temperature profile determination technique. The primary purpose of this investigation is to determine if a physical retrieval method based upon the properties of radiative transfer can improve the accuracy of the FGGE year soundings derived in a statistical manner from satellite-radiosonde colocations. Three first guess options are employed for the physical retrieval: a zonal climatology that varies only as a function of latitude and season, a regional climatology available at 5^{o} latitude-longitude intersections for each month of the year, and the original operational retrieval. The first paper in this report (Koehler and Seman, 1986) provides a more complete description of the different first guess options and the iterative retrieval method. The results are examined in two ways. First, colocation statistics are obtained and evaluated for each of the soundings sets derived from the three first guess alternatives. Second, maps displaying differences between satellite and conventional 700-300 mb thicknesses are compared. The determination of the verification values derived from radiosonde data for this study is described in Koehler (1986). It is important to note that the radiosonde information has been interpolated in both space and time to the satellite soundings in the colocation procedure.

2. The choice of a region and periods of study

Two periods were chosen for this study. The first from 5-6 January 1980 was used in our previous work outlined in Koehler et al. (1983) and provides a case with strong baroclinity, as shown in Fig. 1 which depicts the LFM analyses near the surface and at 500 mb. A second baroclinic period on 12 April 1979 was also chosen to provide a spring season contrast to the January period. Baroclinic situations offer a stringent test for the satellite retrievals.

Locations of the operational TIROS-N soundings for the January period are presented in Fig. 2, with the clear, partly cloudy and cloudy retrieval paths indicated. The region over which the colocation statistics are determined, and on which the thickness difference maps are prepared, is outlined in Fig. 2a. This region is centered over the dense U.S. radiosonde network used to derive the verification information. Soundings from three passes were needed to cover the region. Thus, the satellite data are asynoptic in nature, with soundings on the east coast occuring over three hours before those on the west coast, but generally centered on roughly 0900 GMT and 2100 GMT, as indicated in the figure. Soundings outside the region of interest are not included in the

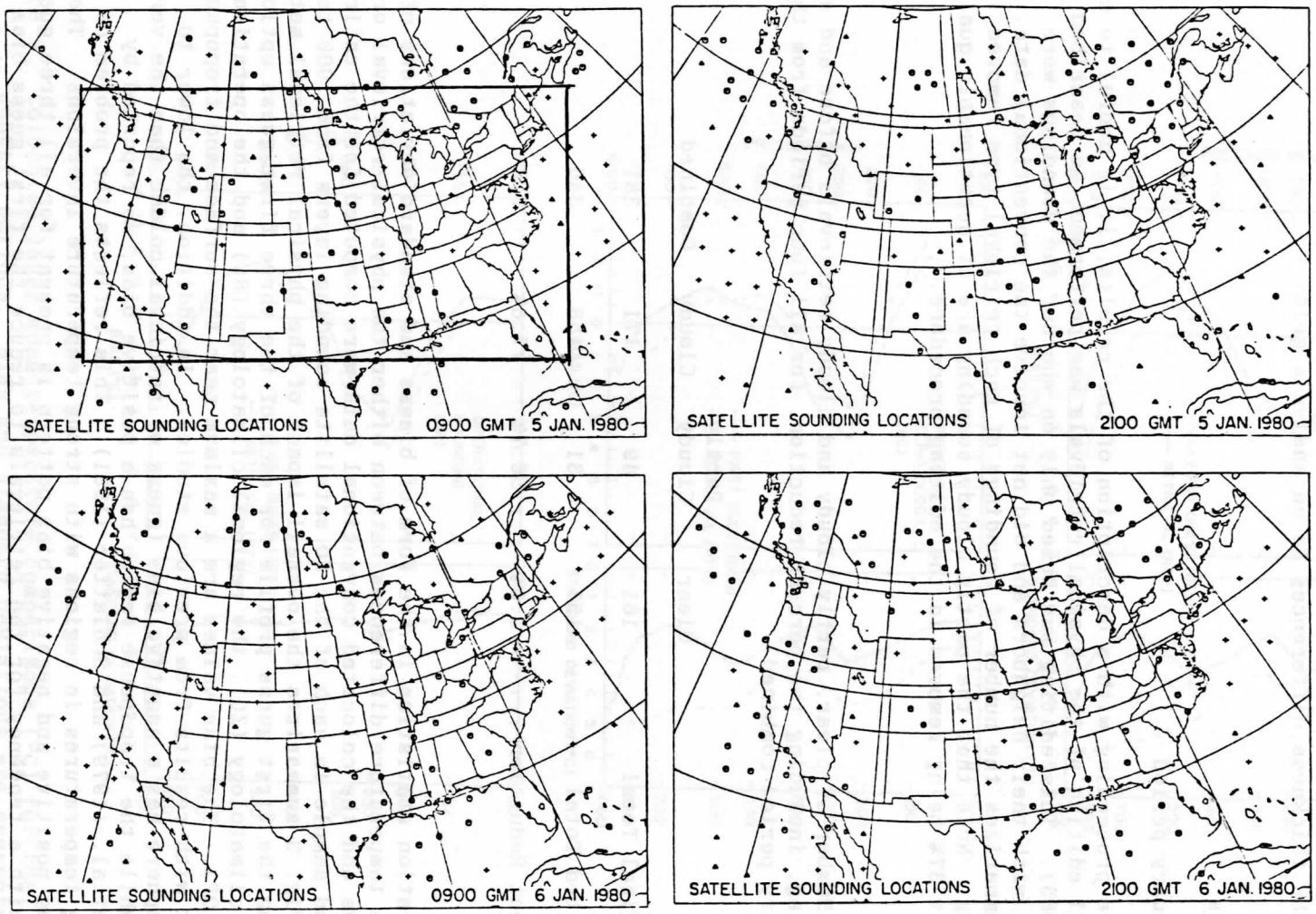

Figure 2. TIROS-N sounding locations for the four January periods studied. Soundings are divided into clear (o), partly cloudy (Δ) and cloudy (+) categories.

statistical evaluations that follow, but were used in the horizontal interpolations of the thickness differences to an analysis grid.

3. Results

A. The January period

Before proceeding with a description of the results, it is useful to note that manual editing of the physical retrievals was performed, as described in Nelson (1983). This editing was based only on whether the soundings were consistent with their neighbors and did not involve the conventional data. Table 1 summarizes the number of soundings of each retrieval type removed in the editing. Note that the partly cloudy sounding are of questionable quality with almost 37% being removed in the editing procedure.

Table 1. Number of clear, partly cloudy and cloudy retrievals before and after editing, including the percent reduction, for all four periods from the January period combined.

	Clear	Partly Cloudy	Cloudy	Combined
Original Total	161	49	171	381
Edited Total	157	31	158	346
Percent Reduction	2.5%	36.7%	7.6%	9.2%

Colocation statistics in the form of biases and standard deviations of layer mean temperature differences between either the physical retrieval or its first guess and the colocated conventional data were computed for the entire four period sample in each of the 20 satellite sounding layers from 1000 to 100 mb. Fig. 3 summarizes the overall impact of the physical retrieval method on changing the first guess profile for each of the three first guess options: the zonal climatology (ZC), the regional climatology (RC) and the operational sounding (OP). The bias values are a maximum near the surface and tropopause, consistent with results from previous studies. In addition, the lower to mid-troposphere has a negative bias (guess or retrieval colder than the verification), while the tropopause region has a positive bias, as reported by Phillips et al. (1979) and Schlatter (1981). This reflects the problem of retrieving temperatures in regions with strong temperature inversions. The alternating positive and negative bias pattern is present for all three guess options, with a tendency for the retrievals to reduce the first guess bias in one layer, while increasing it in another. For example, the large positive bias near the surface in the ZC guess is reduced in the retrieval, while the small negative bias in the mid-troposphere is increased. Thus, there is a tendency for the physical retrieval process to improve one layer at the expense

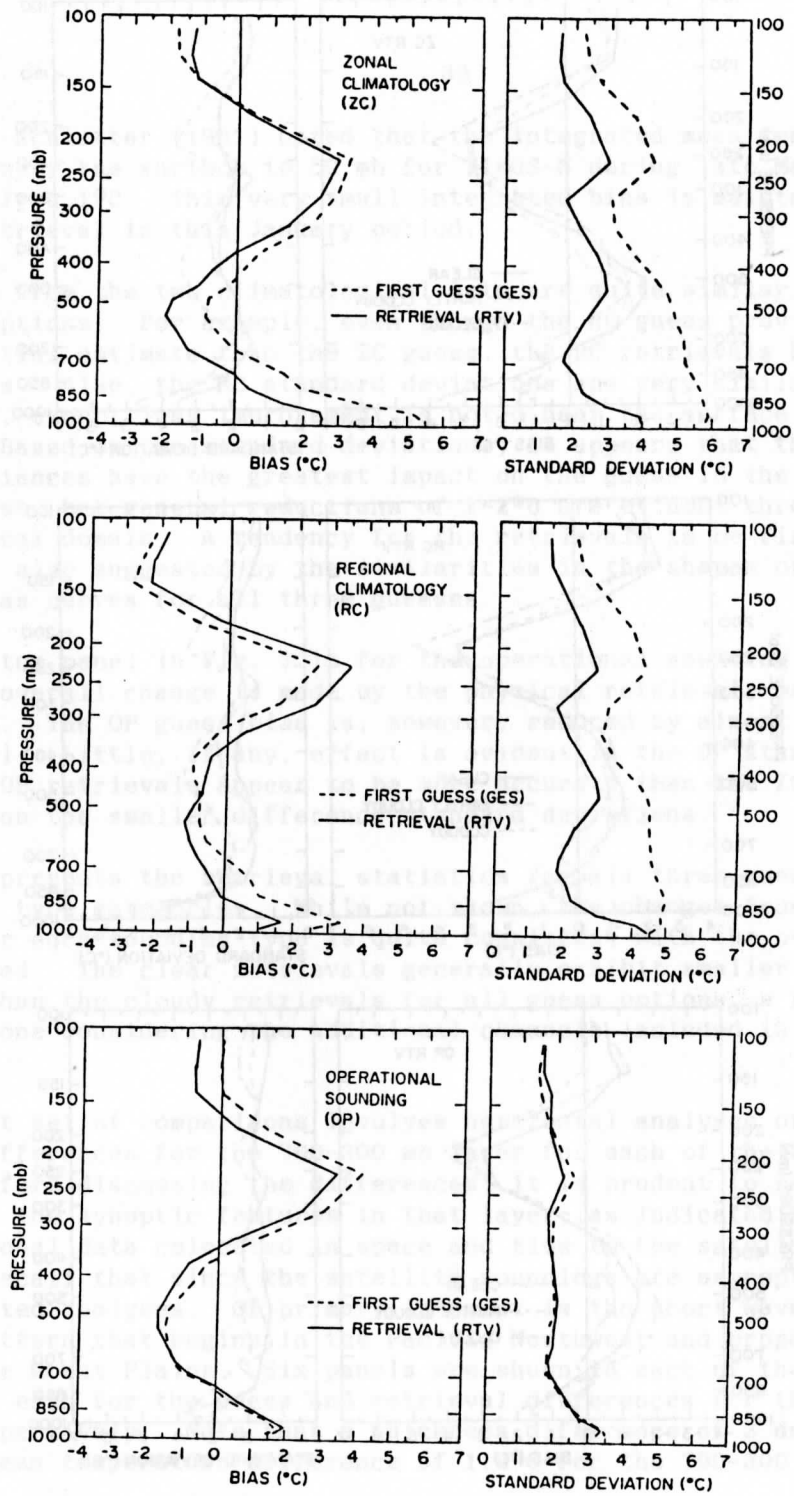

Figure 3. Colocated layer mean temperature comparisons (^{o}C) for the January periods. Bias and standard deviations are presented for both the guess (dashed) and retrieval (solid) differences.

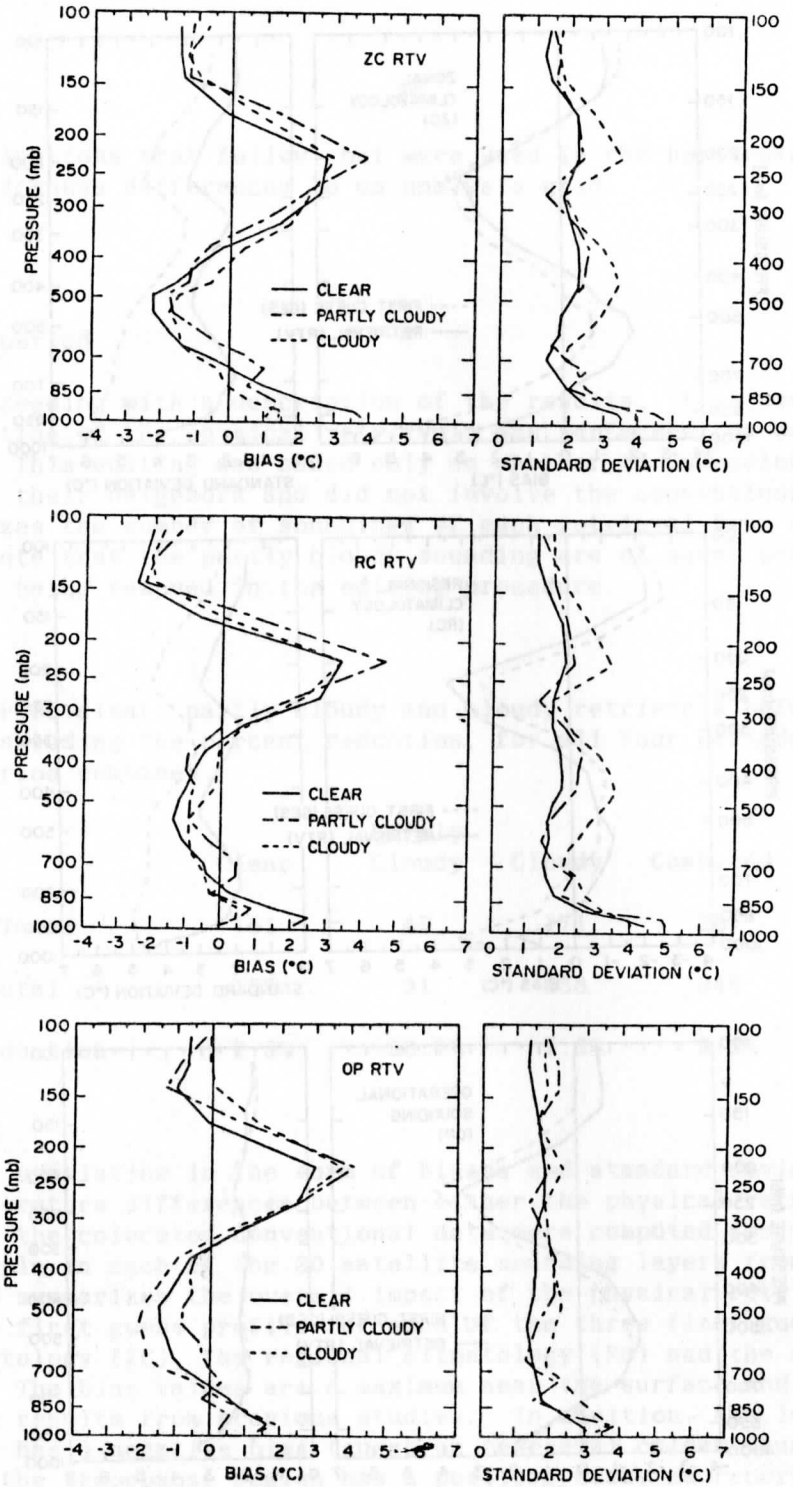

Figure 4. Colocation statistics for the January period except differentiating between sounding type for the retrieval.

of another. Schlatter (1981) noted that the integrated mean temperature error (bias) from near the surface to 50 mb for TIROS-N during late March and early April was only 0.1°C. This very small integrated bias is maintained by the iterative retrieval in this January period.

Results from the two climatological sets are quite similar, with some notable exceptions. For example, even though the RC guess provides a more accurate initial estimate than the ZC guess, the RC retrievals have a larger positive bias. Also, the RC standard deviations are very similar to their ZC counterparts, except less improvement is noted near the surface in the RC retrieval. Based on the standard deviations, it appears that the satellite-measured radiances have the greatest impact on the guess in the layer between 850 and 500 mb, but general reductions of 1-2°C are evident throughout the entire vertical domain. A tendency for the retrievals to be first guess dependent is also suggested by the similarities in the shapes of the guess and retrieval bias curves for all three guesses.

The bottom panel in Fig. 3 is for the operational sounding guess. Note that little overall change is made by the physical retrieval, particularly below 500 mb. The OP guess bias is, however, reduced by almost 0.5°C during the retrieval. Little, if any, effect is evident in the OP standard deviations. The OP retrievals appear to be more accurate than the ZC and RC retrievals, based on the smaller difference standard deviations.

Fig. 4 presents the retrieval statistics for all three guesses broken down in retrieval type categories. While not shown, the changes from guess to retrieval for each sounding type is quite consistent with the overall changes just discussed. The clear retrievals generally exhibit smaller standard deviations than the cloudy retrievals for all guess options, a fact that should surprise no one considering the additional channels included in the clear retrievals.

The next set of comparisons involves horizontal analyses of the colocated thickness differences for the 700-300 mb layer for each of the four January periods. Before discussing the differences, it is prudent to review the time evolution of the synoptic features in that layer, as indicated by analyses of the conventional data colocated in space and time to the satellite locations (Fig. 5). Recall that since the satellite soundings are asynoptic, so too are these colocated analyses. Of primary interest is the short wave trough in the thickness pattern that begins in the Pacific Northwest and propagates southeastward into the Great Plains. Six panels are shown in each of the following figures, one each for the guess and retrieval differences for the ZC, RC and OP guesses, respectively. Note that a thickness difference of 3 dam corresponds to a layer mean temperature difference of 1.2°C for the 700-300 mb layer.

The analyses in Fig. 6 illustrate several of the important features in the entire sequence of Figs. 6-9. The trough and ridge characteristics of the actual synoptic situation are delineated quite well by the positive and negative ZC and RC guess-minus-observed difference centers, respectively. The retrieval differences show similar patterns with reduced amplitudes, providing further evidence of a first guess dependence in the retrievals. The OP difference fields are quite unlike those from the ZC and RC guesses , primarily because of

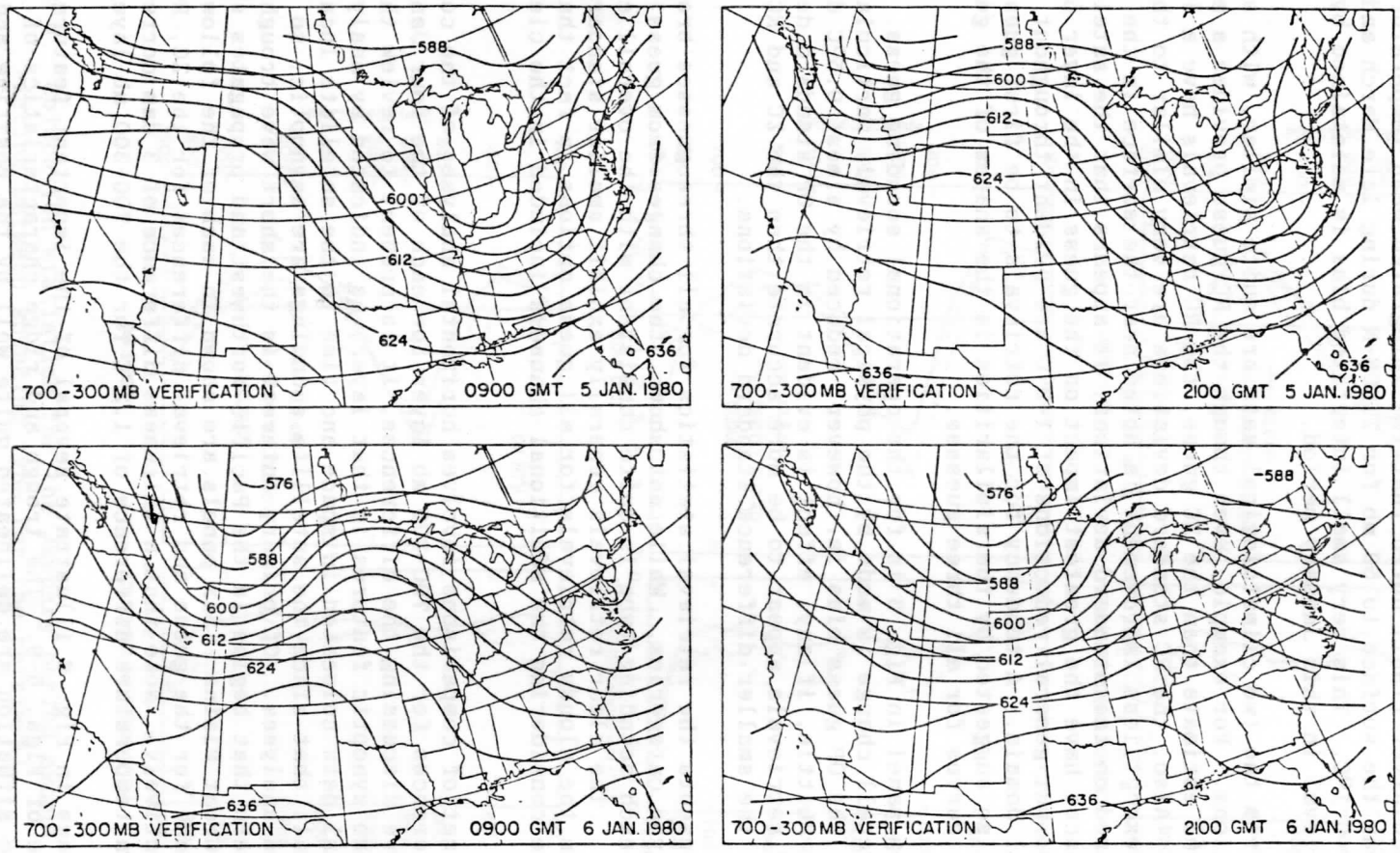

Figure 5. Verification 700-300 mb thicknesses derived from the conventional radiosonde data.

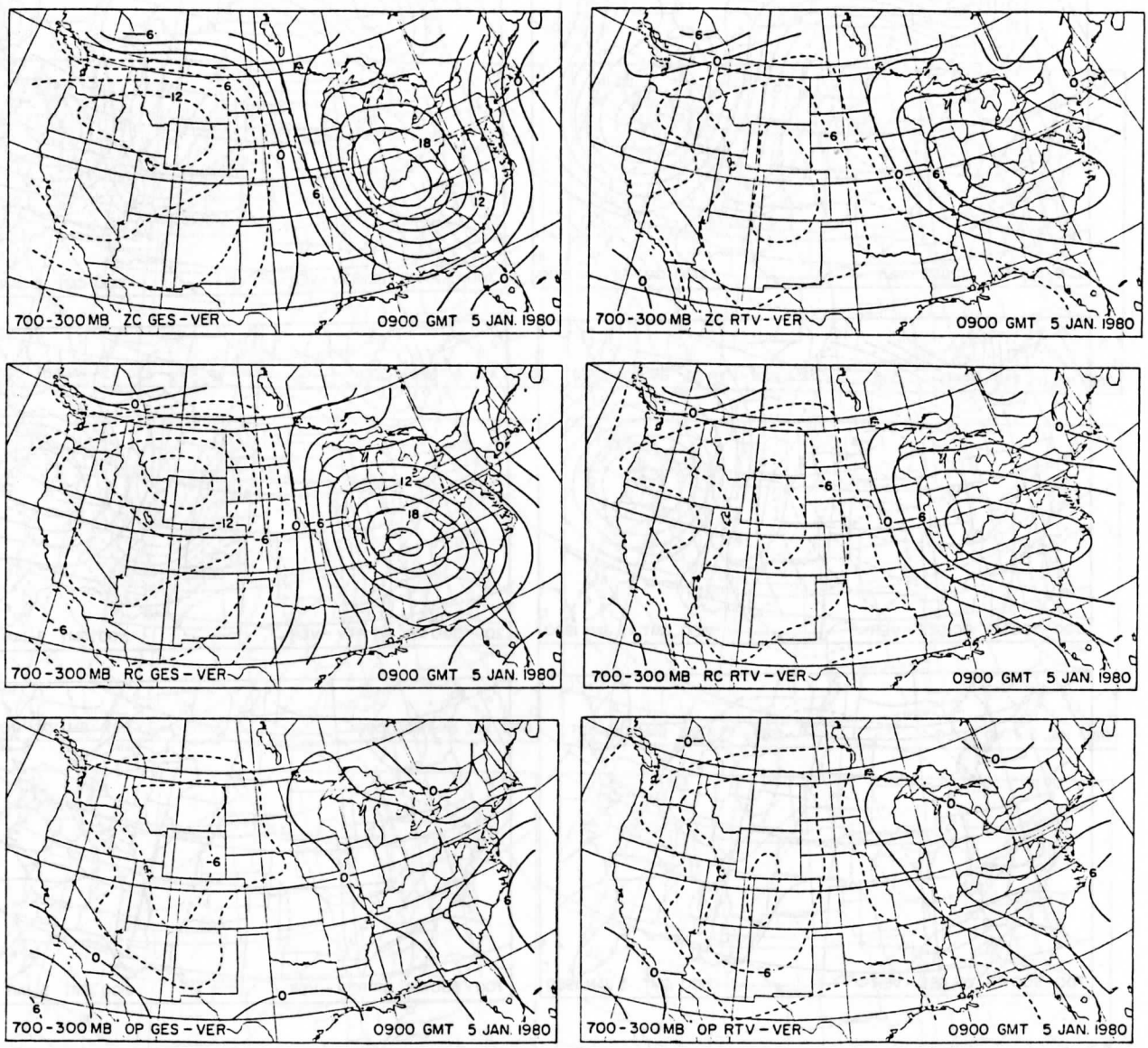

Figure 6. Guess-minus-verification and retrieval-minus-verification 700-300 mb thickness differences (dam) with negative values dashed for 0900 GMT 5 January 1980.

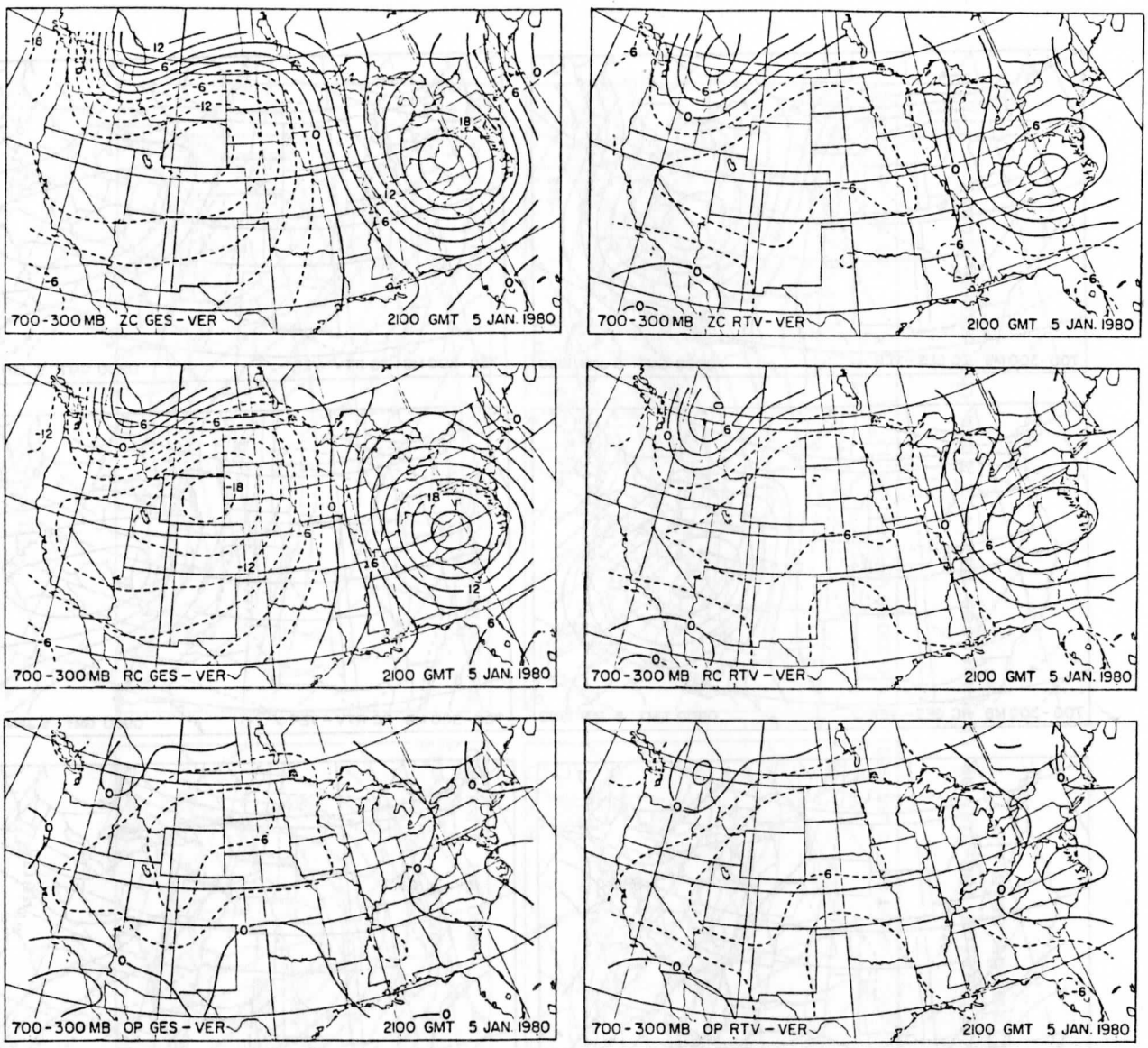

Figure 7. Same as Fig. 6 except for 2100 GMT 5 January 1980.

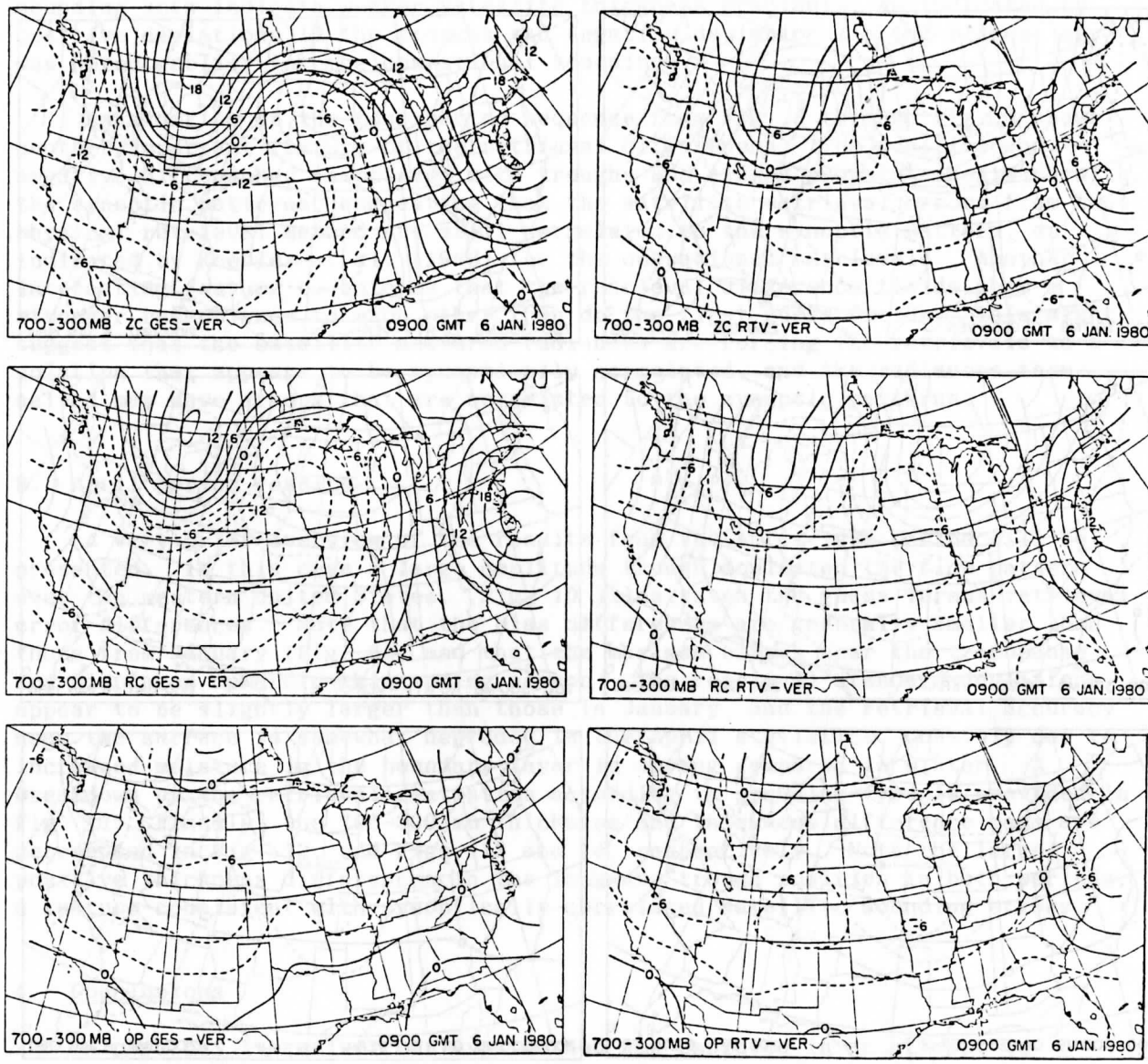

Figure 8. Same as Fig. 6 except for 0900 GMT 6 January 1980.

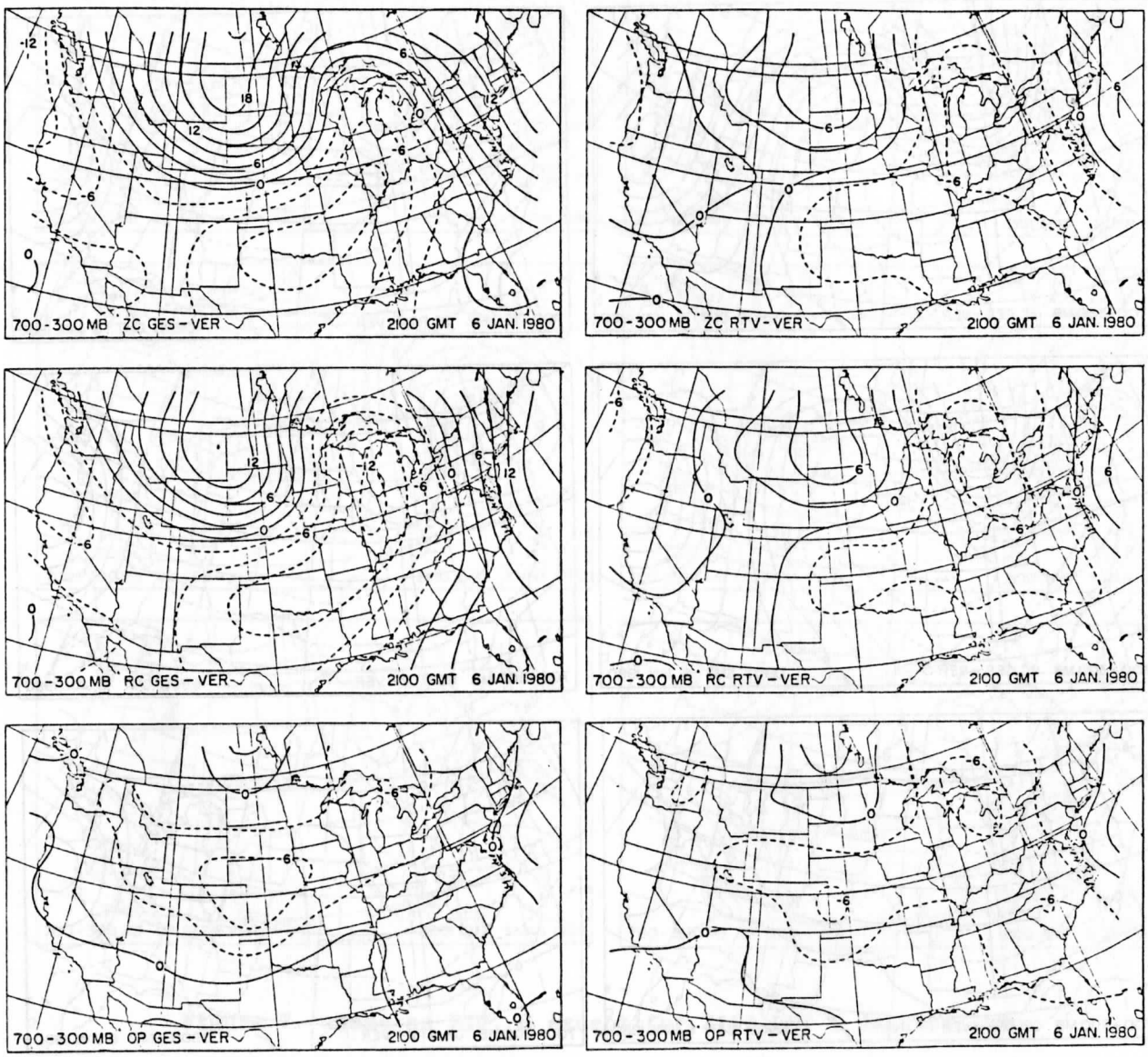

Figure 9. Same as Fig. 6 except for 2100 GMT 6 January 1980.

a quite different structure in the initial guess difference pattern. All of the sounding sets indicate weaker satellite thickness gradients, as indicated by positive deviations in the troughs and negative deviations in the ridges, as was noted earlier for the operational soundings.

Examination of the four period sequence from Fig. 6 through Fig. 9 shows another important feature of the retrieval differences. The positive and negative differences associated with troughs and ridges propagate eastward with the synoptic patterns, suggesting that the satellite retrieval errors from the physical retrieval method are still correlated to the synoptic pattern, as indicated by Koehler et al. (1983) for the operational retrievals. Another interesting feature to note is that the retrieval difference fields show a stronger resemblance to each other than do the first guess fields. This might suggest that the satellite measured radiances are forcing the retrievals to a solution that appears to be synoptically correlated, and the radiances themselves may have errors that are correlated to the synoptic patterns.

B. April period results

A very brief overview of the results from the April 1979 period will be presented. In this case a large amplitude trough dominated the flow pattern over the western United States. Fig. 10 illustrates the guess versus retrieval error differences. Note that the bias differences are generally smaller than those from January (Fig. 3), and that the maximum biases near the tropopause are displaced upwardin this spring season. The retrieval standard deviations appear to be slightly larger than those in January, and the retrieval accuracy near the surface is somewhat degraded in the April statistics, possibly due to increased moisture in the boundary layer in spring compared to winter. A breakdown of the retrieval statistics according to sounding type is provided in Fig. 11. Finally, the 700-300 mb thickness and thickness difference maps are peresented in Fig. 12, and Figs. 13 and 14, respectively. Note the large positive thickness differences in the longwave trough position in both periods, a feature consistent with synoptically-correlated satellite sounding errors.

4. Conclusions

A physical iterative retrieval method was employed in an attempt to improve the operational statistical retrievals derived during two synoptically active cases, one in January 1980 and the other in April 1979. Three different first guess were used, two of which were climatological, while the third came from the operational statistical retrieval. The physical retrieval method significantly reduced the climatological first guess errors but had little effect on improving the operational sounding guess. All the retrieval evaluations indicated that the retrieval errors are most likely correlated to their first guess profiles. Retrievals from the operational guess appeared to be more accurate than those from the climatological guesses.

The physical retrieval was also unable to improve the sounding accuracy with respect to known problems in the operational soundings. Significant errors were still present near the surface and tropopause, and the 700-300 mb

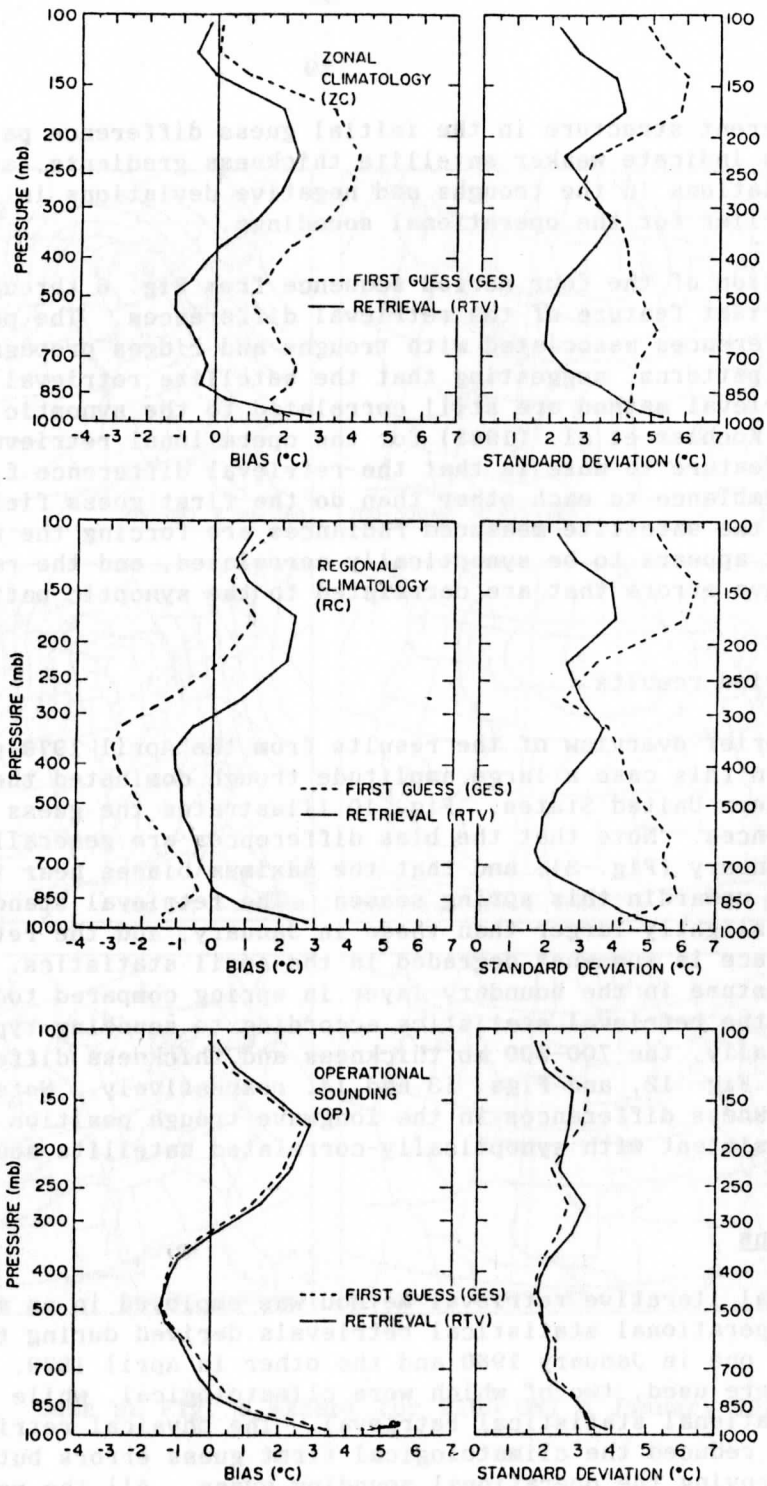

Figure 10. Same as Fig. 3 except for the April period.

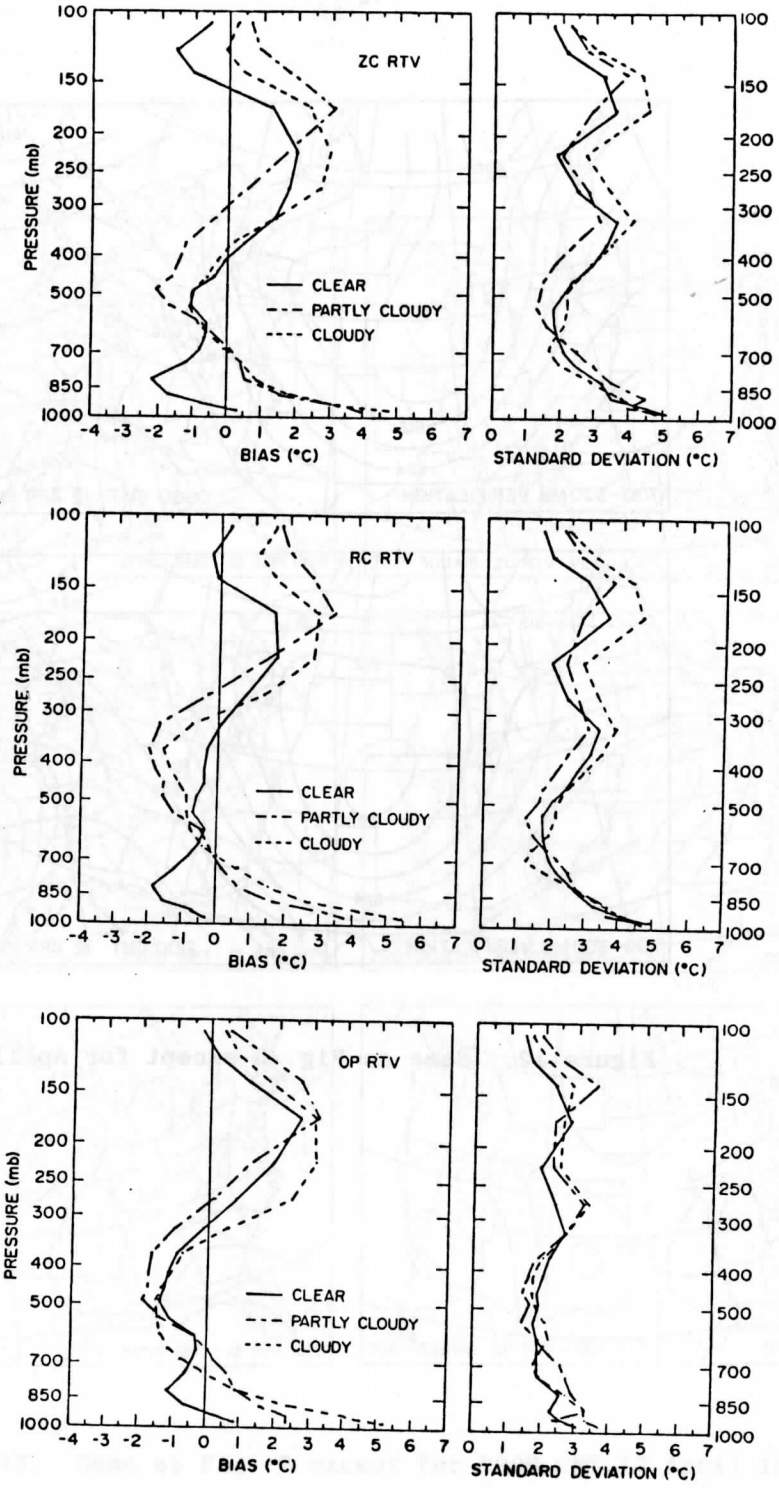

Figure 11. Same as Fig. 4 except for the April period.

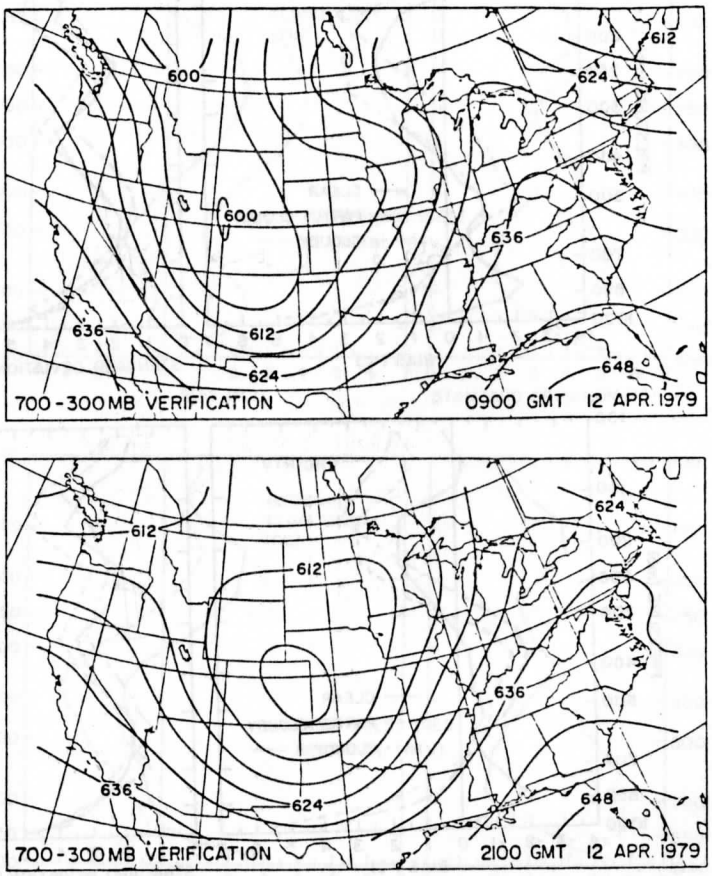

Figure 12. Same as Fig. 5 except for April.

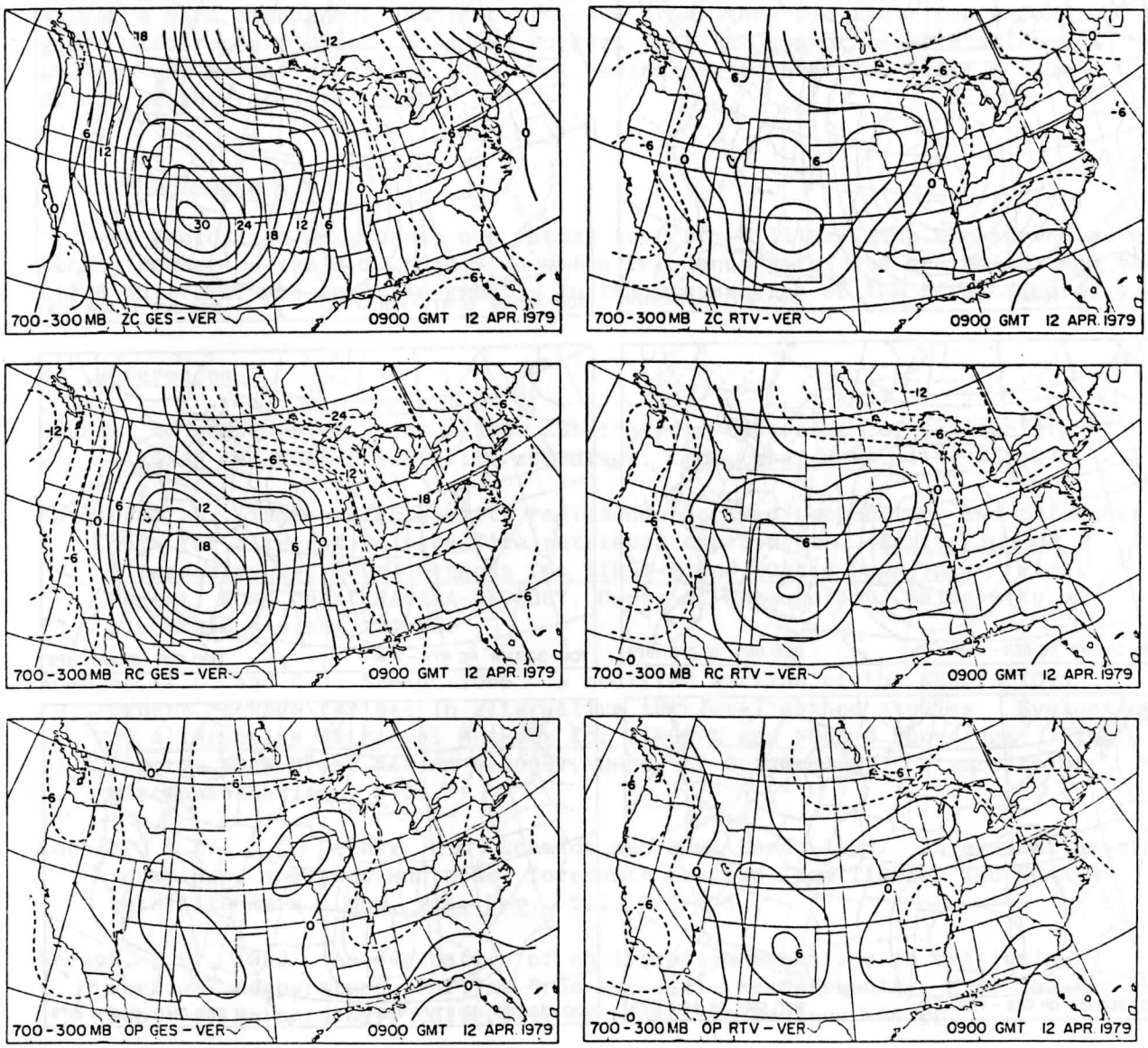

Figure 13. Same as Fig. 6 except for 0900 GMT 12 April 1979.

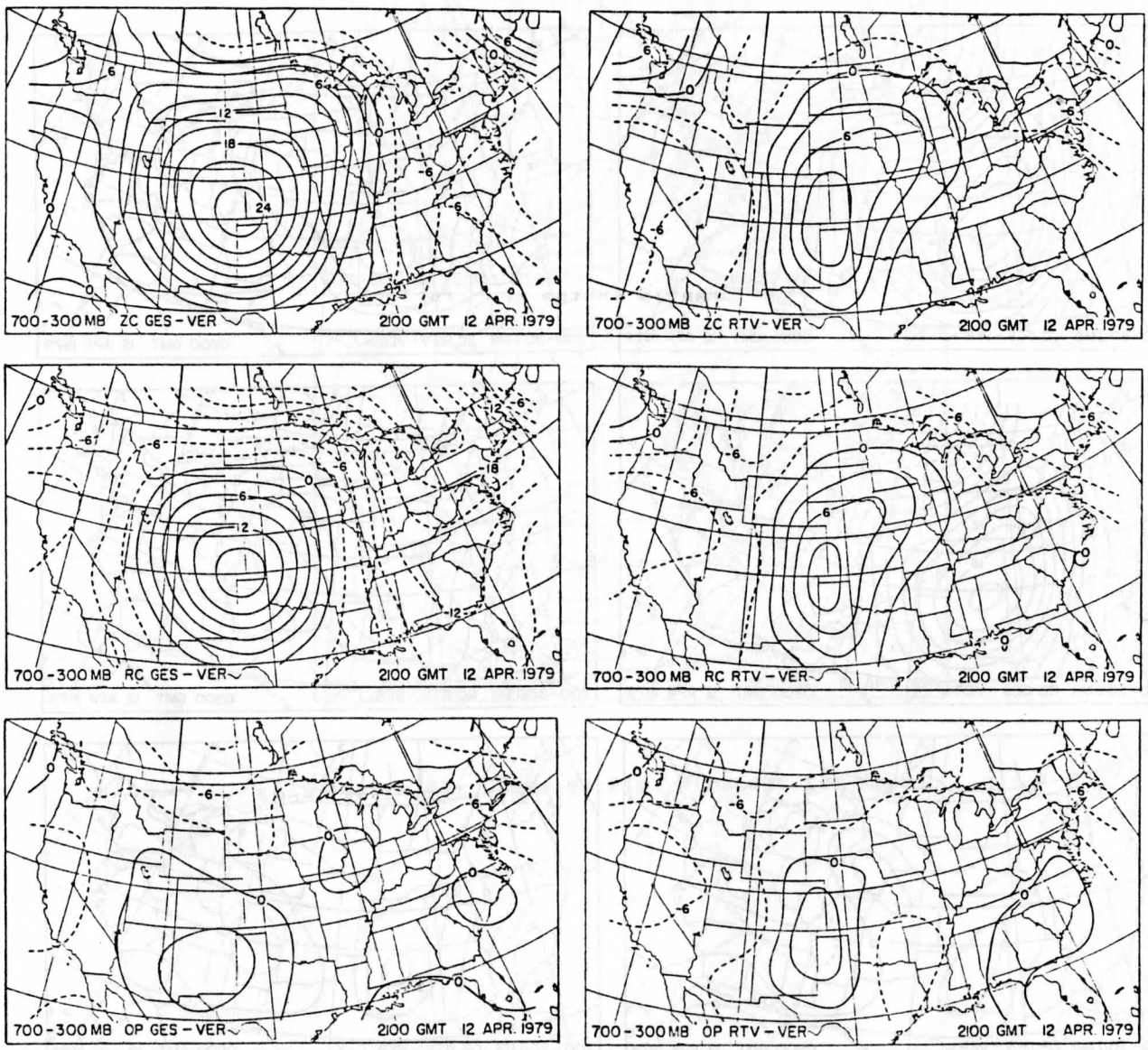

Figure 14. Same as Fig. 6 except for 2100 GMT 12 April 1979.

thickness distributions still exhibited a correlation to the synoptic pattern. In fact, the thickness difference distributions from the three retrieval sets showed a much stronger resemblance to each other than did their corresponding guess difference fields. This may suggest that the synoptic correlation problem may be entering from the input radiances, rather than being a side effect of the retrieval method.

5. Acknowledgements

We would like to express our thanks to Prof. William Smith who served as a second reader on the M.S. thesis on which the January results are based, and to Linda Whittaker who assisted greatly in the preparation of the final figures.

6. References

Gruber, A. and C. D. Watkins, 1982: Statistical assessment of the quality of TIROS-N and NOAA-6 satellite soundings. Mon. Wea. Rev., 110, 867-876.

Koehler, T.L., 1986: High quality radiosonde-derived temperature and thickness data for alternative satellite retrieval experiments. Evaluation of Alternative Retrieval Methods for TIROS-N and NOAA-6 Soundings. Final Report, NOAA Grant NA81AA-D-00087, Dept. of Meteorology, University of Wisconsin-Madison, 22-25.

Koehler, T.L. and C.J. Seman, 1986: A modified version of the NESDIS TOVS Export Package for use in alternative retrieval method studies. Evaluation of Alternative Retrieval Methods for TIROS-N and NOAA-6 Soundings. Final Report, NOAA Grant NA81AA-D-00087, Dept. of Meteorology, University of Wisconsin-Madison, 9-21.

Koehler, T.L., J.C. Derber, B.D. Schmidt and L.H. Horn, 1983: An evaluation of soundings, analyses and model forecasts derived from TIROS-N and NOAA-6 satellite data. Mon. Wea. Rev., 111, 562-571.

Nelson, J.P., 1983: An evaluation of an iterative technique in retrieving vertical temperature profiles from satellite measurements. M.S. Thesis, Dept. of Meteorology, University of Wisconsin-Madison, 46 pp.

Phillips, N., L. McMillin, A. Gruber and D. Wark, 1979: An evaluation of early operational temperature soundings from TIROS-N. Bull. Amer. Meteor. Soc., 60, 1188-1197.

Schlatter, T.W., 1981: An assessment of operational TIROS-N temperature retrievals over the United States. Mon. Wea. Rev., 109, 110-119.

Smith, W.L., 1970: Iterative solution of the radiative transfer equation for the temperature and absorbing gas profile of an atmosphere. Applied Optics, 9, 1993-1999.

Smith, W.L., H.M. Woolf, C.M. Hayden, D.Q. Wark and L.M. McMillin, 1979: The TIROS-N operational vertical sounder. Bull. Amer. Meteor. Soc., 60, 1177-1187.

AN EVALUATION OF DIFFERENT HORIZONTAL RESOLUTION IN RADIANCE COMPOSITING FOR TIROS-N RETRIEVALS

by

Charles J. Seman, Lyle H. Horn and Thomas L. Koehler

Abstract

A physical iterative retrieval method is used to derive 3x3 field-of-view (FOV) and 9x7 FOV satellite soundings from radiance measurements by TIROS-N over the United States during two periods from 6 January 1980. A comparison of the 3x3 and 9x7 iterative retrievals is performed to determine whether the vertical bias and the synoptically correlated warm (cold) bias found in deep troughs (ridges) evident in 9x7 retrievals can be reduced by using fewer fields-of-view per sounding. The one 9x7 and four 3x3 satellite sounding sets generated for each of the two periods are compared using statistical vertical profiles and thickness difference maps for the 700-300 mb layer.

Statistically, the 3x3 iterative retrievals show some improvement over the corresponding 9x7 retrievals. In particular, some of the low to mid tropospheric bias is removed by reducing the number of fields-of-view per sounding, without any significant increase in standard deviations. Further analysis shows that the improved performance of the 3x3 retrievals is sounding-type dependent: clear 3x3 retrievals perform somewhat better than the corresponding 9x7 retrievals, the partly cloudy retrievals show mixed results, while the 3x3 cloudy retrievals offer no improvement. The statistics fail to show that any one of the four 3x3 sounding sets is noticeably superior to the others.

A comparison of the 3x3 and 9x7 700-300 mb thickness fields shows that very little improvement is realized using the higher resolution soundings. The 3x3 thermal fields also show the synoptically correlated errors evident in the NESS operational retrievals, with troughs being too warm and ridges too cold.

1. Introduction

One of the most fundamental problems in atmospheric science is forecasting the future state of the atmosphere, using an initial state based on observations, and a model formulated from the appropriate hydrodynamic equations. Since the advent of numerical weather prediction in the 1950's (Fawcett, 1977), forecasts of upper level flow patterns have steadily improved (Reed, 1977). However, forecasts of major cyclogenesis downstream of data sparse regions were often disappointing. The development of meteorological satellites capable of measuring radiances from which vertical temperature profiles could be derived

promised to alleviate the problems of data shortages over these regions. However, many of the early satellite sounding impact tests indicated that the inclusion of satellite soundings into the conventional data base had little, if any, positive impact on numerical predictions (Tracton and McPherson, 1977). They pointed out that "...remote sounding data are generally of reasonable quality but are not as good as conventional data".

As noted in the the Preface and in the previous paper (Koehler et al., 1986), the quality of statistically derived operational satellite soundings from the FGGE data set was somewhat disappointing when compared to conventional soundings. Several investigations (such as Phillips et al., 1979; Schlatter, 1981; Gruber and Watkins, 1982; and Koehler et al., 1983) have found that the greatest inaccuracies in the operational satellite soundings from TIROS-N and NOAA-6 occur near the surface and near the tropopause. Koehler et al. (1983) also show that the retrievals exhibit errors correlated to the synoptic pattern, with troughs (ridges) being too warm (cold), leading to a reduction of the amplitude of thermal fields associated with synoptic weather systems. Since the FGGE data will be used extensively by the atmospheric science community over the next several years, considerable effort has been made to try to improve the accuracy of the FGGE year soundings.

The research presented in the previous paper in this report by Koehler et al. (1986) desribes an effort to improve retrieval accuracy by using a physical retrieval method as an alternative to the operational statistical method. Only nominal improvement in accuracy was attained from any of their three first guess alternatives when the operational resolution brightness temperatures combined over a 9x7 array of HIRS/2 FOV by NESS provided the basic input data. The research presented here addresses the question of what effect an increased horizontal resolution (a 3x3 FOV array) in the radiance compositing technique might have on the accuracy of the retrievals. Again, the physical retrieval method is employed with a statistical retrieval providing the first guess information.

2. The Experiment

To isolate the effects of increased horizontal resolution in the radiance compositing procedure, two periods of TIROS-N data from 6 January 1980 over the United States is reprocessed using 3x3 arrays of HIRS/2 fields-of-view instead of the 9x7 FOV operational resolution. Note that this is a subset of the period studied by Koehler et al. (1983) that evaluated the accuracy of the operational retrievals, and by Koehler et al. (1986) that examined physical retrievals as an alternative to the operational statistically derived soundings. In reducing the number of FOV used per sounding, it is anticipated that less thermal information will be lost in the averaging of the radiance information, which in turn should result in better definition of the baroclinic structure.

The methodology employed in deriving the higher resolution retrievals is based upon the modified TOVS Export Package software outlined in Koehler and Seman (1986). Limb-corrected HIRS/2 and MSU brightness temperature data from six TIROS-N passes, three centered around 0900 GMT 6 January and three centered

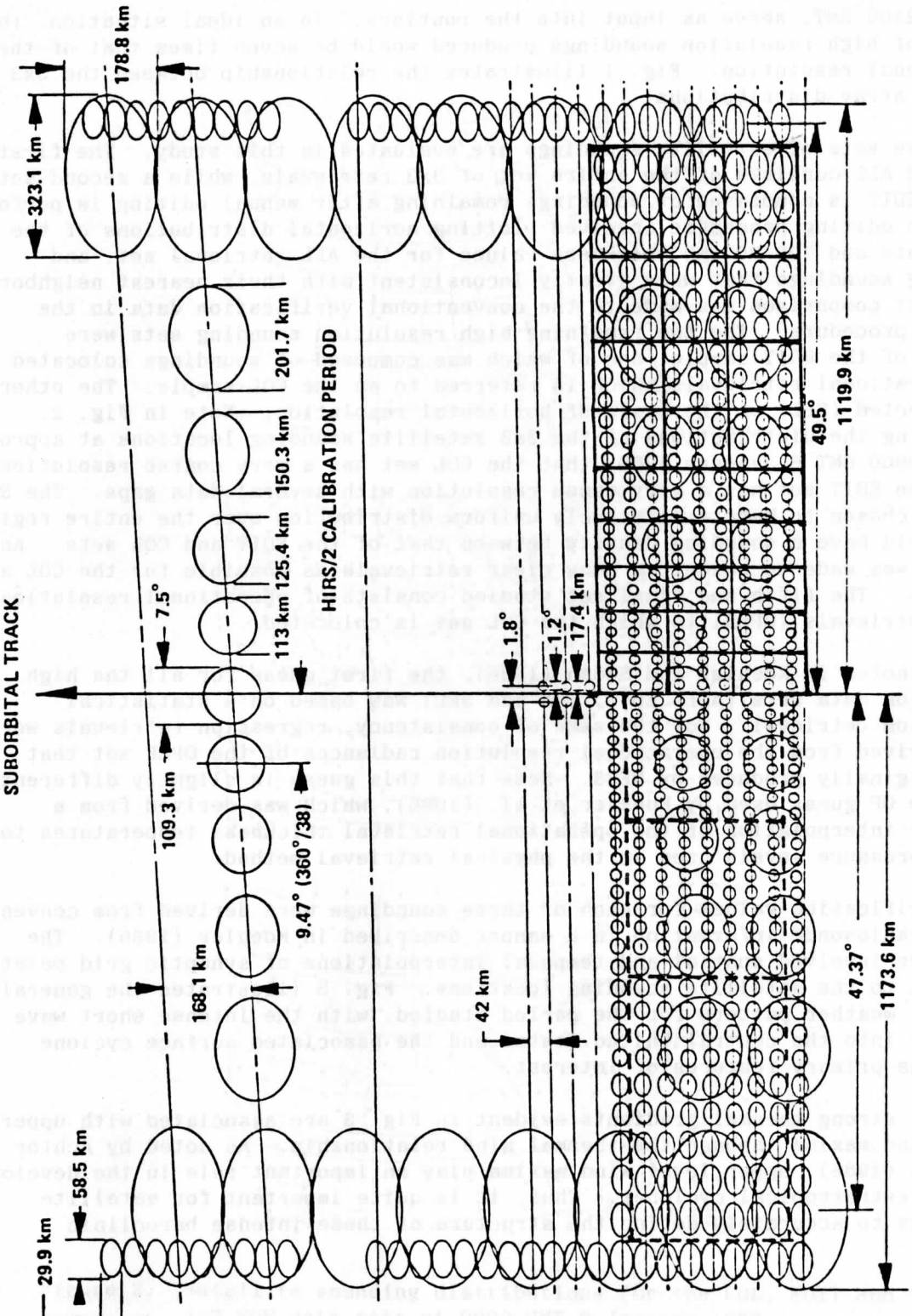

Figure 1. The TOVS instrument scan patterns with 9x7 and 3x3 HIRS/2 field-of-view arrays outlined in dashed and solid lines, respectively.

around 2100 GMT, serve as input into the routines. In an ideal situation, the number of high resolution soundings produced would be seven times that of the operational resolution. Fig. 1 illustrates the relationship between the 3x3 and 9x7 array distributions.

Five sets of satellite soundings are evaluated in this study. The first, labelled ALL consists of the entire set of 3x3 retrievals, while a second set termed EDIT is comprised of soundings remaining after manual editing is performed. The editing procedure involved plotting horizontal distributions of the 700 mb heights and 700-300 mb thickness values for the ALL retrieval set, and removing soundings that were greatly inconsistent with their nearest neighbors. No direct comparison was made to the conventional verification data in the editing procedure. The two remaining high resolution sounding sets were subsets of the EDIT sample, one of which was composed of soundings colocated to the operational retrievals which is referred to as the COL sample. The other was selected (SEL) on the basis of horizontal resolution. Note in Fig. 2, displaying the distributions of the 3x3 satellite sounding locations at approximately 0900 GMT 6 January 1980, that the COL set has a very coarse resolution while the EDIT set has a very dense resolution with several data gaps. The SEL set was chosen to have a relatively uniform distribution over the entire region that would have a sounding density between that of the EDIT and COL sets. An attempt was made to select as many clear retrievals as possible for the COL and SEL sets. The fifth and final set studied consists of operational resolution (9x7) retrievals (OPER) to which the COL set is colocated.

As noted in Koehler and Seman (1986), the first guess for all the high resolution data sets (ALL, EDIT, COL and SEL) was based on a statistical regression retrieval. For the sake of consistency, regression retrievals were also derived from the operational resolution radiances of the OPER set that were originally produced by NESS. Note that this guess is slightly different than the OP guess used by Koehler et al. (1986), which was derived from a vertical interpolation of the operational retrieval thickness temperatures to the 40 pressure levels used in the physical retrieval method.

Verification values for each of these soundings were derived from conventional radiosonde information in a manner described in Koehler (1986). The procedure involved spatial and temporal interpolations of synoptic grid point analyses to the satellite sounding locations. Fig. 3 illustrates the general synoptic weather pattern for the period studied, with the intense short wave plunging into the central United States and the associated surface cyclone being the primary features of interest.

The strong thermal gradients evident in Fig. 3 are associated with upper level wind maxima through the thermal wind relationship. As noted by Achtor and Horn (1986), upper level wind maxima play an important role in the development of extratropical cyclones. Thus, it is quite important for satellite soundings to accurately define the structure of these intense baroclinic zones.

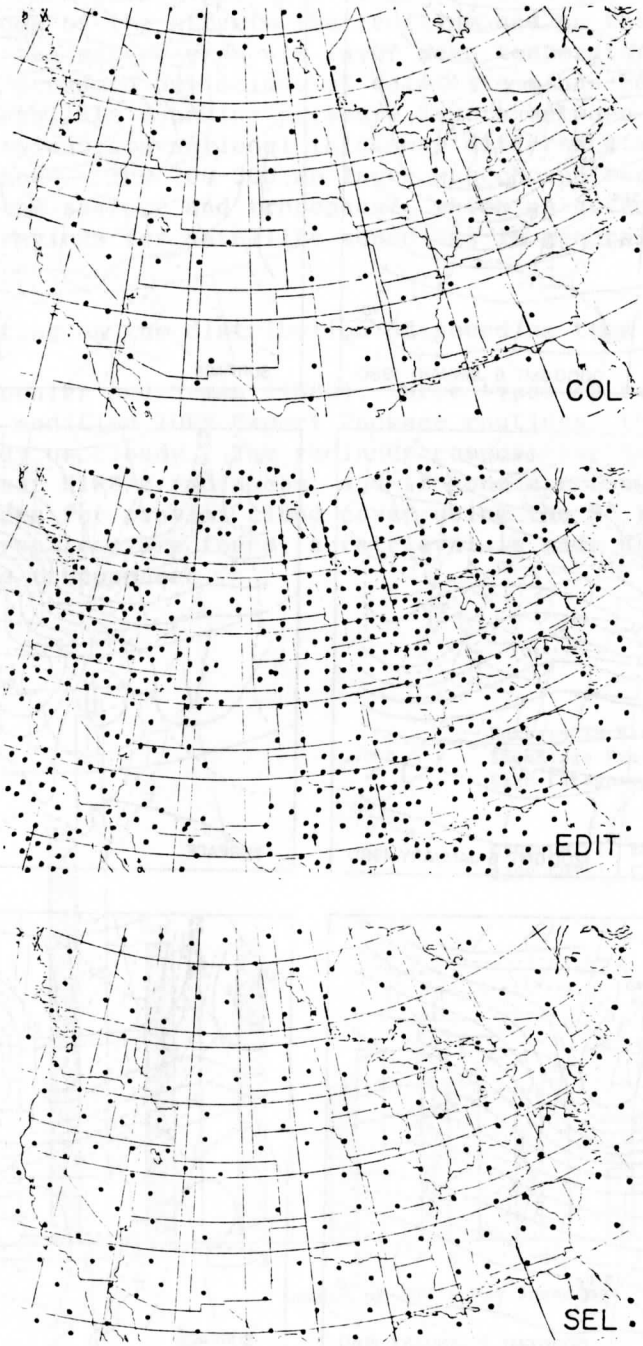

Figure 2. Satellite sounding distributions for the COL, EDIT and SEL 3x3 FOV data sets at 0900 GMT 6 January 1980.

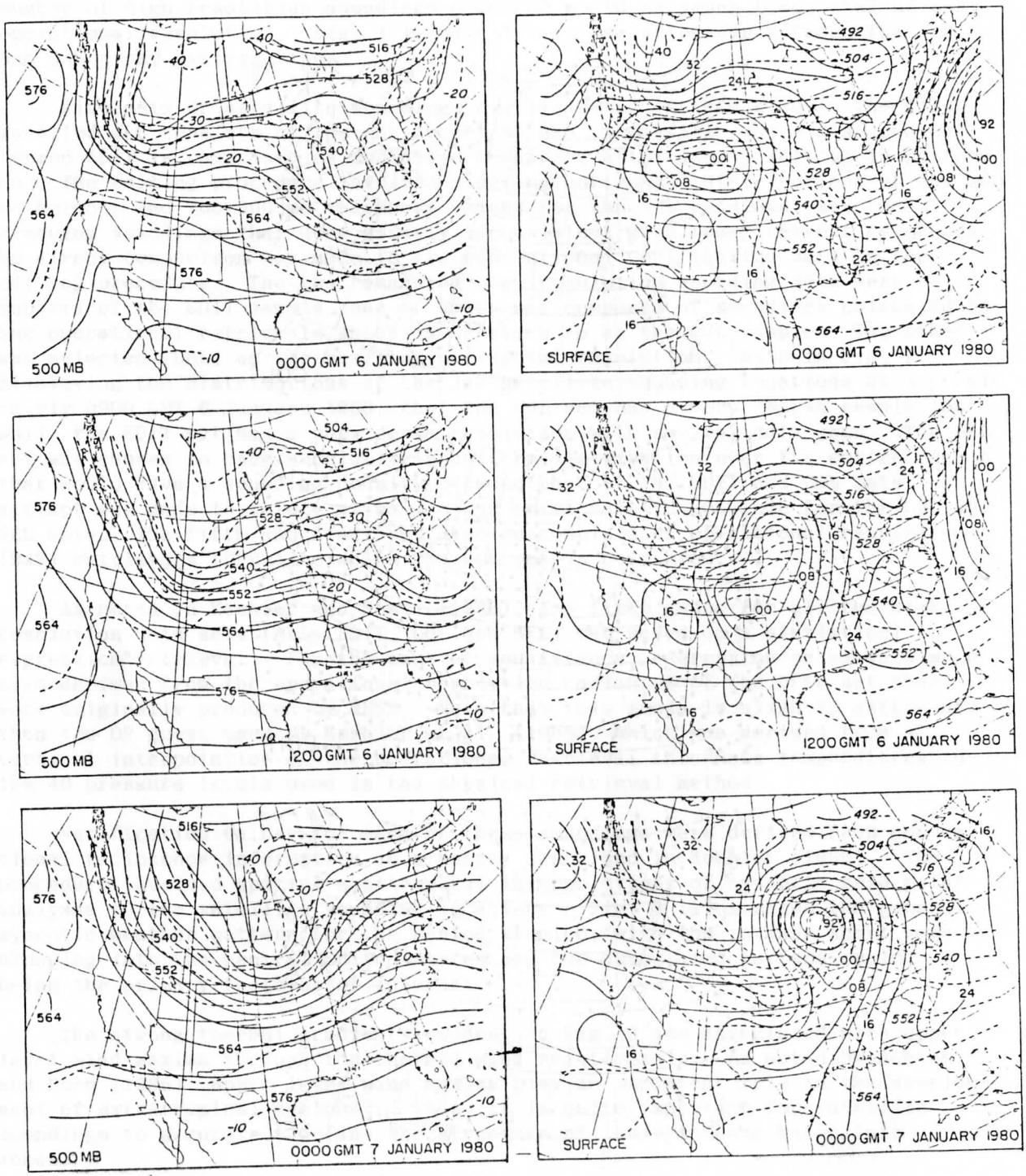

Figure 3. LFM 500 mb and surface analyses for 0000 GMT 6 January to 0000 GMT 7 January 1980. At 500 mb, the dashed contours are temperatures in ^{o}C and the solid lines are height contours in dam. On the surface charts, isobars in mb are solid and the 1000-500 mb thickness lines in dam are dashed.

3. Results

Our findings from this study will be presented in three sections. The first summarizes some of the effects that editing had on the sounding type distributions, and the second presents layer mean temperature statistics in the form of biases and standard deviations of satellite-minus conventional differences for the 20 satellite sounding pressure layers between 1000 and 100 mb. Finally, satellite-minus-conventional thickness difference analyses for 700-300 mb layer will be shown. The 700-300 mb layer was chosen because it does not include data near the surface and tropopause, which as noted before are relatively inaccurate regions for satellite soundings in general.

A. Effects of editing on the distribution of sounding type

As noted by Koehler and Seman (1986), three types of retrievals are produced using the modified TOVS Export Package routines: those designated clear, partly cloudy or cloudy. The radiance compositing techniques first attempt to find clear HIRS/2 radiances, and if none are found, attempts to correct the radiances for partial cloud cover using the N* technique. Finally, if no suitable corrections are found, a retrieval is made using only the MSU measurements in the troposphere.

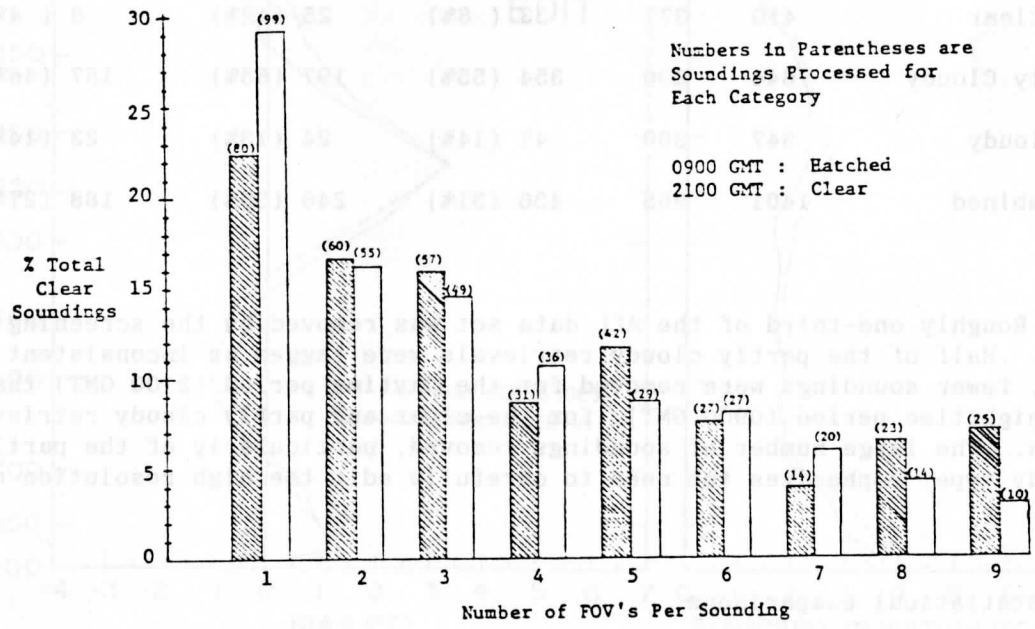

Figure 4. Number of fields-of-view used per clear 3x3 retrieval.

One interesting element of the results from the radiance composing routines is the distribution of the number of HIRS/2 FOV that went into the clear path retrievals, as shown in Fig. 4. Almost one-quarter of the clear retrievals are based on only one HIRS/2 FOV, while only 5% include all 9 FOV. Roughly 42% of the clear soundings combined 3 or fewer FOV. Thus, even though the search for acceptable data involves a 3x3 array, a large fraction of the clear retrievals are representative of an even smaller region. With fewer points used in the average, instrument noise has a greater chance of degrading the final product.

Another general assumption made is that the accuracy of the retrievals decreases as the estimated cloud amount increases. The first place that this hypothesis is tested in our study is in the editing procedure. Table 1 summarizes the results from the manual editing (see Seman, 1985, for a more complete discussion of the editing procedure).

Table 1. Summary of the effect of editing as a function of sounding type. ALL refers to the complete set of 3x3 retrievals, while EDIT refers to the soundings passing the consistency checking procedures.

Sounding Type	ALL	EDIT	Soundings Removed (%) Total	0900 GMT	2100 GMT
Clear	410	377	33 (8%)	25 (12%)	8 (4%)
Partly Cloudy	644	290	354 (55%)	197 (65%)	157 (46%)
Cloudy	347	300	47 (14%)	24 (13%)	23 (14%)
Combined	1401	965	436 (31%)	246 (35%)	188 (27%)

Roughly one-third of the ALL data set was removed by the screening procedure. Half of the partly cloudy retrievals were tagged as inconsistent. Also, fewer soundings were removed for the daytime period (2100 GMT) than for the nighttime period (0900 GMT), for the clear and partly cloudy retrieval types. The large number of soundings removed, particularly of the partly cloudy type, emphasizes the need to carefully edit the high resolution data sets.

B. Statistical comparisons

The focus of this section is to provide a statistical evaluation of the layer mean temperature differences between the satellite soundings and colocated values derived from the conventional radiosonde data. The differences were computed for the 20 satellite retrieval layers from 1000 to 100 mb for each of the five data sets described earlier. Vertical profiles of the bias and standard deviations of the differences are presented for the different data

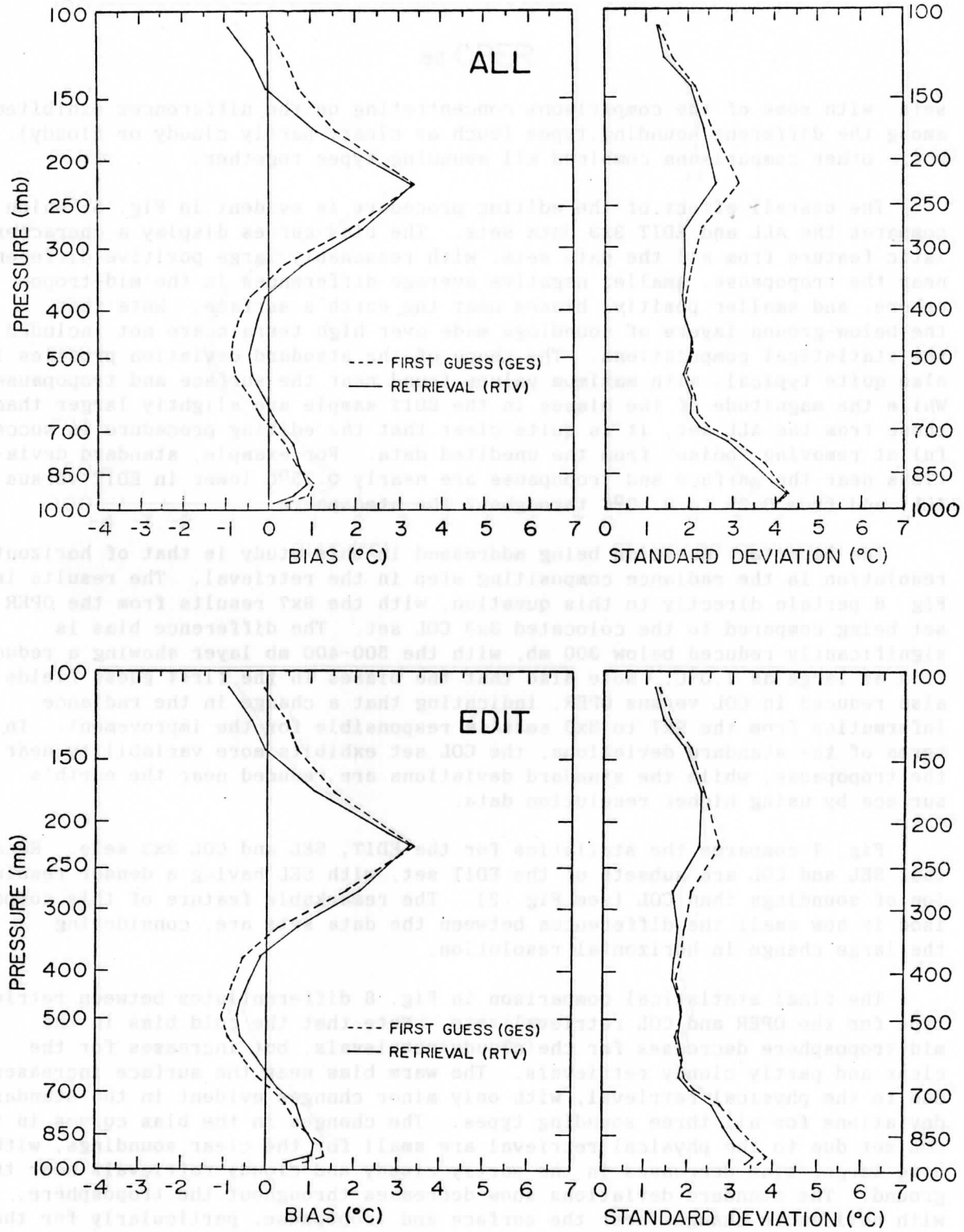

Figure 5. Statistics for the 3x3 ALL and EDIT data sets. Retrieved (solid) and first guess (dashed) layer mean temperatures for all sounding types.

sets, with some of the comparisons concentrating on the differences exhibited among the different sounding types (such as clear, partly cloudy or cloudy), while other comparisons combined all sounding types together.

The overall effect of the editing procedure is evident in Fig. 5, which compares the ALL and EDIT 3x3 data sets. The bias curves display a characteristic feature from all the data sets, with reasonably large positive differences near the tropopause, smaller negative average differences in the mid-troposphere, and smaller positive biases near the earth's surface. Note that the below-ground layers of soundings made over high terrain are not included in the statistical computations. The shape of the standard deviation profiles is also quite typical, with maximum values found near the surface and tropopause. While the magnitude of the biases in the EDIT sample are slightly larger than those from the ALL set, it is quite clear that the editing procedure is successful at removing "noise" from the unedited data. For example, standard deviations near the surface and tropopause are nearly 0.75°C lower in EDIT versus ALL, and from 0.25 to 0.50°C throughout the atmosphere.

The important question being addressed in this study is that of horizontal resolution in the radiance compositing step in the retrieval. The results in Fig. 6 pertain directly to this question, with the 9x7 results from the OPER set being compared to the colocated 3x3 COL set. The difference bias is significantly reduced below 300 mb, with the 500-400 mb layer showing a reduction as large as 1.0°C. Note also that the biases in the first guess fields are also reduced in COL versus OPER, indicating that a change in the radiance information from the 9x7 to 3x3 sets is responsible for the improvement. In terms of the standard deviations, the COL set exhibits more variability near the tropopause, while the standard deviations are reduced near the earth's surface by using higher resolution data.

Fig. 7 compares the statistics for the EDIT, SEL and COL 3x3 sets. Recall that SEL and COL are subsets of the EDIT set, with SEL having a denser resolution of soundings than COL (see Fig. 2). The remarkable feature of this comparison is how small the differences between the data sets are, considering the large change in horizontal resolution.

The final statistical comparison in Fig. 8 differentiates between retrieval type for the OPER and COL retrieval sets. Note that the cold bias in the mid-troposphere decreases for the cloudy retrievals, but increases for the clear and partly cloudy retrievals. The warm bias near the surface increases due to the physical retrieval, with only minor changes evident in the standard deviations for all three sounding types. The changes in the bias curves in the COL set due to the physical retrieval are small for the clear soundings, with some larger bias decreases in the partly cloudy and cloudy retrievals near the ground. The standard deviations show decreases throughout the troposphere, with noticeable changes near the surface and tropopause, particularly for the partly cloudy and cloudy soundings.

In comparing the OPER and COL retrievals as a function of sounding type, interesting conclusions arise. The 3x3 resolution soundings are generally warmer than their 9x7 counterparts above 700 mb. The bias near the surface in the OPER set is reduced for the clear soundings, but not for the others. In

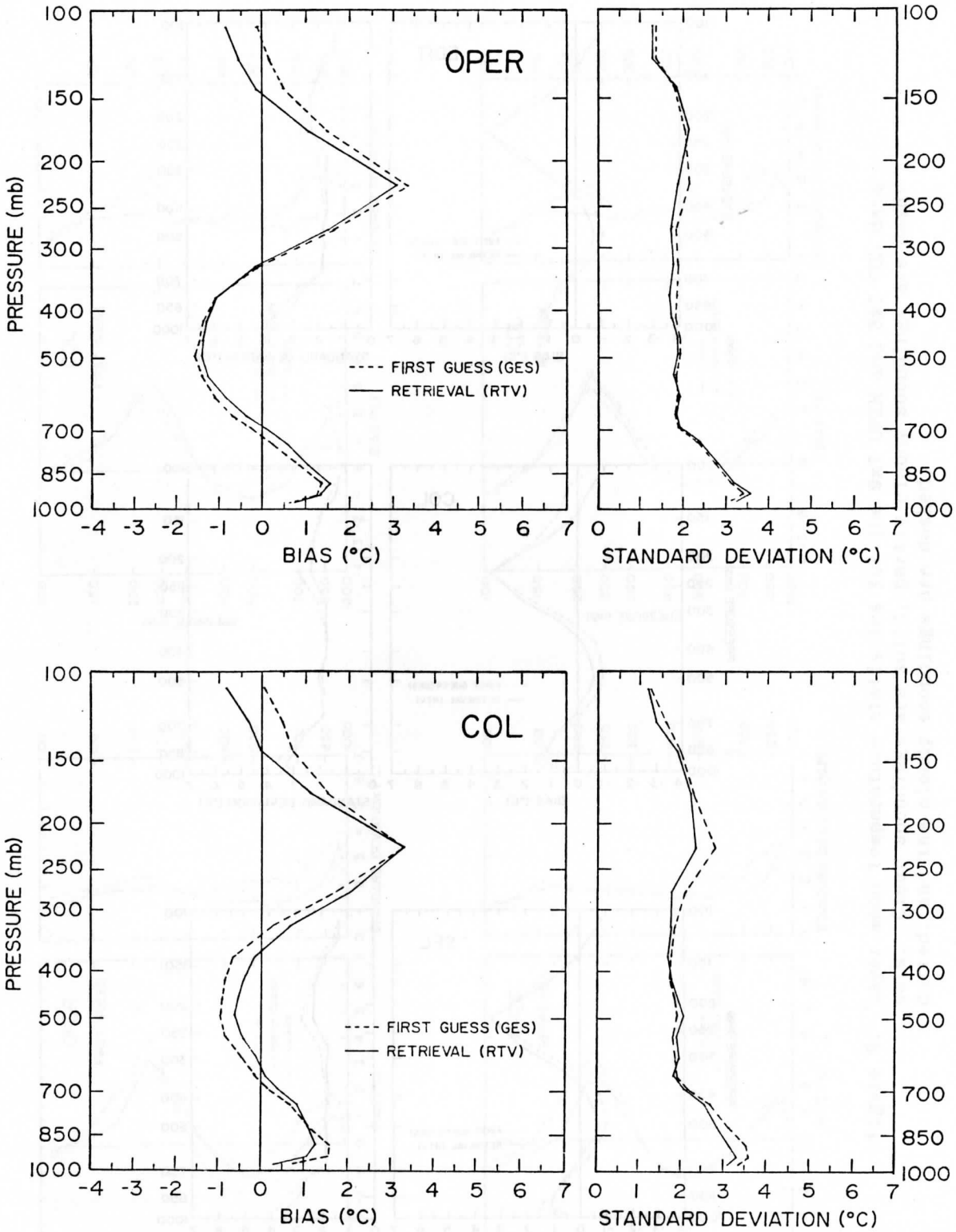

Figure 6. Statistics for the 9x7 OPER and 3x3 COL data sets. Retrieved (solid) and first guess (dashed) layer mean temperatures for all sounding types.

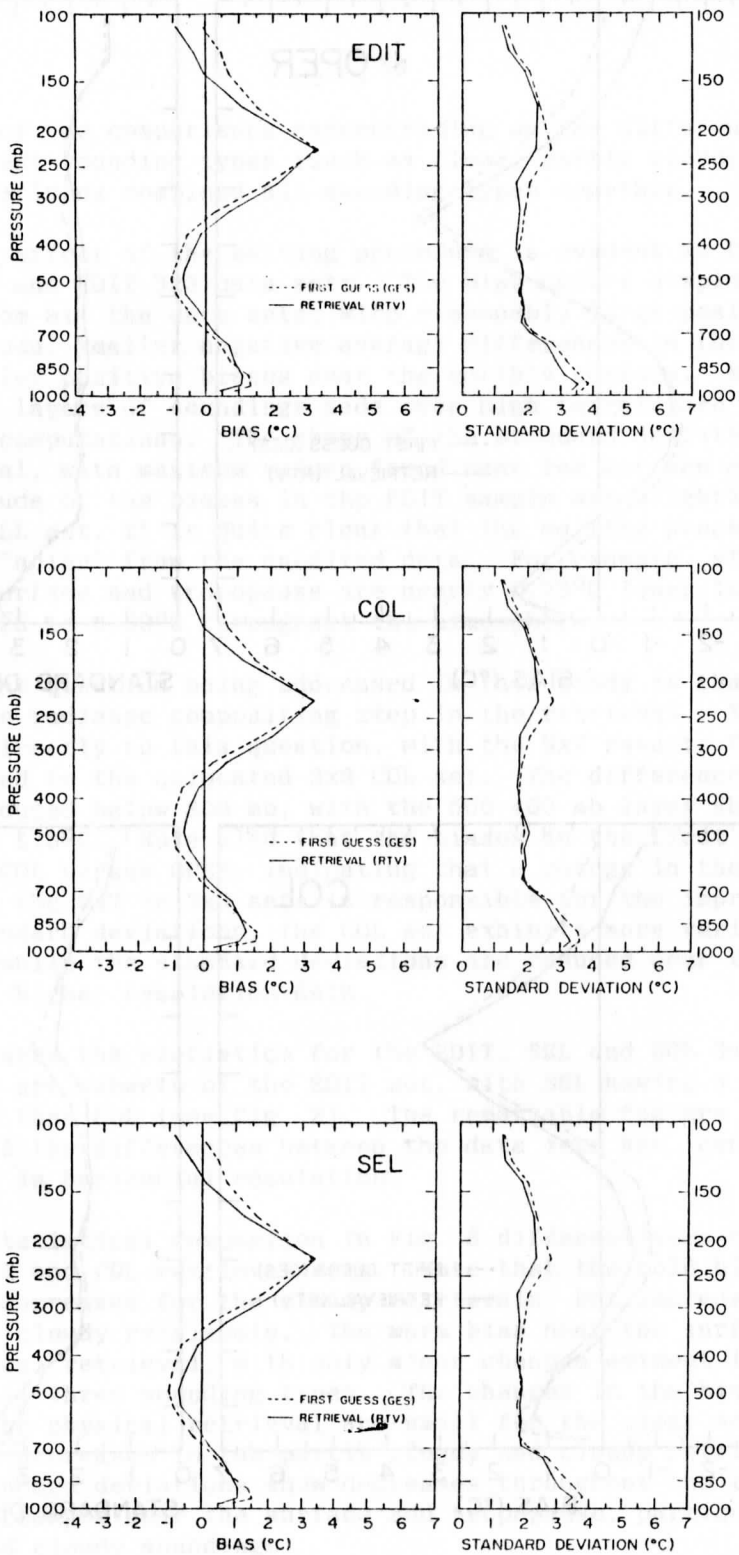

Figure 7. Statistics for the 3x3 EDIT, COL and SEL data sets. Retrieved (solid) and first guess (dashed) layer mean temperatures for all sounding types.

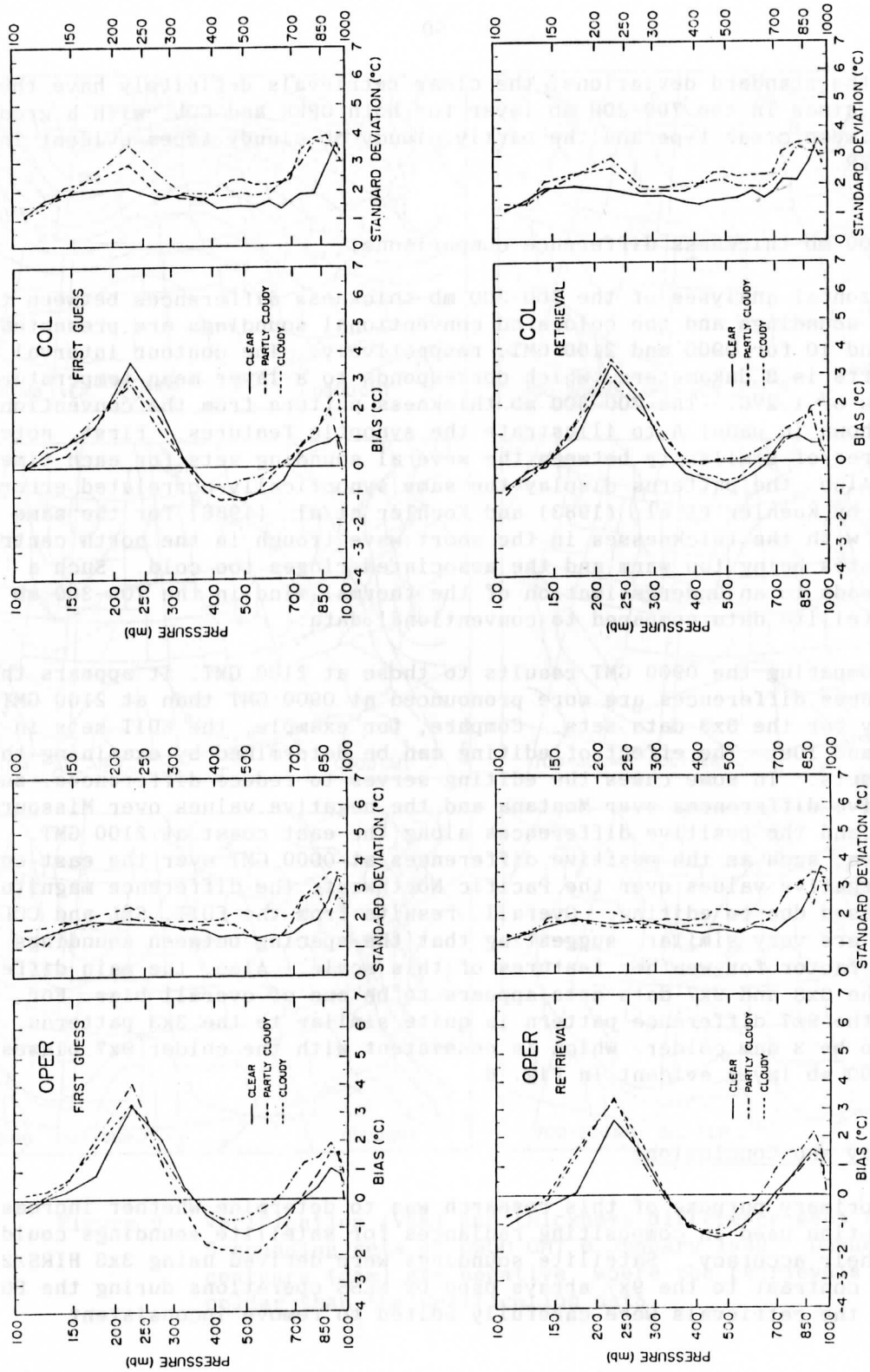

Figure 8. Layer mean temperature statistics for the 9x7 OPER and 3x3 COL data sets. Clear soundings are solid, partly cloudy soundings are dash-dotted, and the cloudy soundings are dashed.

terms of the standard deviations, the clear retrievals definitely have the smallest values in the 700-300 mb layer for both OPER and COL, with a greater spread between clear type and the partly cloudy or cloudy types evident in COL versus OPER.

C. 700-300 mb thickness difference comparisons.

Horizontal analyses of the 700-300 mb thickness differences between the satellite soundings and the colocated conventional soundings are presented in Figs. 9 and 10 for 0900 and 2100 GMT, respectively. The contour interval on these charts is 3 dekameters, which corresponds to a layer mean temperature difference of 1.2°C. The 700-300 mb thickness pattern from the conventional data is shown in panel A to illustrate the synoptic features. First, note the large degree of similarity between the several sounding sets for each time period. Also, the patterns display the same synoptically-correlated error described by Koehler et al. (1983) and Koehler et al. (1986) for the same period of study, with the thicknesses in the short wave trough in the north central United States being too warm and the associated ridges too cold. Such a pattern leads to an underestimation of the thermal wind in the 700-300 mb layer in the satellite data compared to conventional data.

In comparing the 0900 GMT results to those at 2100 GMT, it appears that the thickness differences are more pronounced at 0900 GMT than at 2100 GMT, especially for the 3x3 data sets. Compare, for example, the EDIT sets in Figs. 9e and 10e. The effect of editing can be determined by examining the ALL and EDIT sets. In some cases the editing serves to reduce differences, such as the positive differences over Montana and the negative values over Missouri at 0900 GMT, and the positive differences along the east coast at 2100 GMT. In other cases, such as the positive differences at 0900 GMT over the east coast and the negative values over the Pacific Northwest, the difference magnitudes are increased due to editing. Overall, results from the EDIT, SEL and COL 3x3 data sets are very similar, suggesting that the spacing between soundings is not a crucial factor for weather features of this scale. Also, the main difference between the 3x3 and 9x7 data sets appears to be one of overall bias. For example, the 9x7 difference pattern is quite similar to the 3x3 patterns, but appears to be 3 dam colder, which is consistent with the colder 9x7 biases in the 700-300 mb layer evident in Fig. 6.

4. Summary and Conclusions

The primary purpose of this research was to determine whether increasing the resolution used in compositing radiances for satellite soundings could improve their accuracy. Satellite soundings were derived using 3x3 HIRS/2 arrays in contrast to the 9x7 arrays used by NESS operations during the FGGE year, and the retrievals were carefully edited to remove inconsistent soundings.

The first general result is that editing of the high resolution retrievals is important, with almost one-third of the retrievals being labelled as inconsistent. Far more partly cloudy retrievals were removed, with a greater number

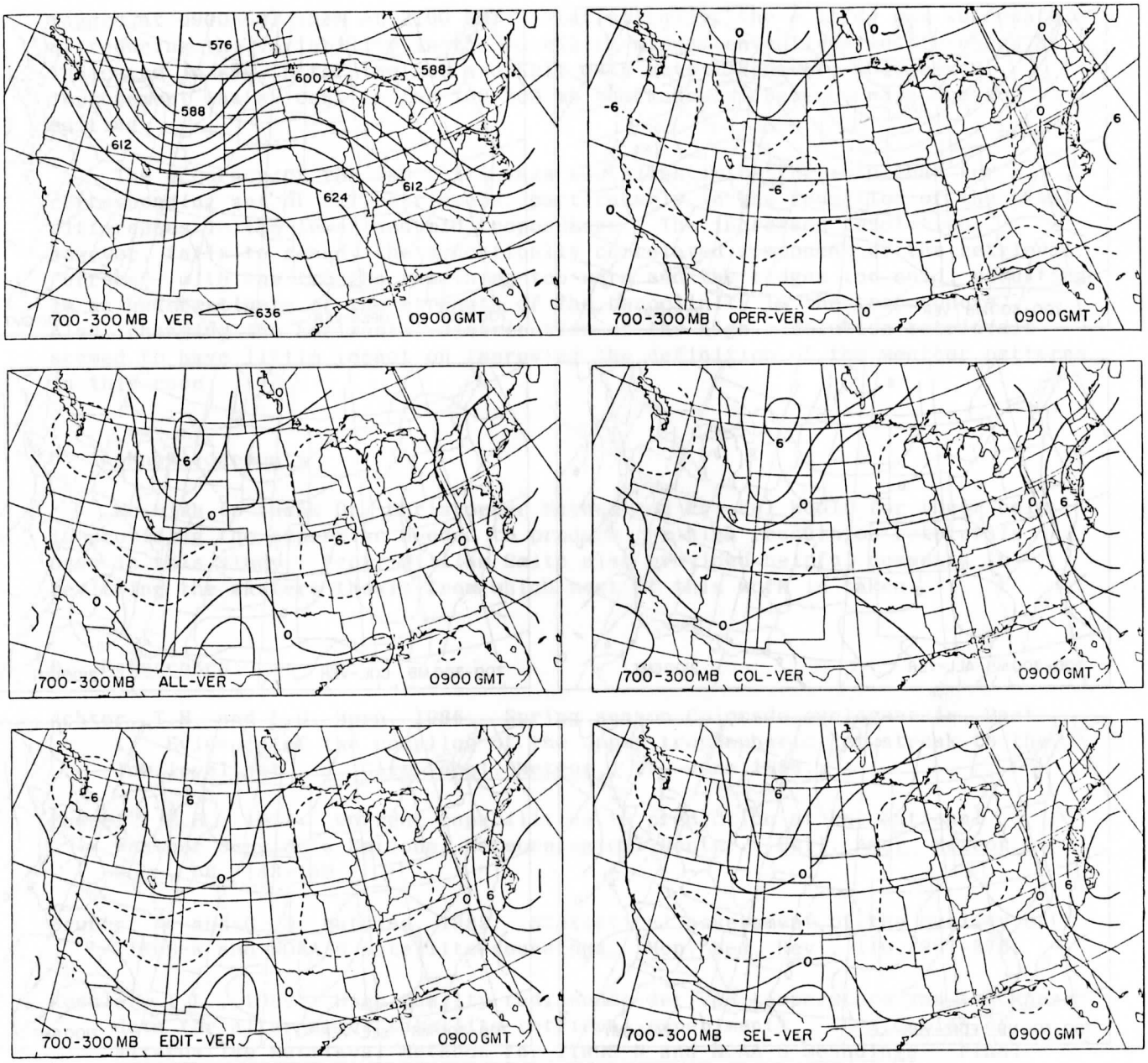

Figure 9. Verification (VER) and thickness difference maps for 5 sounding sets at 0900 GMT 6 January 1980. Dashed contours (dam) are negative, where the retrievals are colder than the verification data.

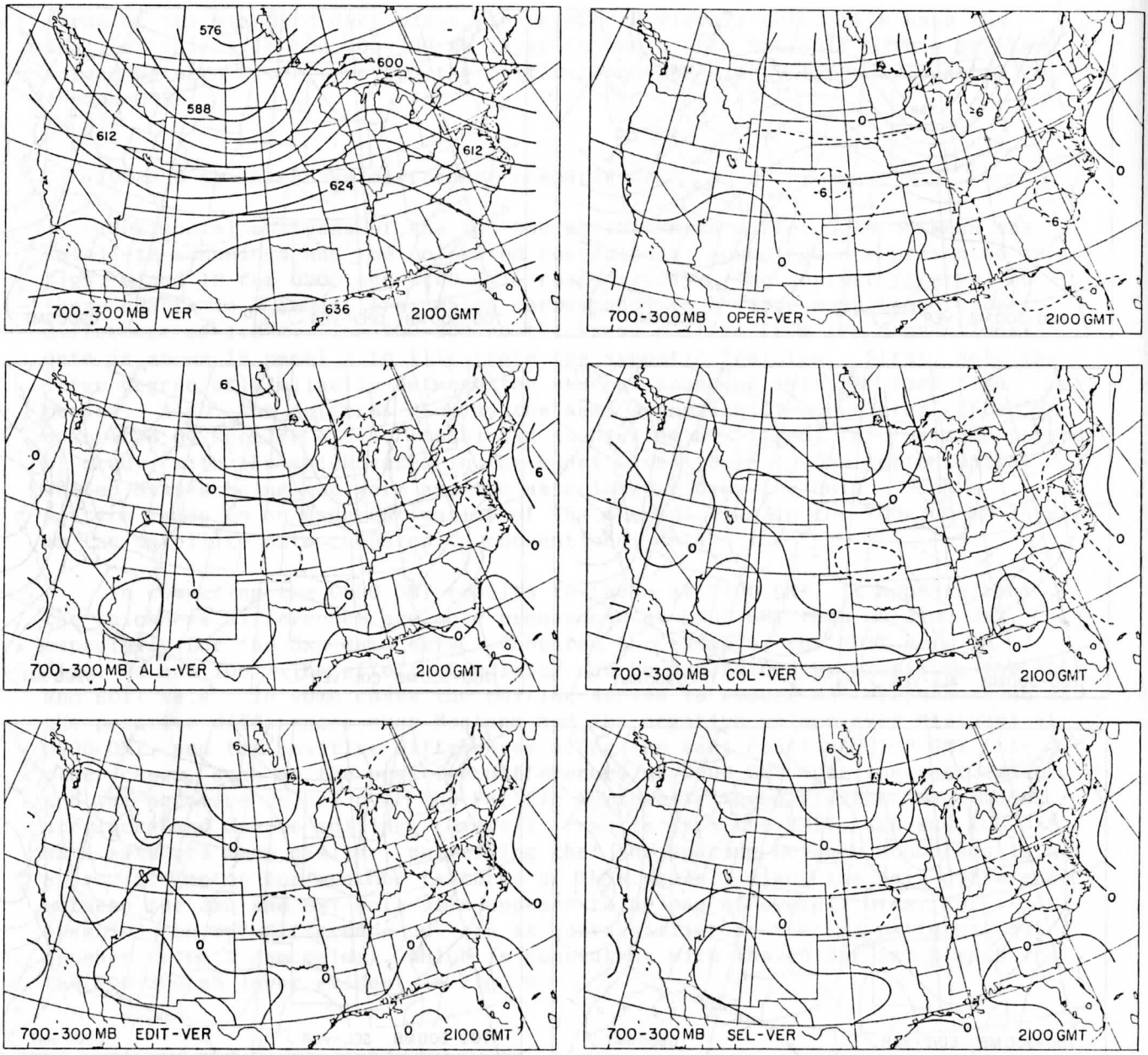

Figure 10. Same as Fig. 9, except for 2100 GMT 6 January 1980.

tagged at 0900 GMT than at 2100 GMT. Statistically, the editing was successful at reducing the variability in the satellite-minus-conventional differences as indicated in Fig. 5 for the ALL and EDIT data sets. However, only mixed improvement was evident in the 700-300 mb thickness difference maps due to editing.

The accuracy of the 3x3 retrievals was slightly better than that for a corresponding set of 9x7 retrievals, particularly in the reduction of the bias differences in the lower and mid-troposphere. The increased resolution, however, fails to remedy the synoptically correlated component of the retrieval "errors", with the troughs remaining too warm and the ridges too cold, resulting in an underestimate of the strength of the baroclinity in the troposphere. Also, changing the horizontal distribution of the high resolution retrievals seemed to have little impact on improving the definition of the weather patterns in this case.

5. Acknowledgements

We wish to thank Dr. Christopher Hayden and Mr. Hal Woolf for their help in providing the expertise needed to produce the high resoultion retrievals used in this study. Prof. William Smith also provided helpful comments in reviewing the masters thesis from which most of this work is taken.

6. References

Achtor, T.H. and L.H. Horn, 1986: Spring season Colorado cyclogenesis. Part I: Evidence of the coupling of the upper tropospheric jet streak to the low level jet. J. Clim. Appl. Meteor., 25, June 1986.

Fawcett, E.B., 1977: Current capabilities in prediction at the National Weather Service's National Meteorological Center. Bull. Amer. Meteor. Soc., 58, 143-149.

Gruber, A. and C. D. Watkins, 1982: Statistical assessment of the quality of TIROS-N and NOAA-6 satellite soundings. Mon. Wea. Rev., 110, 867-876.

Koehler, T.L., 1986: High quality radiosonde-derived temperature and thickness data for alternative satellite retrieval experiments. Evaluation of Alternative Retrieval Methods for TIROS-N and NOAA-6 Soundings. Final Report, NOAA Grant NA81AA-D-00087, Dept. of Meteorology, University of Wisconsin-Madison, 22-25.

Koehler, T.L. and C.J. Seman, 1986: A modified version of the NESDIS TOVS Export Package for use in alternative retrieval method studies. Evaluation of Alternative Retrieval Methods for TIROS-N and NOAA-6 Soundings. Final Report, NOAA Grant NA81AA-D-00087, Dept. of Meteorology, University of Wisconsin-Madison, 9-21.

Koehler, T.L., J.C. Derber, B.D. Schmidt and L.H. Horn, 1983: An evaluation of soundings, analyses and model forecasts derived from TIROS-N and NOAA-6 satellite data. Mon. Wea. Rev., 111, 562-571.

Koehler, T.L., J.P. Nelson and L.H. Horn, 1986: An evaluation of a physical retrieval method as an alternative to the statistical method used in the NESS operational sounding processing during FGGE. Evaluation of Alternative Retrieval Methods for TIROS-N and NOAA-6 Soundings. Final Report, NOAA Grant NA81AA-D-00087, Dept. of Meteorology, University of Wisconsin-Madison, 26-46.

Phillips, N., L. McMillin, A. Gruber and D. Wark, 1979: An evaluation of early operational temperature soundings from TIROS-N. Bull. Amer. Meteor. Soc., 60, 1188-1197.

Reed, R.J., 1977: The development and status of modern weather prediction (Bjerknes Memorial Lecture). Bull. Amer. Meteor. Soc., 58, 390-400.

Schlatter, T.W., 1981: An assessment of operational TIROS-N temperature retrievals over the United States. Mon. Wea. Rev., 109, 110-119.

Seman, C.J., 1985: A case study evaluating different horizontal resolution in radiance compositing for TIROS-N retrievals. M.S. Thesis, Dept. of Meteorology, University of Wisconsin-Madison, 89 pp.

Tracton, M.S. and R.D. McPherson, 1977: On the impact of radiometric sounding data upon operational numerical weather prediction at NMC. Bull. Amer. Meteor. Soc., 58, 1201-1209.

AN EVALUATION OF SCAN ANGLE DEPENDENCE IN LIMB-CORRECTED MSU BRIGHTNESS TEMPERATURES

by

Thomas L. Koehler

Abstract

Evaluations of the limb correction technique applied by NESS to the TIROS-N MSU observed brightness temperatures are presented. Observed brightness temperatures both before aand after limb correction are compared to simulated brightness temperatures derived from conventional radiosonde measurements.

Results suggest a left to right bias in the limb-corrected MSU data, with the left side colder than the right side. The data before limb correction can be reproduced more accurately in simulation. Incorporating the actual MSU antenna patterns into the simulations removes part of the left to right bias.

1. Introduction

The accuracy of the satellite derived temperature profiles produced operationally by NESS during the FGGE year has been the topic of several studies, including Phillips et al. (1979), Schlatter (1981), Gruber and Watkins (1982), and Koehler et al. (1983). Errors in satellite retrievals can arise from several sources, such as radiance measurement errors, errors in the retrieval algorithm, and basic physical limitations in the determination of atmospheric temperature profiles from satellite radiance measurements. The two preceding papers in this project report (Koehler et al. 1986, and Seman et al. 1986) have focused on alternatives to two aspects of the retrieval technique. They found very little improvement in the accuracy of the retrievals from either using a physical retrieval algorithm instead of the operational statistical method, or from compositing the radiance information over 3x3 HIRS/2 field-of-view arrays, instead of the 9x7 arrays used in the operational method. Another study by LeMarshall and Schreiner (1985) suggests that limb correction of the basic radiance data may contribute to satellite sounding errors. The study presented here will examine the accuracy of the limb correction procedure for the microwave channels by comparing the MSU observed brightness temperatures both before and after limb correction to simulated brightness temperatures derived from conventional temperature measurements. Attention will be focused on measurements made by the Microwave Sounding Unit aboard the TIROS-N satellite.

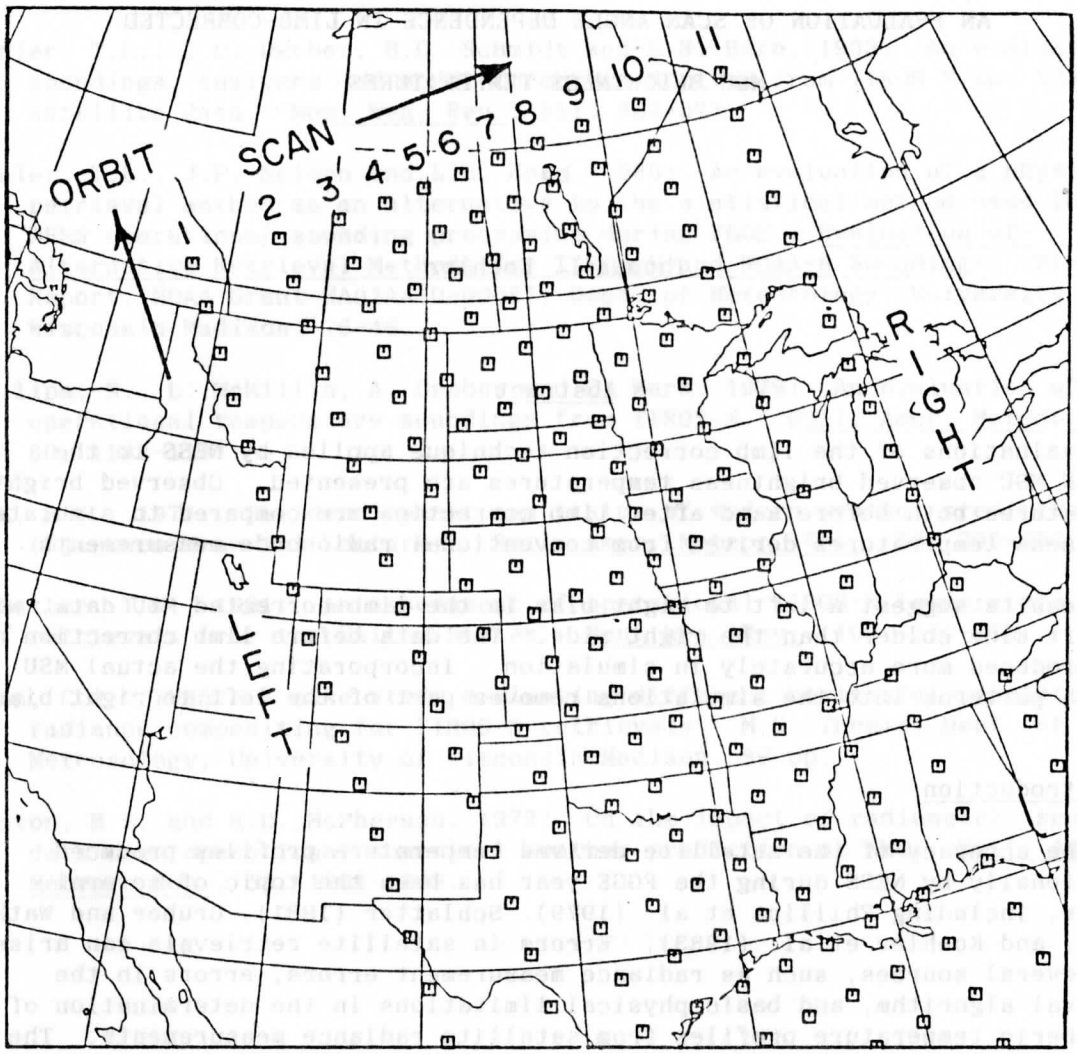

Figure 1. MSU scan locations for 2100 GMT 6 Januray 1980. The numbering system for the different scan positions is shown going from 1 to 11 moving from left to right. As in the figures that follow, the arrow is drawn on the left of the pass and points in the direction of the orbit.

While both the HIRS/2 and MSU measurements are limb corrected, the assessment of the limb correction procedure was confined to the microwave measurements for two reasons. First, spatial coverage for the evaluation is better in the microwave than in the infrared part of the spectrum, since the microwave measurements are only marginally affected by the presence of clouds. Second, due to relative insensitivity to the presence of clouds, the microwave measurements are used frequently in several steps in the operational retrieval algorithm, such as detecting possible cloud contamination in the infrared measurements, and in estimating the appropriate retrieval coefficients to be applied in the statistical determination of atmospheric temperatures from radiance measurements.

2. A description of MSU measurements

While descriptions of the MSU instrument are available in the literature (e.g., Grody, 1983), a brief overview of the microwave instrument and principles of microwave measurements is essential to understanding the numerical techniques and results from this study. The MSU consists of two 10.2 cm antenna systems that make measurements at four frequencies (50.30, 53.74, 54.96 and 57.95 GHz). The antenna scans from left to right in eleven 9.47^{o} steps across the orbital track. Fig. 1 illustrates a typical distribution of the center points of the microwave observations from one orbit over the central United States. The numbering system for identifying the scan positions used in this paper is also shown in the figure, with position 6 corresponding to the nadir position, and positions 1 and 11 corresponding to the extreme scan angles of -47.35^{o} and $+47.35^{o}$ respectively. Actual microwave measurements are really volumetric in nature, with most of the energy coming from a conical volume whose intersection at the earth's surface forms a circle at nadir with a diameter of approximately 110 km, and an ellipse at the extreme angles with major and minor axes of 325 and 179 km, respectively. Since the wavelength being measured (0.5 cm) is not negligible compared to the instrument dimensions, the MSU exhibits diffraction properties, causing what are called side lobes in the antenna pattern. These side lobes produce a small proportion of the total measured energy that emanates from outside the nominal field-of-view described above.

The energy measured by a microwave sensor aboard an orbiting satellite is related to the vertical temperature distribution through the radiative transfer equation. The version of this equation valid for the microwave frequencies is

$$T_B(\nu) = \tau(p_s)\, T_s \varepsilon_s + \tau(p_s)(1-\varepsilon_s) \int_o^{p_s} T(p)\, \frac{\partial \tau'(p)}{\partial \ln p}\, d \ln p$$

$$+ \int_{p_s}^{o} T(p)\, \frac{\partial\, \tau\, (p)}{\partial \ln p}\, d \ln p \qquad (1)$$

where

$$\tau\,(p) = \exp\left[- \int_o^{p_s} \alpha(\nu, p, T)\ \sec \Theta\, dp \right] \qquad (2)$$

and

$$\tau'(p) = \tau(p_s)/\tau(p) \qquad (3)$$

In these expressions, T_B is the brightness temperature at a specified frequency (γ) which is proportional to the energy detected, T is the temperature as a function of pressure (p), T_s is the surface radiating temperature, ε_s is the surface emissivity, τ is the atmospheric transmittance of energy radiated toward space at a given pressure, τ' is the transmittance of energy radiated toward the earth's surface, and α is the atmospheric absorptivity at a particular pressure and frequency that varies as a function of temperature. Each term on the right side of Eq. 1 refers to a particular radiative process. The first term represents energy emitted by the earth's surface that reaches the satellite, the second is that portion of the atmospheric emission radiated downward toward the earth's surface then reflected back toward the satellite, and the final term represents direct upwelling atmospheric radiation.

The dependence of brightness temperature measurements on scan angle enters through the sec θ term in Eq. 2, where θ is the zenith angle of the satellite measured from the earth's surface. (See Appendix A for the relationship of θ to scan angle.) At greater scan angles, the upwelling energy must pass through a longer path in the atmosphere, which displaces the weighting function ($-\partial\tau/\partial \ell n\ p$) higher into the atmosphere, as illustrated in Fig. 2 for MSU Channels 2 and 3, the primary tropospheric sounding channels. The resulting effect of the vertical displacement of these weighting functions on T_B computed from the standard atmosphere with $\varepsilon_s = 1$ is shown in Fig. 3. Values at the edge of the orbit are almost 12 K colder than at the center for Ch. 2, but only 6.5 K colder for Ch. 3. This so-called "limb" effect is more pronounced for Ch. 2 than Ch. 3 because most of the signal for Ch. 2 comes from below 200 mb, a region with a constant 6.5 K/km lapse rate in the standard atmosphere, while more of the signal for Ch. 3 comes from the isothermal region from 200 to 70 mb, where vertical displacement of the weighting functions will have less of an impact on the resultant brightness temperatures.

3. The operational limb correction procedure

The NESS operational retrieval technique was designed to use brightness temperatures that were corrected for the effect of scan angle. The limb correction procedure for the MSU channels corrects not only for limb effects, but also attempts to compensate for several other factors that affect the actual microwave measurements, including precipitating clouds, variable surface emissivity, and side lobes in the antenna pattern. While the microwave measurements are rather insensitive to the presence of cloud droplets, precipitation, especially convective precipitation, can affect the measurements, as shown for example in Grody (1983). Also, the surface emissivities for the microwave channels are more variable than for infrared channels, with the emissivity varying from 0.5 over water to nearly 1.0 over dry land. Finally, as mentioned earlier, antenna response patterns for the microwave instruments display side lobes produced by diffraction properties of the instrument. The antenna pattern applied in the limb correction technique is labelled SCAMS in Fig. 4 (Woolf, personal communication, 1984a). While most of the response occurs

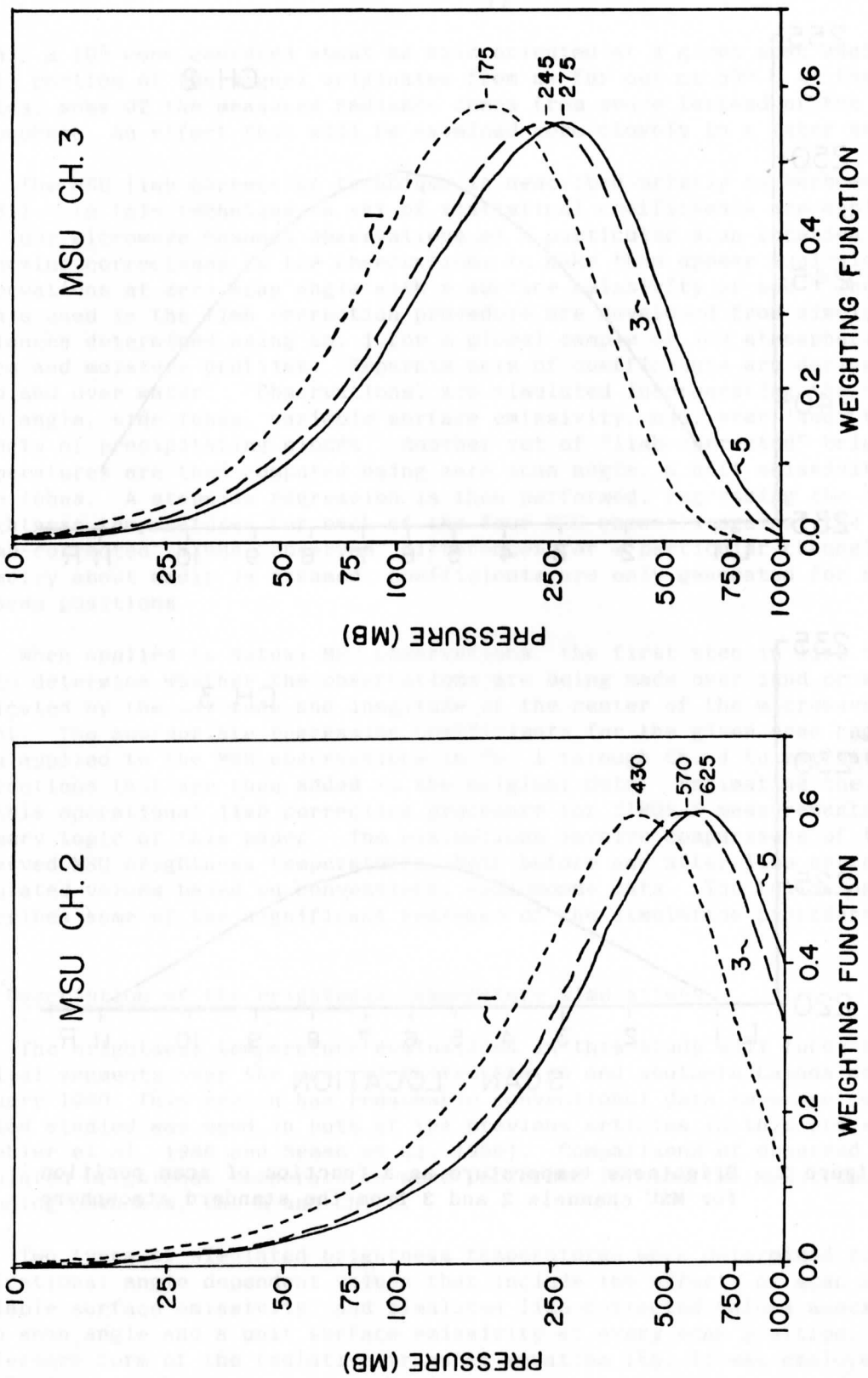

Figure 2. Brightness temperature weighting functions from the standard atmosphere for MSU channels 2 and 3 at scan positions 1, 3 and 5.

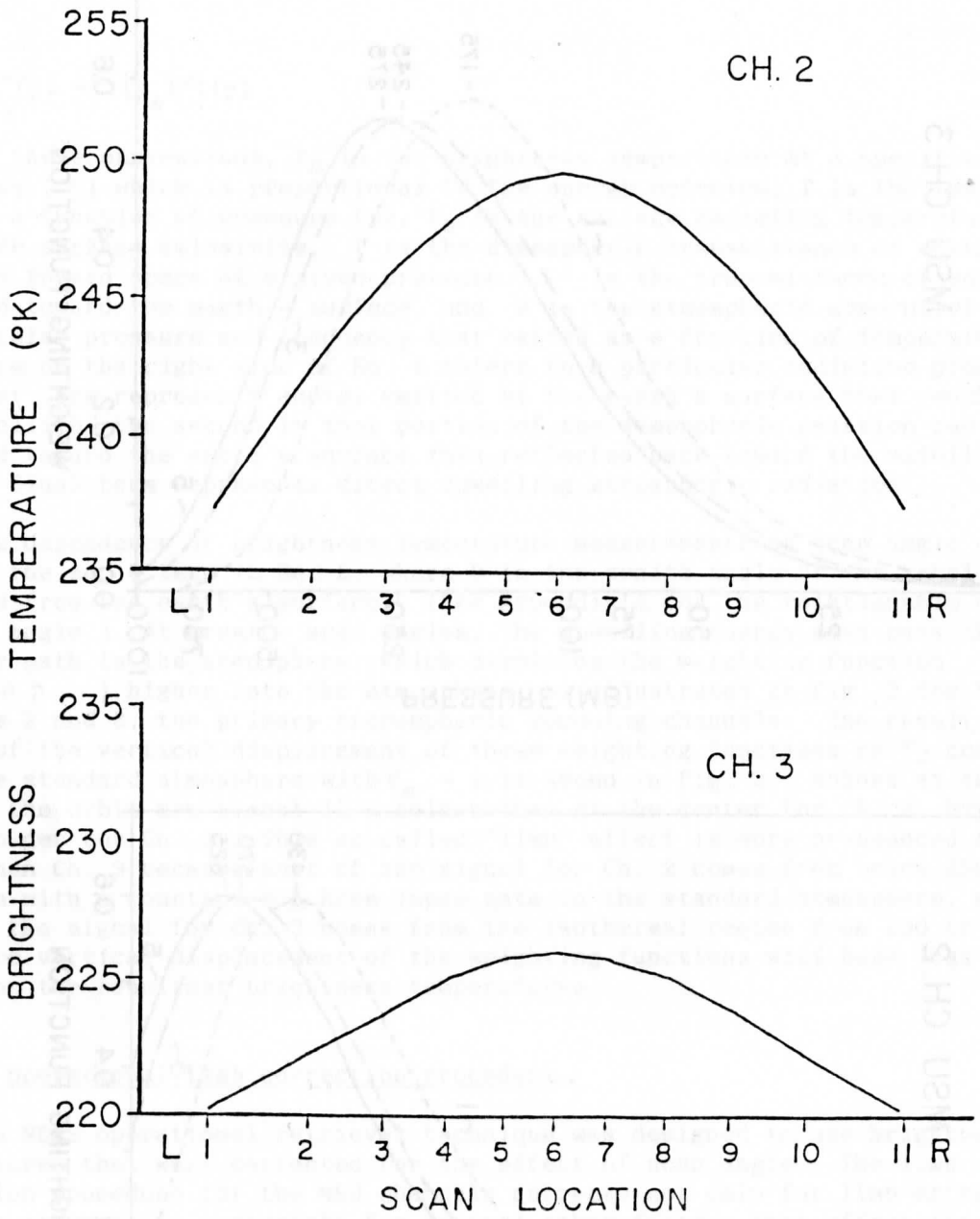

Figure 3. Brightness temperature as a function of scan position for MSU channels 2 and 3 from the standard atmosphere.

within a 10^{o} cone centered about an axis oriented at a given scan angle, a small portion of the signal originates from as far out as 63^{o}. At the far scan angles, some of the measured radiance comes from space instead of the earth's atmosphere, an effect that will be examined more closely in a later section.

The MSU limb correction technique is described briefly in Werbowetzki (1981). In this technique, a set of statistical coefficients are applied to the four microwave channel observations at a particular scan location to determine corrections to the observations to make them appear equivalent to observations at zero scan angle with a surface emissivity of one. The coefficients used in the limb correction procedure are developed from simulated radiances determined using Eq. 1 for a global sample of 100 atmospheric temperature and moisture profiles. Separate sets of coefficients are derived over land and over water. "Observations" are simulated incorporating the effects of scan angle, side lobes, variable surface emissivity, and, over land, the effects of precipitating clouds. Another set of "limb-corrected" brightness temperatures are then computed using zero scan angle, a unit emissivity and no side lobes. A stepwise regression is then performed, regressing the "observed" brightness temperatures for each of the four MSU channels against the "limb-corrected" minus "observed" differences for a particular channel. Since symmetry about nadir is assumed, coefficients are only generated for 6 of the 11 scan positions.

When applied to actual MSU observations, the first step in limb correction is to determine whether the observations are being made over land or water, as indicated by the latitude and longitude of the center of the microwave footprint. The appropriate regression coefficients for the given scan angle are then applied to the MSU observations in Ch. 1 through Ch. 4 to estimate corrections that are then added to the original data. Estimating the accuracy of this operational limb correction procedure for TIROS-N measurements is the primary topic of this paper. The evaluations involve comparisons of the observed MSU brightness temperatures, both before and after limb correction, to simulated values based on conventional radiosonde data. The following section describes some of the significant features of the simulation procedure.

4. Description of the brightness temperature simulations

The brightness temperature evaluations in this study will focus on four orbital segments over the central United States and southern Canada on 5-6 January 1980. This region has reasonable conventional data coverage, and the period studied was used in both of the previous articles in this project report (Koehler et al. 1986 and Seman et al. 1986). Comparisons of observed and simulated brightness temperatures were performed for the two MSU tropospheric sounding channels, Ch. 2 and Ch. 3.

Two types of simulated brightness temperatures were determined for the evaluations: angle dependent values that include the effects of scan angle and variable surface emissivity, and simulated limb-corrected values assuming a zero scan angle and a unit surface emissivity at every scan position. A finite difference form of the radiative transfer equation (Eq. 1) was employed in the simulation, which required atmospheric temperature estimates and transmittance

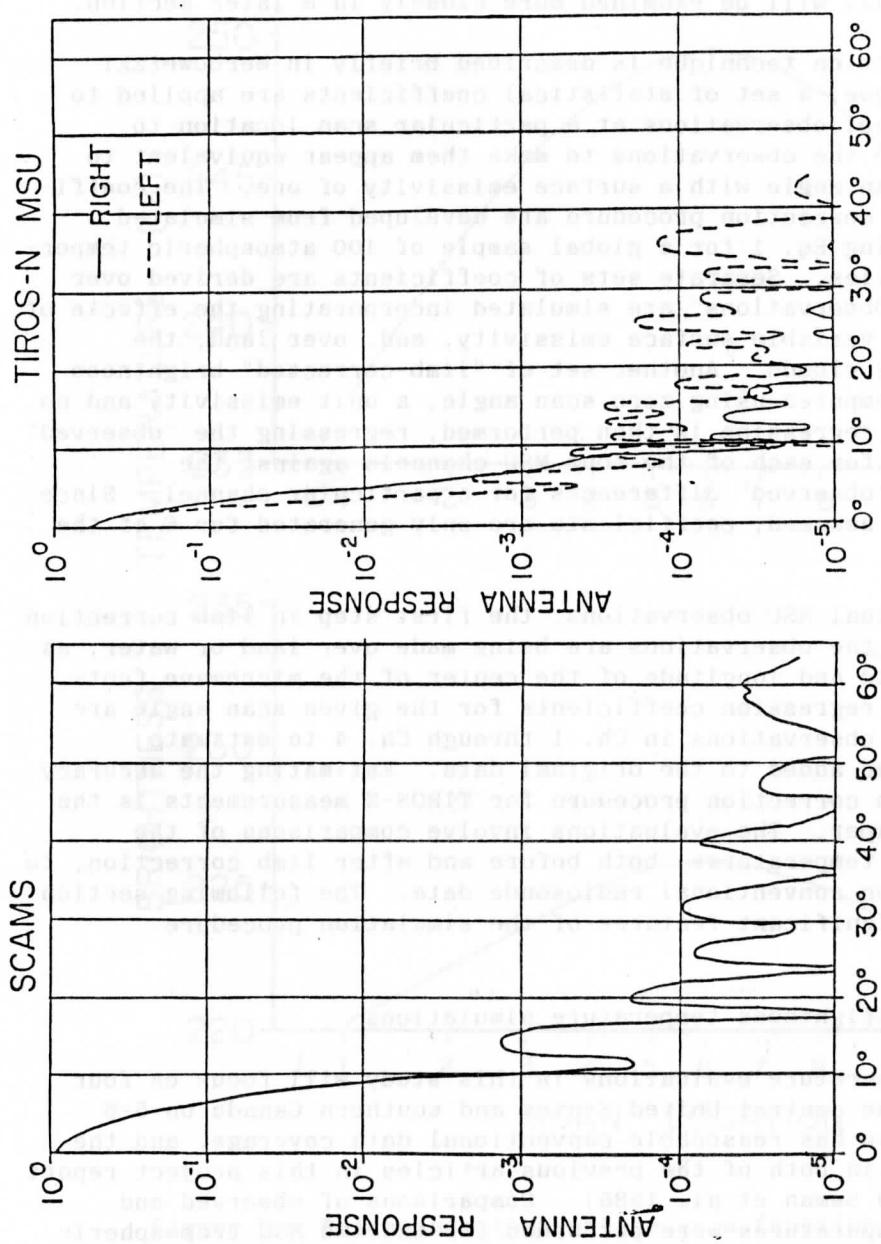

Figure 4. Microwave antenna response functions for the SCAMS nominal footprint used in the development of the TIROS-N limb correction coefficients and the actual TIROS-N response function for Ch. 2 at nadir. Left and right refer to the side of the footprint facing the direction of the satellite motion.

coefficients at the 40 isobaric levels from 1000 to 0.1 mb used in the standard NESDIS retrieval algorithms. Estimates of the surface pressure, skin temperature and surface emissivity at each scan location were also needed.

Temperature values for the 21 tropospheric levels from 1000 to 100 mb are interpolated in time and space to the MSU observation location from horizontal analyses of temperature derived from conventional radiosonde observations in a manner described in Koehler (1986). Temperatures at and above 50 mb were taken from the regional climatology described in Koehler and Seman (1986). To avoid an abrupt discontinuity between the conventional tropospheric temperature data and the climatological values in the upper atmosphere, adjustments were made to the climatological values based on the observed and climatological temperature difference at 100 mb. A fraction of the 100 mb difference was added to the climatological values at 85 and 70 mb based on the following expression.

$$T(p) = T_C(p) + \left[T(100mb) - T_C(100mb) \right] \frac{\ln (p/50mb)}{\ln (100mb/50mb)} \qquad (4)$$

where T_C is the climatological temperature.

Surface pressure was determined hydrostatically using the colocated observed temperatures and 1000 mb height, and a terrain elevation for the center of the microwave footprint. The skin temperature was assumed to equal the air temperature at the surface, and the surface emissivity was estimated from Ch. 1 in a manner described in Appendix B.

Finally, two sets of transmittance coefficients were applied in parts of this study. The set used most often is the standard NESDIS coefficients described in Weinreb et al. (1981), while the other set was developed by the NESDIS Development Laboratory in Madison, WI. This latter set will be referred to as the angle-dependent transmittances, because the coefficients were determined at different scan angles, assuming symmetry about nadir (Woolf, 1984b, personal communication).

Before proceeding to discussions of the observed-minus-simulated results, it is important to recognize the possible sources for these differences that can be found in either the observations or in the simulated brightness temperatures. The most obvious source of error is measurement error by the MSU instrument, which should be random in nature, and has been estimated to be about 0.5 K for Chs. 2 and 3. The limb correction provides another "observational" source of error. In essence, the limb correction procedure attempts to: 1) adjust the measurements to a zero scan angle, 2) remove the effect of varying surface emissivity and possible precipitation, and 3) account for side lobes in the MSU antenna pattern. All this is accomplished by applying linear regression to the four observations at the different MSU frequencies. Errors in limb correction may enter from deriving the regression coefficients from too limited a sample of atmospheric distributions. Sources of error in simulated brightness temperatures include: 1) measurement errors in the original radiosonde temperature observations, 2) analysis errors in transferring these temperatures to a uniform grid, 3) errors in the colocation procedure to the MSU scan location, 4) the use of climatological data above 100 mb, 5) possible

limitations in modeling the transmittance functions, and 6) ineffective treatment of the instrument side lobes. It is impossible to identify the exact proportion of each of the sources of error in any given observed-minus-simulated difference. However, some insight into the sensitivity of several of these components can be gained from the comparisons to be presented in the following section.

5. Results

The following presentation is divided into three subsections. The limb-corrected observed-minus-simulated differences are presented first, followed by results without limb correction in which the side lobe effects were ignored when the simulated brightness temperatures were computed. The final set of comparisons involve the basic brightness temperatures versus simulated values computed using different models of the MSU antenna side lobes.

A. Evaluation of the limb-corrected data

Map analyses of the differences between the limb-corrected MSU observations and simulated brightness temperatures derived from conventional temperature observations assuming zero scan angle and unit surface emissivity for MSU Ch. 2 are shown in Fig. 5. Four orbital segments separated in time by about 12 hours over the central United States and southern Canada are presented. The arrow in the diagram drawn on the left side of the orbit indicates the direction of the orbital path. The 0900 GMT orbits are descending orbits, while the 2100 GMT orbits are ascending orbits. Note also that negative differences are shaded, indicating areas in which the limb-corrected observations are colder than their simulated counterparts. Negative differences can arise either from the observations being too cold or the simulated values being too warm.

Two consistent patterns emerge from the results from this channel which peaks near 625 mb. First, large positive differences appear in the northern parts of the orbit where cold air is situated in the conventional 850 mb analyses shown in Fig. 6. Other large positive differences are also found on the right edge of the orbits. The largest negative differences are on the left side of the orbits, displaced one or two scan positions in from the left edge, with values greater than -2.0 K found over the Rockies at 2100 GMT 5 January. Note also the very strong gradient in brightness temperature differences extending from central Wyoming northward through Montana, and that the orientation of the difference isotherms corresponds well with the isotherm orientation on the 1200 GMT 5 January 850 mb chart. A similar orientation is found over the Northern Plains 24 hours later.

The effects of water vapor, clouds and precipitation were not fully considered in the simulation. Fig. 7 depicts the cloud and precipitation patterns and surface frontal positions at the time of the satellite orbits. These depictions were derived from NMC surface and radar charts, and satellite pictures. The consistent patterns in the brightness temperature difference fields just noted seem to bear little resemblance to the cloud and precipitation

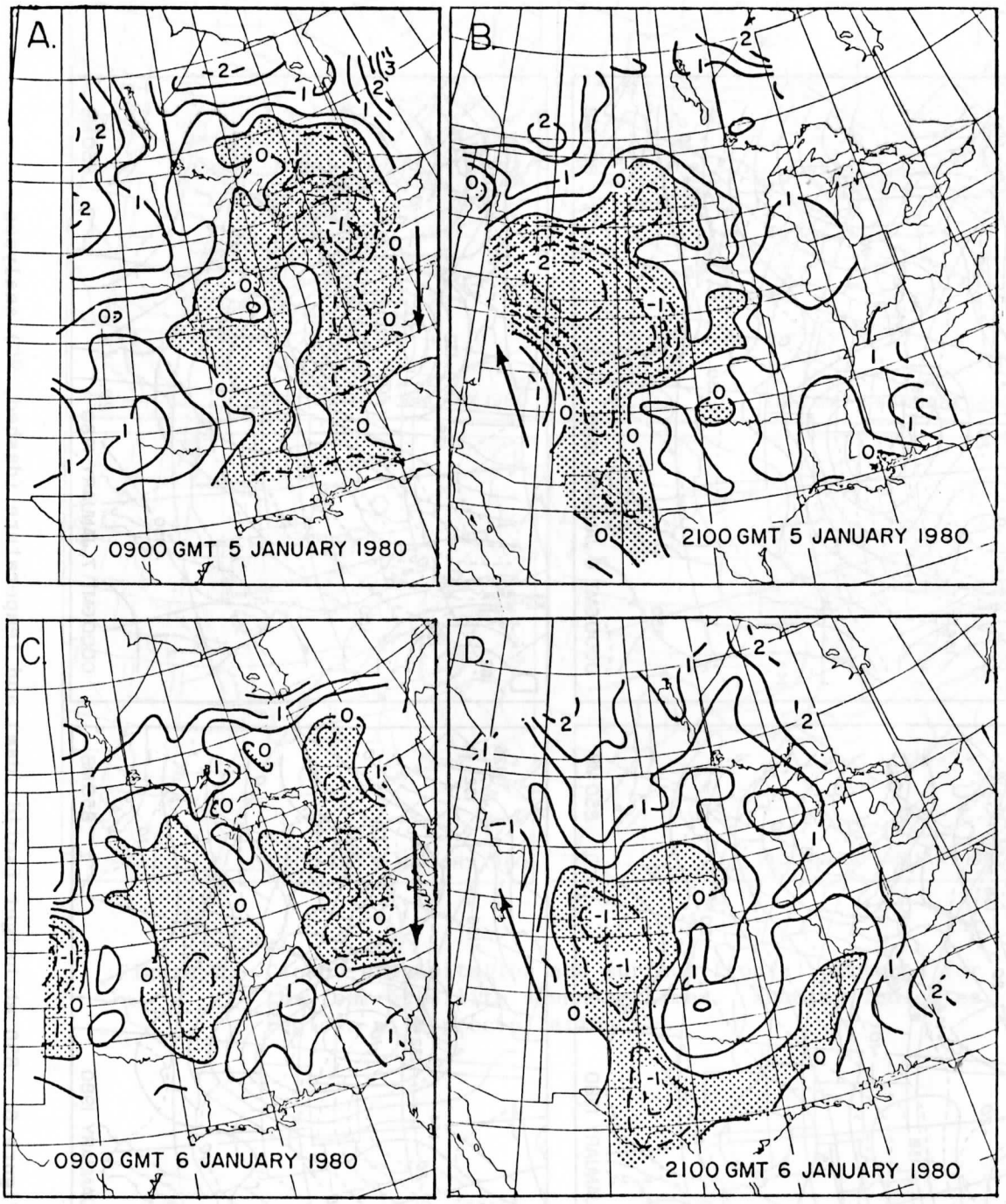

Figure 5. Differences between the limb-corrected observed brightness temperatures and their simulated counterparts (K).

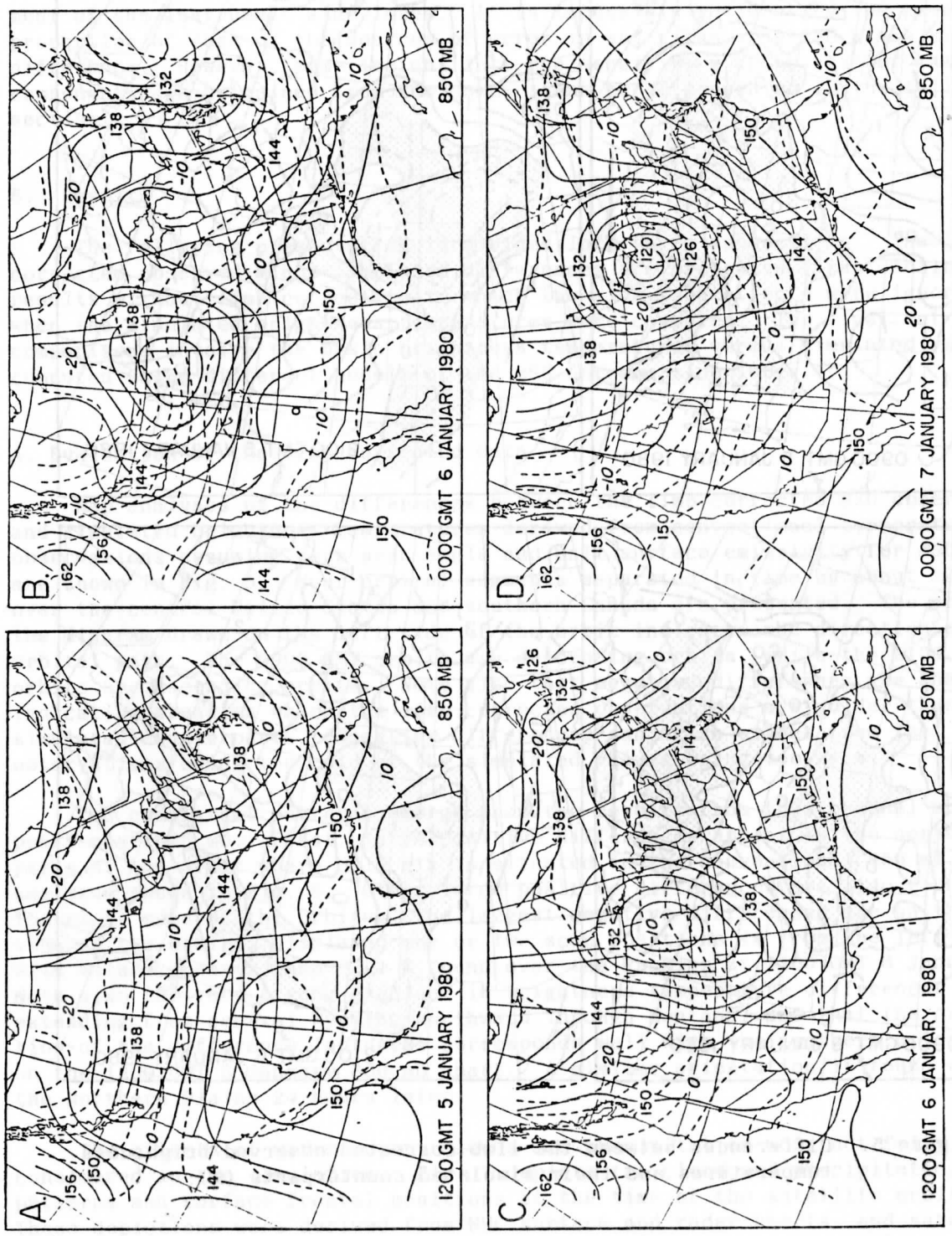

Figure 6. 850 mb height (solid, dam) and temperature (dashed, ^{o}C) analyses.

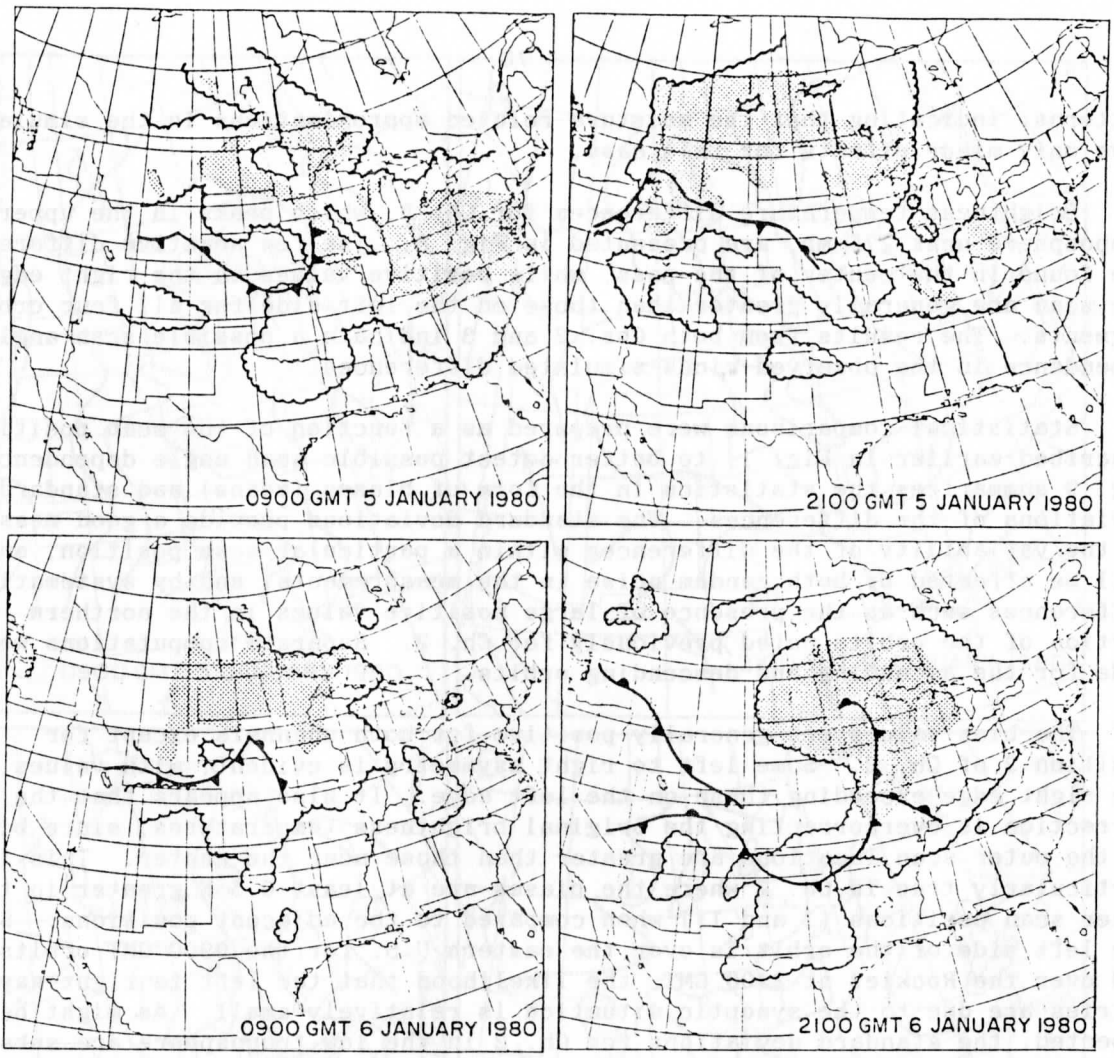

Figure 7. Cloud, precipitation and surface frontal patterns for the four satellite sounding times. Shading indicates regions with precipitation.

patterns, indicating that the moisture-related approximations in the simulation have only minor effects for this case.

Brightness temperature differences for Ch. 3, which peaks in the upper troposphere near 275 mb, are presented in Fig. 8. The few negative differences are found in the center of the pass, while positive values on the right edge of the scan are generally greater than those on the left side for all four orbital segments. The results from both Chs. 2 and 3 indicate a possible scan angle dependence in the observed-minus-simulated differences.

Statistical comparisons were prepared as a function of the scan positions described earlier in Fig. 1, to better detect possible scan angle dependence. Fig. 9 summarizes the statistics in the form of biases (means) and standard deviations of the differences. The standard deviations provide a good measure of the variability of the differences within a particular scan position, and will be affected by both random noise in the measurements, and by systematic differences such as the presence of large positive values in the northern portion of the orbits noted previously for Ch. 2. Separate computations were made for the ascending and descending orbits.

The bias values are generally positive for both channels except for position 2 of Ch. 2. Some left to right asymmetry is evident, with values on the right edge exceeding those on the left edge. It also appears that the limb correction is overcorrecting the original brightness temperatures, since biases at the outer scan locations are greater than those near the center. This is particularly true in Ch. 2 where the biases are at least 0.5 K greater in the outer scan positions (1 and 11) when compared to the adjacent positions. Since the left side of the orbit is over the eastern U.S. for the 0900 GMT orbits, and over the Rockies at 2100 GMT, the likelihood that the left to right asymmetries are due to the synoptic situation is relatively small. As might be expected, the standard deviations for Ch. 2 in the low troposphere are substantially greater for the positions over the Rockies, primarily on the left side of the 2100 GMT ascending orbits. The effect of terrain is considerably less important for Ch. 3. In summary, the limb-corrected brightness temperature difference bias statistics indicate a possible left to right asymmetry in the MSU observations and suggest overcorrection of the original brightness temperature measurements at the outer scan positions. Standard deviations of the differences are nearly twice as large for Ch. 2 compared to Ch. 3, and increase for Ch. 2 in regions with high terrain.

B. Evaluations of the original uncorrected brightness temperatures

As noted previously, the differences between the observed and simulated brightness temperature arise from several sources. Thus the accuracy of the limb correction procedure cannot be judged solely on the difference distributions just presented. Insight can be gained by comparing brightness temperature difference distributions both with and without limb correction. This section presents results based on differences between the original brightness temperature observations (without limb correction), and simulated values derived from two different models of the MSU observations. Both of the simulations incorporate the effects of varying scan angle and surface emissivity. In comparing

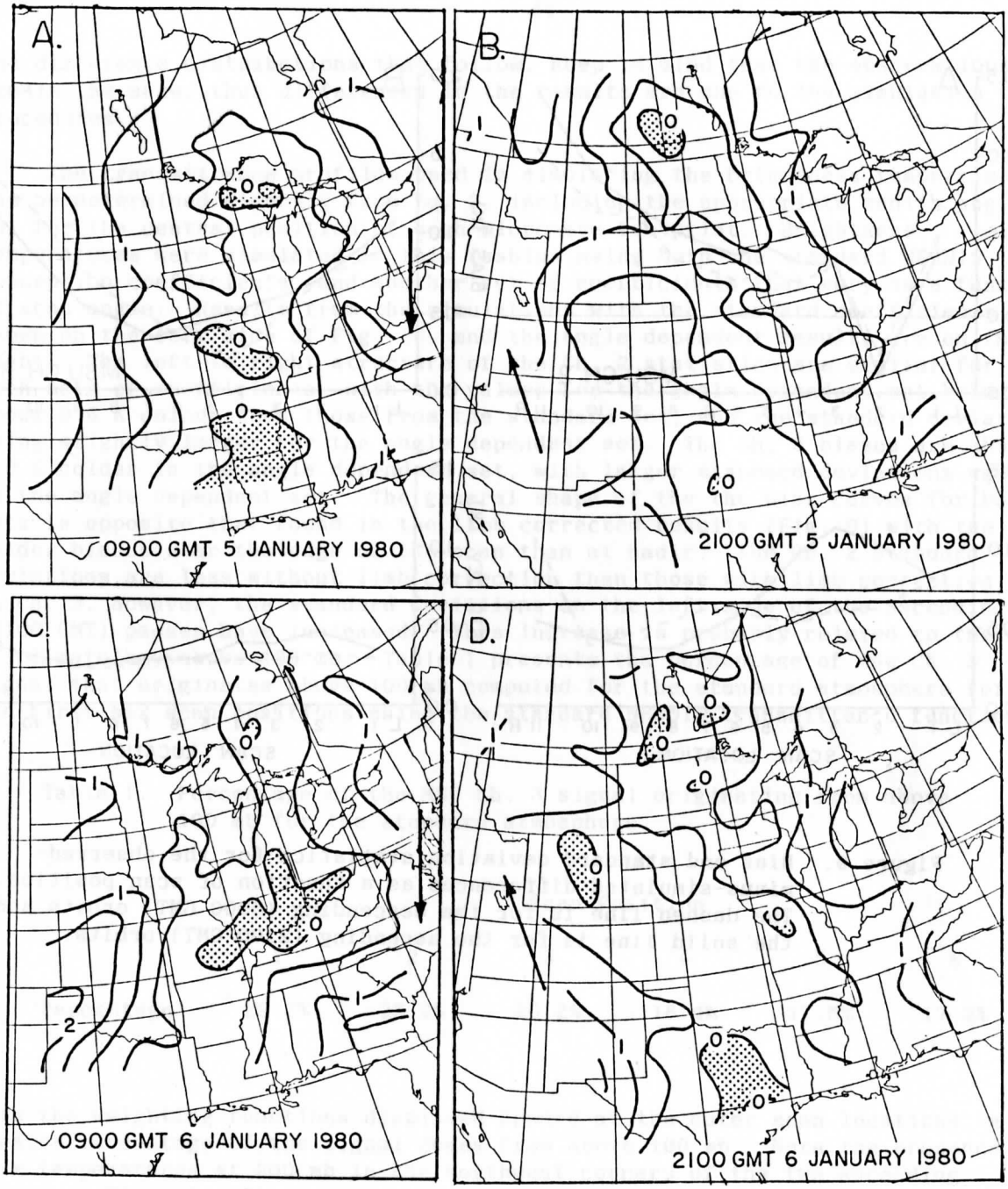

Figure 8. Same as Fig. 5 except for Ch. 3.

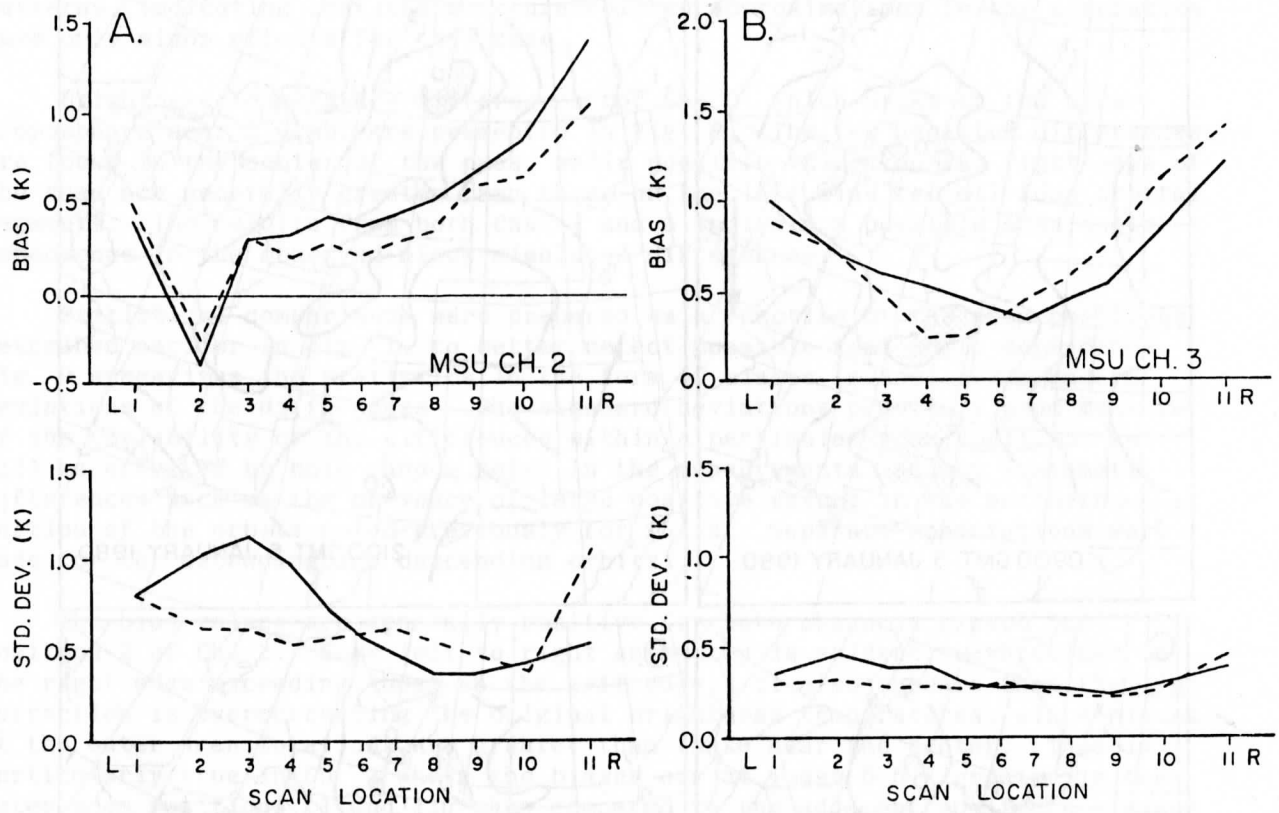

Figure 9. Bias and standard deviation statistics for the observed-minus-simulated differences as a function of scan position. The dashed line is for the descending (0900 GMT) orbits and the solid line is for the ascending (2100 GMT) orbits.

the difference distributions that follow, keep in mind that the observations remain the same, thus differences in the results are due to the simulation procedures.

The transmittance profiles used in simulating the brightness temperatures can be determined directly from Eq. 2, including the appropriate zenith angle (θ) for the central position of each microwave footprint. Brightness temperatures were simulated in this fashion using both the standard NESDIS absorption coefficients, and another set of coefficients that vary as a function of scan angle. Results from the simulations with the standard coefficients are shown on the left side of Fig. 10, and the angle dependent results are on the right. The left to right structure of the Ch. 2 statistics are similar for both sets of coefficients, with the values for the angle dependent set being about 0.6 K colder than those from the standard set, and the standard deviations being slightly larger for the angle dependent set. The Ch. 3 biases are about 1.0 K colder in the angle dependent set, with larger standard deviations again in the angle dependent set. The general shape of the the bias curves for both sets is opposite that found in the limb corrected results (Fig. 9) with the colder biases near the edge of the scan than at nadir. The Ch. 2 standard deviations are less without limb correction than those with limb correction. In Ch. 3, however, the standard deviations on the left side of the ascending (2100 GMT) passes have increased. This increase is probably related to the use of climatology above 100 mb. Table 1 presents the percentage of the Ch. 3 signal that originates above 100 mb computed for the standard atmosphere for the first six scan positions using the standard NESDIS transmittance functions.

Table 1. Percentage of the MSU Ch. 3 signal originating from above 100 mb for the standard atmosphere.

	Scan Position					
	1	2	3	4	5	6
Percentage	29.2%	23.2%	20.2%	18.4%	17.5%	17.2%

With the weighting functions displaced upward at the outer scan locations, a greater percentage of the signal comes from above 100 mb. Note the presence of warm temperatures at 200 mb in the northwest corners of the two ascending orbits in Fig. 11. These warm temperatures are associated with the propagating shortwave trough and denote a low tropopause in these regions. The lower stratospheric temperatures in a region of low tropopause exhibit large deviations from climatology. Thus the use of climatological values above 100 mb is likely responsible for the larger Ch. 3 standard deviations on the left side of the scan in the 2100 GMT orbits, because the climatological values are receiving more weight in the simulation without limb correction than in the simulation with limb correction.

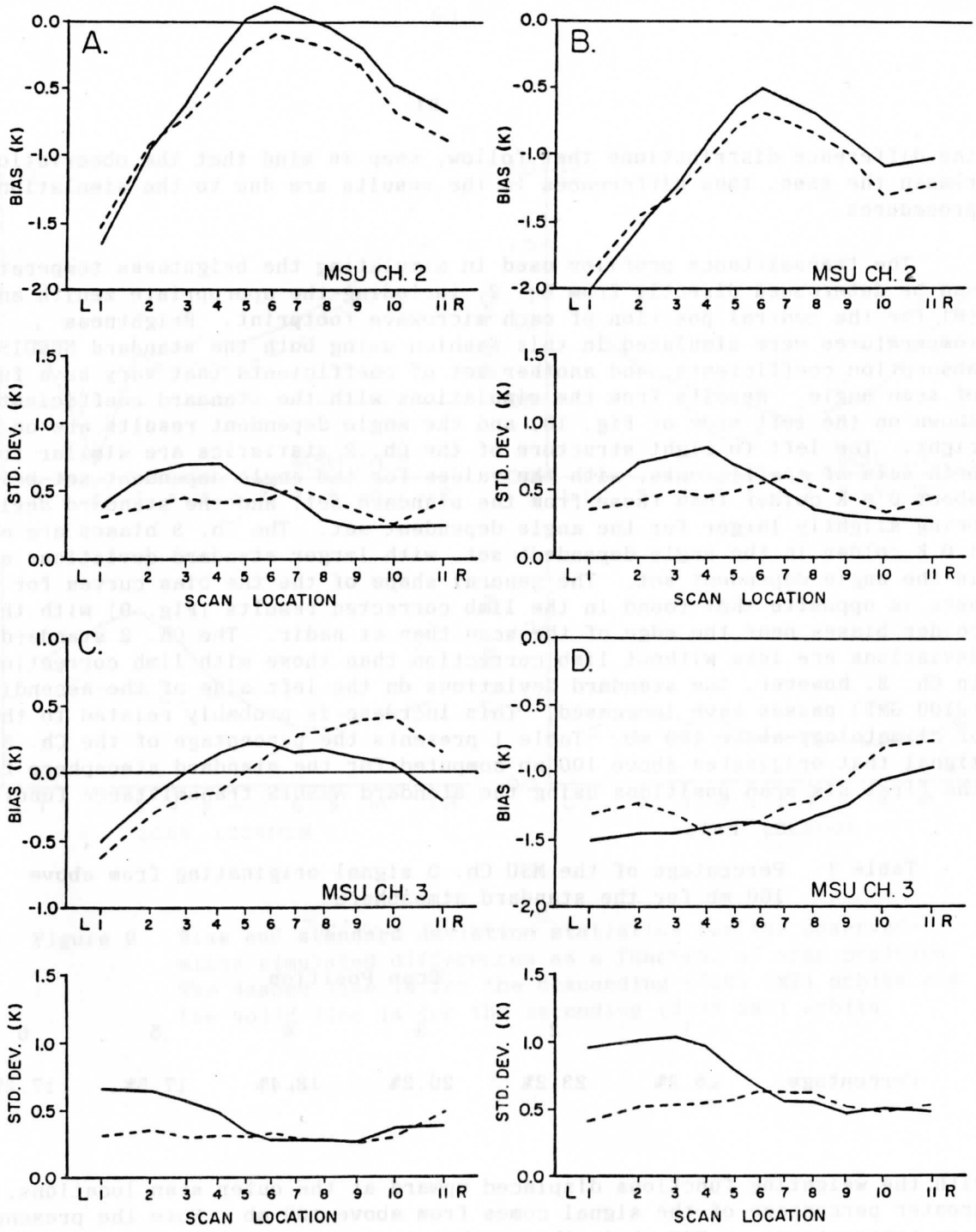

Figure 10. Brightness temperature difference statistics for the observations without limb correction and with no side lobe correction. Panels A and C for the standard NESDIS transmittance functions, and panels B and D for the angle dependent transmittances.

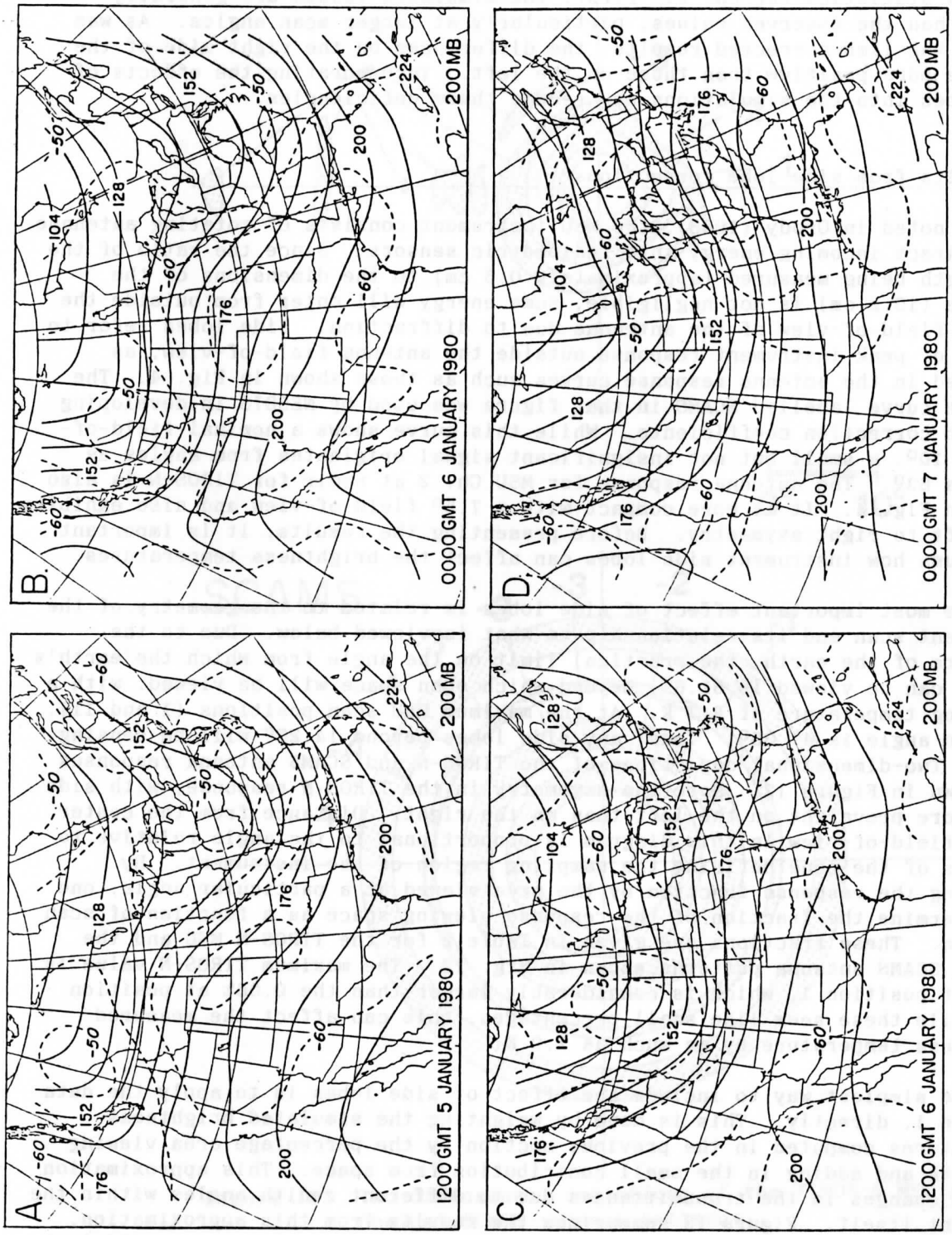

Figure 11. Same as Fig. 6 except for 200 mb.

Two deficiencies arising from these simple simulations are most evident in the bias statistics for Ch. 2. First, the simulated values are generally warmer than the observed values, particularly at larger scan angles. As was seen in the limb-corrected results, the differences on the right side of the scan are more positive than those on the left. Incorporating the effects of side lobes into the simulations may reduce these deficiencies.

C. Results from side lobe corrections

As noted in Grody (1983), the MSU instrument consists of rotating antennae which direct incoming energy into radiometric sensors. Since the ratio of the wavelength being measured (approximately 0.5 cm) to the dimensions of the antennae (10.2 cm) is not negligible, some energy will enter from outside the nominal field-of-view of the antennae due to diffraction. Side lobes refer to regions of peak instrument response outside the antenna field-of-view, as indicated in the antenna response curves such as those shown in Fig. 4. The response curve labelled SCAMS in that figure was used by NESDIS in developing the limb correction coefficients. While this curve shows a nominal field-of-view of 10^{o}, a small but not insignificant signal originates from angles as great as 63^{o}. The antenna response for MSU Ch. 2 at nadir for TIROS-N is also shown in Fig. 4. It is more compact with a 7.5^{o} field-of-view and also exhibits some left to right asymmetry. Before presenting the results, it is important to discuss how instrument side lobes can affect the brightness temperatures.

The most important effect of side lobes is related to the geometry of the instrument scan and its relationship to what is viewed below. Due to the curvature of the earth, the practical limit on the angle from which the earth's surface can be viewed is 61.6^{o}, beyond which open space will be viewed, with a radiating temperature of 2.7 K. At the maximum MSU scan positions (1 and 11), the scan angle is 47.35^{o}. Thus, any side lobes beyond 14.25^{o} will be sensing space. Two-dimensional depictions of the TIROS-N and SCAMS antenna responses are shown in Figure 12. Note the asymmetry in the TIROS-N response, with side lobes more prevalent on the left than on the right. Distance from the center of the field-of-view in this diagram is proportional to the angle relative to the axis of the cone defining the sampling region of the instrument. By weighting the response function by the area viewed at a particular angle, one can determine the fraction of the response viewing space as a function of scan position. These fractions are given in Table 2 for the TIROS-N MSU and the nominal SCAMS antenna patterns shown in Fig. 12. The maximum TIROS-N value is 0.39% at position 1, which is considerably larger than the 0.06% at position 11. While these seem like small percentages, this can affect the measured brightness temperature by as much as 1.0 K.

The simplest way to include the effect of side lobes is to apply the data in Table 1, directly. This is done by weighting the simulated brightness temperatures computed in the previous section by the percentage area viewing the earth and adding in the small contribution from space. This approximation ignores changes in the transmittances due to different zenith angles within the footprint itself. Figure 13 summarizes the results from this approximation. Panels A and C are derived using the standard NESDIS transmittance coefficients and the SCAMS and MSU antenna patterns, respectively, while Panel B is for the

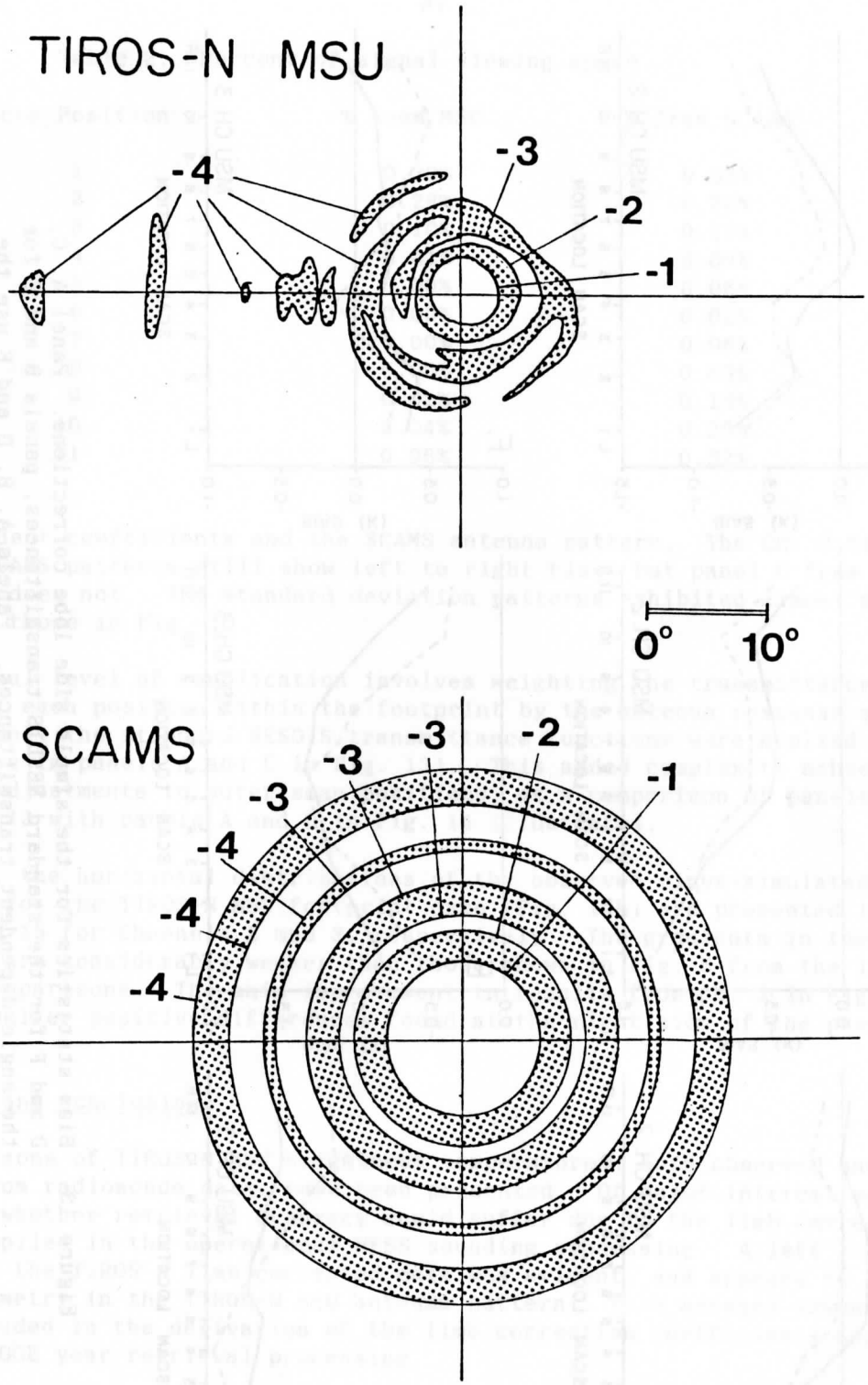

Figure 12. Two-dimensional depictions of the TIROS-N MSU and nominal SCAMS antenna patterns.

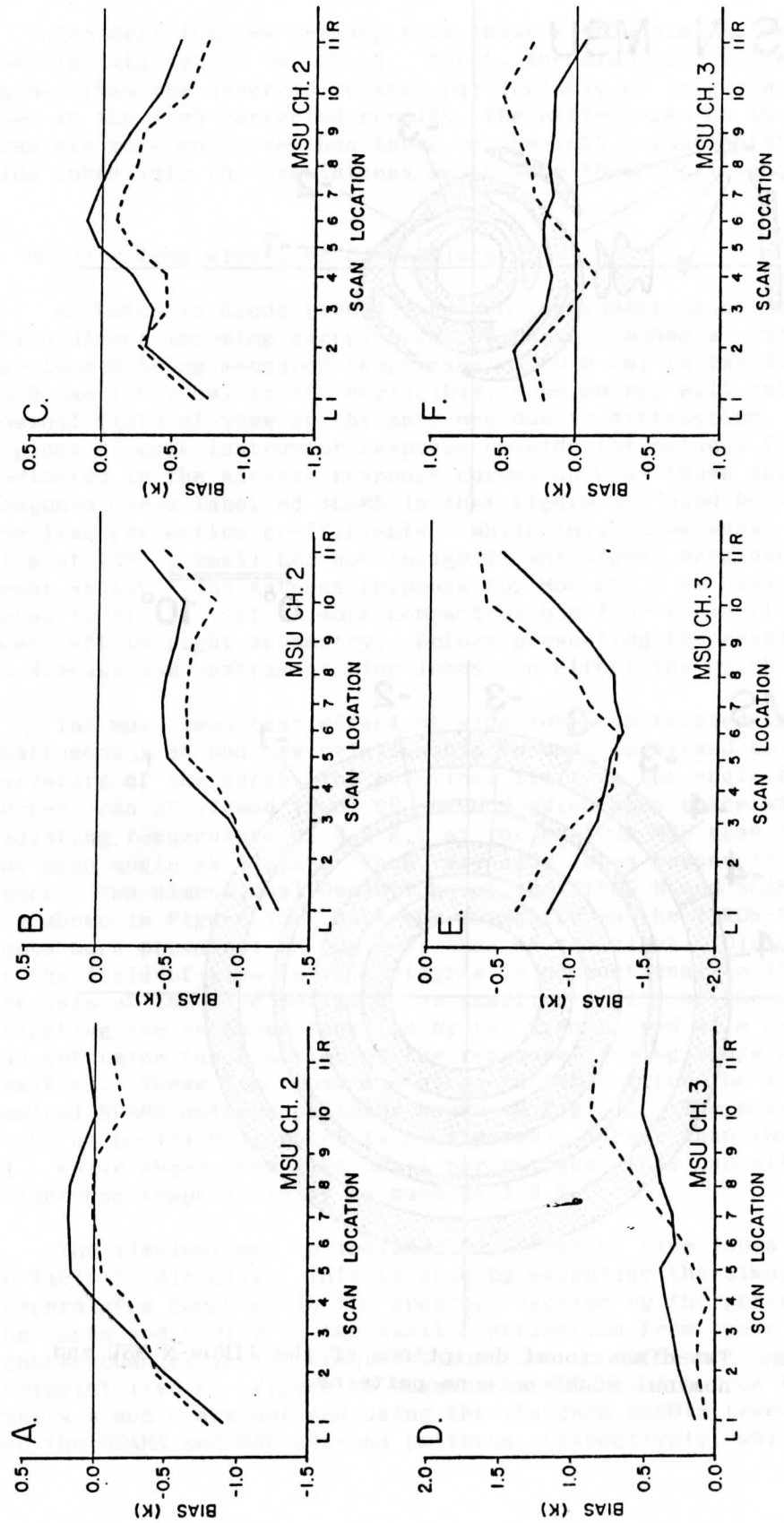

Figure 13. Bias statistics for the simple side lobe corrections. Panel A, C, D and F for the standard NESDIS transmittances, panels B and E for the angle dependent transmittances. Panels A, B, D and E use the SCAMS footprint, while panels C and F use the TIROS-N footprint.

Table 2. Percent of signal viewing space.

Scan Position	% from MSU	% from SCAMS
1	0.39%	0.32%
2	0.28%	0.20%
3	0.10%	0.13%
4	0.01%	0.09%
5	0.00%	0.06%
6	0.00%	0.02%
7	0.00%	0.06%
8	0.00%	0.09%
9	0.02%	0.13%
10	0.04%	0.20%
11	0.06%	0.32%

angle dependent coefficients and the SCAMS antenna pattern. The Ch. 2 biases using the SCAMS patterns still show left to right bias, but panel C from the MSU pattern does not. The standard deviation patterns exhibited almost no change from those in Fig. 10.

The final level of complication involves weighting the transmittance functions at each position within the footprint by the antenna response at that position. Only the standard NESDIS transmittance functions were applied in this case (as in panels A and C in Fig. 13). This added complexity achieves only minor adjustments to outer scan positions, as a comparison of panels A and C from Fig. 13 with panels A and B in Fig. 14 illustrates.

Lastly, the horizontal distributions of the observed-minus-simulated differences for the TIROS-N MSU footprint case (Fig. 14b) are presented in Figs. 15 and 16 for Channels 2 and 3, respectively. The gradients in the Ch. 2 differences are considerably weaker than those shown in Fig. 5 from the limb-corrected comparisons. The main improvement in results from Ch. 3 in Fig. 16 is in the smaller positive differences found at the right side of the pass.

6. Summary and conclusions

Comparisons of TIROS-N MSU brightness temperatures, both observed and simulated from radiosonde data, have been presented. Of major interest was the question of whether retrieval accuracy could suffer due to the limb correction procedure applied in the operational NESS sounding processing. A left to right asymmetry in the TIROS-N limb-corrected data was evident, and appears to arise from an asymmetry in the TIROS-N MSU antenna pattern. This antenna asymmetry was not included in the derivation of the limb correction coefficients applied during the FGGE year retrieval processing.

Another interesting facet of the results is that the Ch. 2 brightness temperatures are warmer than the simulated values in the cold air in the northern portions of the passes, consistent with the synoptically correlated errors described in the earlier papers in this report. Finally, the bias

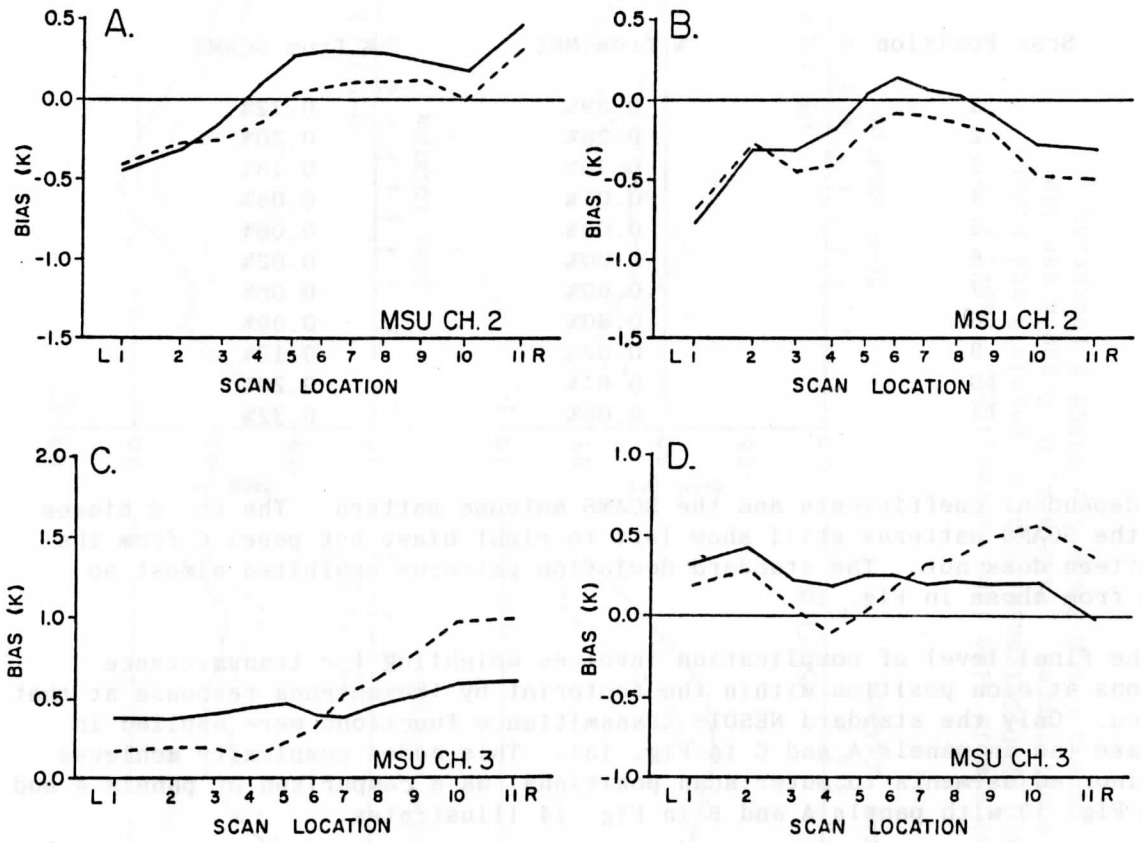

Figure 14. Bias statistics for the more complex side lobe corrections. All panels are for the standard NESDIS transmittance functions. Panels A and C are for the SCAMS footprint, and panels B and D are for the TIROS-N MSU footprint.

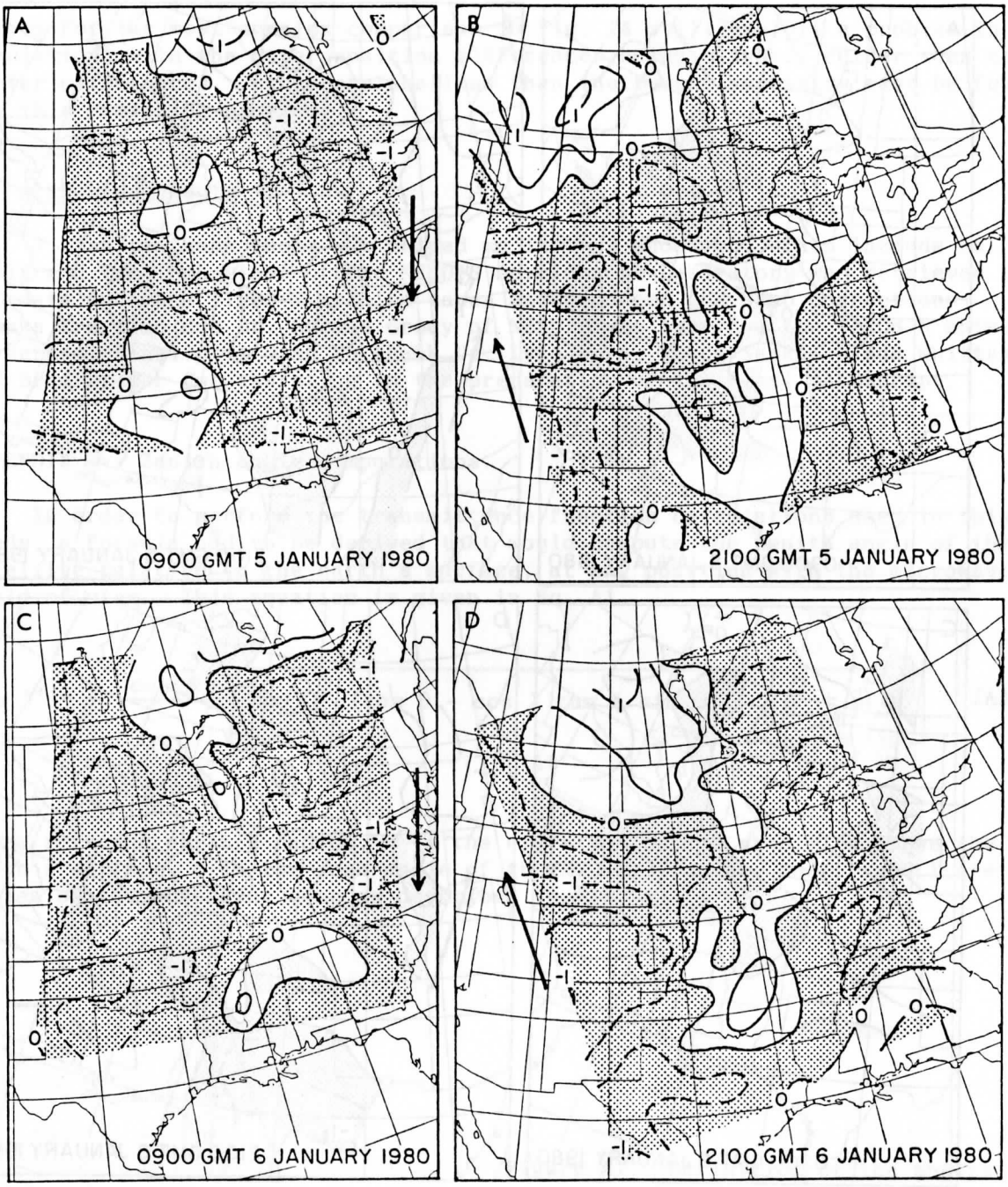

Figure 15. Brightness temperature differences for Ch. 2 data without limb correction and simulated data derived from the more complex side lobe correction.

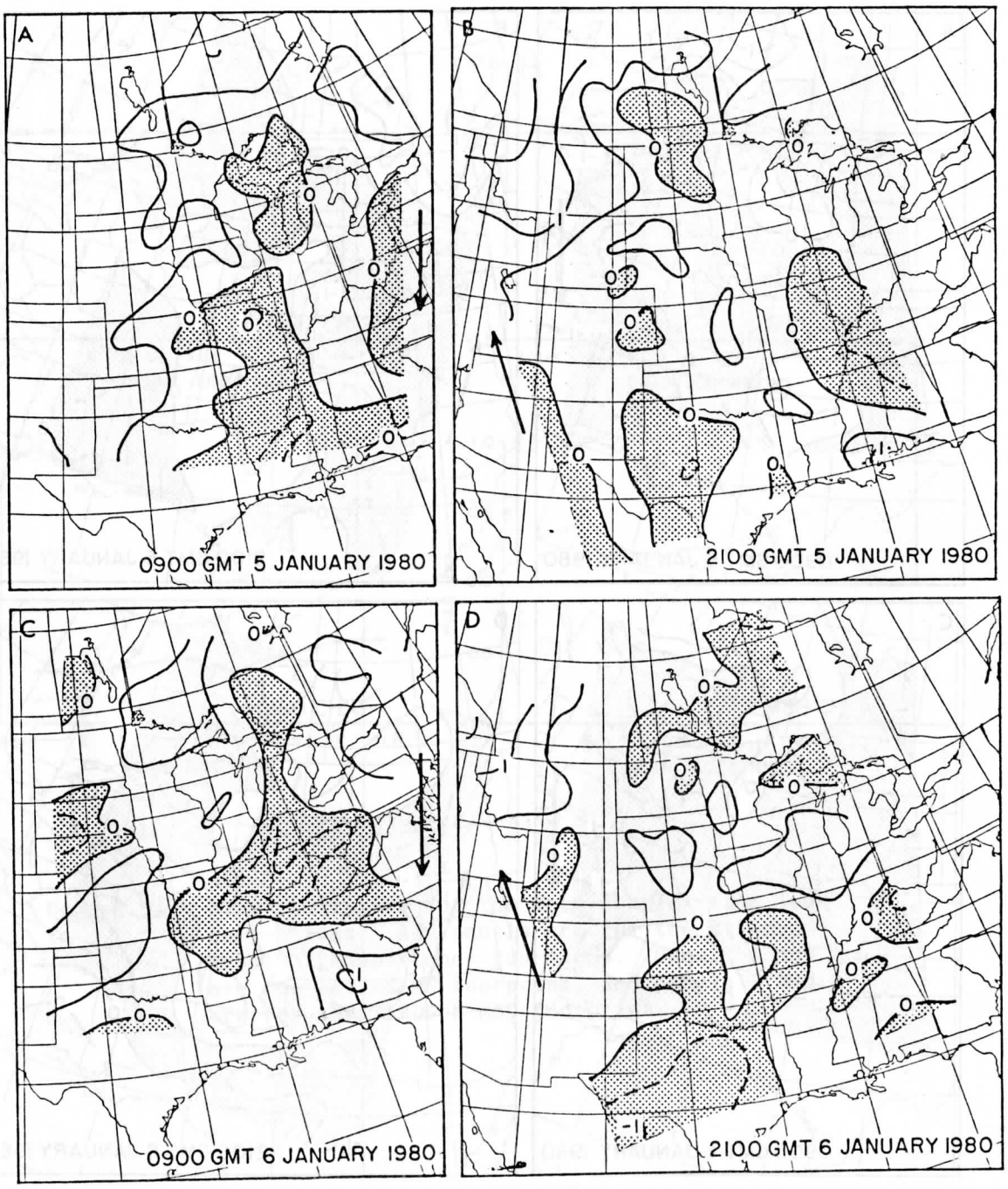

Figure 16. Same as Fig. 15 except for Ch. 3.

curves for the most complex comparison in Fig. 14 still exhibit a problem in the simulation, with the outer position differences being slightly colder than the center differences. Other explanations than instrument asymmetry must be found for this remaining problem.

7. Acknowledgements

I wish to thank those who helped me in this endeavor. Thes include Hal Woolf and Tony Schreiner of the NESDIS Development Laboratory who retrieved the MSU data from the TIROS-N archive tapes and produced the limb corrections. Thanks are also due Dr. Norman Grody of NESDIS who provided the TIROS-N antenna patterns. Finally, I wish to thank Dr. Lyle Horn, Chuck Seman, Linda Whittaker and Brad Bramer for assisting in the preparation of the final manuscript.

APPENDIX A - Zenith angle computations.

In order to perform the transmittance function calculations used in this study, a formula had to be derived that would compute the zenith angle of the satellite relative to the earth's surface, at any position with the microwave field of view. This equation is given in Eq. A1.

$$\cos \gamma' = - \frac{\cos \phi}{r} \sqrt{\left[(r+h)^2 \, (\cos \Theta - \cos \lambda \tan \phi \sin \Theta)^2 - \frac{(h^2 + 2rh)}{\cos^2 \phi} \right]} \qquad \text{(A1)}$$

where r is the earth's radius, h is the elevation of the satellite above the earth's surface, Θ in the scan angle of the MSU instrument, and ϕ and λ are angles of the observing cone as described in Fig. A1.

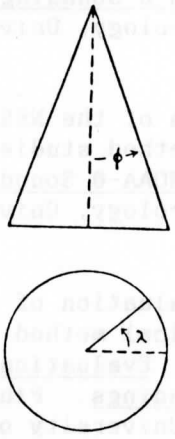

Figure A1. Definition of the angles of the cone.

APPENDIX B - Surface emissivity estimates for the simulations without limb correction

An estimate of the emissivity is required in order to compute the simulated brightness temperatures for the data that are not limb corrected. This estimate is determined from solving Eq. 1 for the surface emissivity using the observed value for Ch. 1 and the simulated value for Ch. 1 from the raob data. This expression is shown in Eq. B1. It is then assumed that the emissivity from Ch. 1 is equal to that in the other MSU channels.

$$\varepsilon_s = \frac{T_B - \int_o^{p_s} T \left[\tau_s \frac{\partial \tau'}{\partial \ln p} - \frac{\partial \tau}{\partial \ln p} \right] d \ln p}{\left[T_s - \int_o^{p_s} T \frac{\partial \tau'}{\partial \ln p} \, d \ln p \right] \tau_s} \qquad \text{(B1)}$$

8. References

Grody, N. C., 1983: Severe storm observations using the Microwave Sounding Unit. J. Clim. Appl. Meteor., 22, 609-625.

Gruber, A. and C. D. Watkins, 1982: Statistical assessment of the quality of TIROS-N and NOAA-6 satellite soundings. Mon. Wea. Rev., 110, 867-876.

Koehler, T.L., J.C. Derber, B.D. Schmidt and L.H. Horn, 1983: An evaluation of soundings, analyses and model forecasts derived from TIROS-N and NOAA-6 satellite data. Mon. Wea. Rev., 111, 562-571.

Koehler, T.L., 1986: High quality radiosonde-derived temperature and thickness data for alternative satellite retrieval experiments. Evaluation of Alternative Retrieval Methods for TIROS-N and NOAA-6 Soundings. Final Report, NOAA Grant NA81AA-D-00087, Dept. of Meteorology, University of Wisconsin-Madison, 22-25.

Koehler, T.L. and C.J. Seman, 1986: A modified version of the NESDIS TOVS Export Package for use in alternative retrieval method studies. Evaluation of Alternative Retrieval Methods for TIROS-N and NOAA-6 Soundings. Final Report, NOAA Grant NA81AA-D-00087, Dept. of Meteorology, University of Wisconsin-Madison, 9-21.

Koehler, T.L., J.P. Nelson and L.H. Horn, 1986: An evaluation of a physical retrieval method as an alternative to the statistical method used in the NESS operational sounding processing during FGGE. Evaluation of Alternative Retrieval Methods for TIROS-N and NOAA-6 Soundings. Final Report, NOAA Grant NA81AA-D-00087, Dept. of Meteorology, University of Wisconsin-Madison, 26-46.

LeMarshall, J.F. and A.J. Schreiner, 1985: Limb effects in satellite temperature sounding. J. Clim. Appl. Meteor., 24, 287-290.

Phillips, N., L. McMillin, A. Gruber and D. Wark, 1979: An evaluation of early operational temperature soundings from TIROS-N. Bull. Amer. Meteor. Soc., 60, 1188-1197.

Schlatter, T.W., 1981: An assessment of operational TIROS-N temperature retrievals over the United States. Mon. Wea. Rev., 109, 110-119.

Seman, C.J., L.H. Horn and T.L. Koehler, 1986: An evaluation of different horizontal resolution in radiance compositing for TIROS-N retrievals. Evaluation of Alternative Retrieval Methods for TIROS-N and NOAA-6 Soundings. Final Report, NOAA Grant NA81AA-D-00087, Dept. of Meteorology, University of Wisconsin-Madison, 47-64.

Weinreb, M.P., H.E. Fleming, L.M. McMillin and A.C. Neuendorffer, 1981: Transmittances for the TIROS Operational Vertical Sounder. NOAA Tech. Rep. NESS 85, 60 pp.

Werbowetzki, A., Ed., 1981: Atmospheric sounder users guide. NOAA Tech. Rep. NESS 83, 82 pp.